THE UNIVERSITY OF SOUTH ALABAMA
COLLEGE OF ENGINEERING

PHYSICAL MODELING OF WAVE TRANSMISSION FOR SUBMERGED AND EMERGENT BREAKWATERS USED IN LIVING SHORELINES

BY

Richard J. Allen

A Thesis

Submitted to the Graduate Faculty of the
University of South Alabama
in partial fulfillment of the
requirements for the degree of

Master of Science

in

Department of Civil Engineering

May 2013

Approved: Date:

____

Chair of Thesis Committee: Dr. Bret M. Webb

____

Committee Member: Dr. Scott L. Douglass

____

Committee Member: Dr. Sean P. Powers

____

Chair of Department: Dr. Kevin D. White

____

Director of Graduate Studies: Dr. Thomas G. Thomas

____

Dean of the Graduate School: Dr. B. Keith Harrison

PHYSICAL MODELING OF WAVE TRANSMISSION FOR SUBMERGED AND EMERGENT BREAKWATERS USED IN LIVING SHORELINES

A Thesis

Submitted to the Graduate Faculty of the
University of South Alabama
in partial fulfillment of the
requirements for the degree of

Master of Science

in

Department of Civil Engineering

by
Richard J. Allen
B.S., University of South Alabama, 2011
May 2013

ACKNOWLEDGMENTS

This research was made possible through support provided by the U.S. Department of Commerce through the National Oceanic and Atmospheric Administration through The University of Southern Mississippi under terms of Agreement No. **NA10OAR4170078**. The opinions expressed herein are those of the authors and do not necessarily reflect the views of the U.S. Department of Commerce, the National Oceanic and Atmospheric Administration or The University of Southern Mississippi.

The author would like to take the time to thank all of the individuals who made this research possible. Foremost, the author appreciates the support received from the Department of Civil Engineering faculty, namely Dr. Bret Webb and Dr. Scott Douglass for acquiring funding, and Dr. Eric Steward for assistance in determining the physical properties of the oyster shell substrate used in the ReefBLKs^{SM}. Furthermore, thanks should be given to Carl Ferraro from the Alabama Department of Conservation and Natural Resources - Coastal Division for the acquisition of oyster shell and netting material used in the bagged oyster shell experiments as well as Scott Rickard from the Auburn Shellfish Laboratory for supplying the oyster shell used in the ReefBLK^{SM} experiments. The geotechnical descriptions of the substrate used in the bagged oyster shell experiments is accredited to Lewis Copeland, Vice President, of Southern Earth Sciences. John Lyon is acknowledged for his fabrication expertise in constructing the frames for the ReefBLK^{SM}. Additionally, set up and execution of the physical experiments could not have been accomplished without the support of Timothy Wicker, Drew Harrison, and Caren Reid Dixon. Finally, the financial and physical support of the author's parents, Rick and Jan Allen, is attributed to the success of this research.

TABLE OF CONTENTS

LIST OF TABLES

Appendix A

Table Page

Appendix B

Table Page

LIST OF FIGURES

Appendix A

Figure | Page

LIST OF SYMBOLS

B	=	Crest width
d	=	Water depth
h_c	=	Structure height
H_i	=	Incident wave height
H_t	=	Transmitted wave height
K_t	=	Transmission coefficient, H_t / H_i
K_{tl}	=	Lower limit transmission coefficient (Van der Meer et al. 2005)
K_{tu}	=	Upper limit transmission coefficient (Van der Meer et al. 2005)
L_i	=	Wave length (Calculated using S.A.W.T.)
R_c, F	=	Breakwater freeboard, $h_c - d$
S_{op}	=	Wave steepness, $S_{op} = 2\pi H_i / (gT^2)$
T	=	Wave period
$\tan \alpha$	=	Seaward slope of breakwater
ξ	=	Surf similarity parameter, $\xi = \tan \alpha / (S_{op})^{0.5}$

ABSTRACT

Allen, Richard J., M.S., University of South Alabama, May 2013. Physical Modeling of Wave Transmission for Submerged and Emergent Breakwaters used in Living Shorelines. Chair of Committee: Dr. Bret M. Webb.

Breakwaters used in living shoreline projects are referred to as engineered reefs and are used to modify wave characteristics along estuarine shorelines in such a way as to promote ecological and biological enhancement, with stabilization of the shoreline often an expressed goal. Studies show engineered reefs are a successful alternative to traditional rubble mound breakwaters in the environmental aspect; however, the true success of these structures has not been quantified in terms of wave energy dissipation. Through physical modeling of engineered reefs using the University of South Alabama's wave basin, much of the engineering design related to wave energy was determined. The testing included bagged oyster shell breakwaters, apex-truncated square concrete pyramids, and ReefBLKs^{SM} subjected to multiple wave forms and water depths. Results from the testing showed that wave transmission through bagged oyster shell and concrete pyramid devices can mostly be explained using published methodologies. In terms of structure geometry, the non-dimensional height, h_c/d, is the primary factor when designing the engineered reefs. The bagged oyster shell and ReefBLKs^{SM} are more effective in attenuating shorter wave lengths while concrete pyramids are more affective in attenuating longer wave lengths. The dependence of structure performance on wave period is a new finding.

INTRODUCTION

Shoreline stabilization is prevalent along estuarine shorelines in the United States. For example, Douglass and Pickel (1999) quantify the amount of shoreline armoring in Mobile Bay, Alabama and show between 1955 and 1997 shoreline armoring increased from 8% to 30% and is a direct function of the population; hence, as the population increases, the amount of armoring will increase proportionally. The armoring described in Douglass and Pickel (1999) primarily consists of vertical bulkheads, armor stone, and other less aesthetically pleasing materials. Shoreline stabilization utilizing techniques described by Douglass and Pickel (1999) is known to protect upland erosion, but hard structures are not favorable for the local ecology (Swann 2008).

Implementing hard structures for shoreline stabilization and upland property protection decreases wetland/salt marsh habitat by inhibiting sediment transport, removing intertidal habitat, and increasing wave reflection (Benoit et al. 2007).Wetlands provide vital marine habitat in the intertidal zone, create a buffer for storm surge, and serve as treatment for storm water runoff (Stout 1990). A study by Dahl (2006) shows wetland areas in the United States have been reduced by half of the historical values, which is a concern for many scientists and government officials.

Quantifying the environmental factors for design purposes, such as sediment transport and wave energy, associated with the reduction of wetlands is addressed in the published literature. In terms of sediment transport, Airoldi et al. (2005) summarizes a number of projects overseen by DELOS (Environmental Design of Low Crested Coastal Defense Structures) and suggests projects should be designed to allow a natural shoreline to form with minimal post-construction infringement but should not impede the hydrodynamic properties needed to abate negative impacts on the local ecology (stagnant water, invasive species, etc.), as well as regional processes. The wave energy threshold required for the establishment/survival of wetlands is quantified by Roland and Douglass (2005). Roland and Douglass (2005) find marsh grass, specifically *Spartina alterniflora*, can survive with no erosion when the median significant wave height is below 0.1 m. The limits or goals of sediment transport and wave energy thresholds needed for the successful design of a more natural shoreline must be considered; however, achieving a more natural shoreline requires a new strategy employing alternatives to hardened structures and an innovative design process incorporating these goals.

Alternatives to hardened structures for shoreline stabilization are becoming popular by planners and policy makers. The alternatives attempt to use the natural ecology and less invasive techniques to protect shorelines (Yozzo et al. 2003; Adams 2002). These ecologically-friendly projects have come to be known as “living shorelines.” The definition of a living shoreline given by the National Oceanic and Atmospheric Administration (NOAA, 2013) is:

> *”A shoreline management practice that provides erosion control benefits; protects, restores, or enhances natural shoreline habitat; and maintains coastal processes through the strategic placement of plants, stone, sand*

fill, and other structural organic materials (e.g. biologs, oyster reefs, etc)."

The components within the definition may be obtained individually using traditional methods, but combining all aspects into one design requires the cooperation of multiple disciplines including, but not limited to: coastal engineers, ecologists, biologists, geologists, and policy makers (Borsje et al. 2010; Hardaway et al. 2010a; Walker et al. 2011). Coastal engineers can stabilize a shoreline easily using traditional hard structures such as vertical bulkheads, but these eliminate vital marine habitats. Additionally, projects focused on marine habitats beneficial for promoting growth can be built (Davis et al. 2006; DeQuattro 2010; Hardaway et al. 2010b). Furthermore, all shorelines are not the same, so what might be a good design in one location may be completely wrong in another (Bendell 2006).

Incorporating structures such as engineered reefs into living shoreline projects is sometimes required, based on the wave climate (Duhring 2006). Engineered reefs are defined in this study as a structure composed of formed concrete units or any structure used to manipulate the geometry of a substrate for the purpose of attenuating wave energy. Some examples of engineered reefs are: ReefBLK℠, Reef Balls™, bagged oyster shell, and apex-truncated square concrete pyramids. See Figures A1-A4 of Appendix A for photos of these technologies. Engineered reefs modify wave characteristics along estuarine shorelines in such a way as to promote ecological and biological enhancement, with stabilization of the shoreline often an expressed goal. To achieve these goals, engineered reefs used in living shorelines must be designed to meet the limits presented by Roland and Douglass (2005) for the survival of salt marsh habitat and to account for sediment transport as described by Airoldi et al. (2005).

A method for calculating the wave height leeward of engineered reefs must be used to obtain the desired wave conditions suitable for salt marsh habitat. However, methodologies published for engineered reefs are limited to specific materials and geometries. Engineered reefs lacking published methodologies for wave transmission are employed in demonstration projects where the desired leeward wave height is sometimes estimated using methodologies published for other types of reefs or breakwaters and is, in most cases, inadequate. The implications of applying traditional methods can lead to the failure of an engineered reef to provide adequate shoreline stabilization or the over design of the structure, which can produce adverse ecological factors, increased costs, and a less aesthetically pleasing site due to larger than required structures. The research performed in this study addresses the lack of published methodologies for three engineered reef designs: bagged oyster shell, apex-truncated square concrete pyramids, and ReefBLKs℠.

LITERATURE REVIEW

The coastal engineering design of detached breakwaters is based primarily on wave height reduction. The reduction in wave height by a breakwater is commonly referred to as wave attenuation. Wave attenuation is defined using the ratio of the incident wave height, H_i, to the transmitted wave height, H_t. This ratio is called the wave transmission coefficient, K_t, shown mathematically in Equation 1 (Jeffreys 1944).

$$K_t = \frac{H_t}{H_i} \qquad \text{(Eq. 1)}$$

Based on this equation, the smaller the value of K_t the more effective the breakwater is in attenuating the wave energy. Hence, if K_t were zero there would be no transmitted wave height in the lee of the breakwater; whereas, K_t values equal to one indicate the structure has no effect on the incident wave height. Wave attenuation is achieved through the geometry of the structure (Goda et al. 1967). Goda et al. 1967 suggests wave transmission is a function of five non-dimensional relationships defined using ratios of the geometry of the structure as well as the incident wave characteristics and water depth (Equation 2). Symbols in Equation 2 and in the remainder of this document are defined in the List of Symbols on page *xiii*.

$$K_t = \frac{H_t}{H_i} = f\left(\frac{F}{H_i}, \frac{B}{d}, \frac{h_c}{d}, \frac{d}{L_i}, \frac{H_i}{d}\right) \quad \text{(Eq. 2)}$$

Wave transmission based on geometry for traditional coastal engineering defense breakwaters is studied by many researchers (Hall and Hall 1940; Jeffreys 1944; Goda et al. 1967; Dick and Brebner 1968; Dattatri et al. 1978; Seelig 1980; Ahrens 1984; Van der Meer and d'Angremond 1991; d'Angremond et al. 1996; Seebrook and Hall 1998). Wave transmission based exclusively on geometry is still applicable to modern designs, and equations from these earlier studies are still provided in the Coastal Engineering Manual (U.S. Army Corp of Engineers 2002). However, improving on the previous research for wave transmission is a never-ending research objective, which now includes other breakwater properties such as porosity, slope, and orientation (Lynett et al. 2000; Mizutani and Mostafa 2001; Golshani et al. 2002; Ting et al. 2004; Kramer et al. 2005; Van der Meer et al. 2005; Perez-Romero et al. 2009; Rageh 2009; Vanneste and Troch 2010; Ahmed and Anwar 2011; Ahmadian and Simons 2012).

One of the recent studies performed by Van der Meer et al. (2005) compiled laboratory testing and equations from the available literature into formulae for normally incident waves passing over a fully-submerged trapezoidal rubble mound structure. The formulae do not include any relationship to the structure end geometry or location relative to the shoreline. The formulae depend primarily upon non-dimensional relationships between the incident wave height and the cross-sectional physical characteristics of the structure. The final equations published in Van der Meer et al. (2005) are shown in Equations 3 and 4.

For $\frac{B}{H_i} < 8$ $$K_t = -0.40\frac{R_c}{H_i} + 0.64\left(\frac{B}{H_i}\right)^{-0.31}(1 - e^{-0.50\xi}) \qquad \text{(Eq. 3)}$$

For $\frac{B}{H_i} > 12$ $$K_t = -0.35\frac{R_c}{H_i} + 0.51\left(\frac{B}{H_i}\right)^{-0.65}(1 - e^{-0.41\xi}) \qquad \text{(Eq. 4)}$$

Explanation of the terms in Equation 3 and 4 can be found in the List of Symbols at the beginning of this document. Note that a gap exists in the range $8 < B/H_i < 12$, where the Van der Meer et al. (2005) equations yield a discontinuity and it is suggested that linear interpolation is used for values of B/H_i that fall within this range. Additionally, Van der Meer et al. (2005) suggests limits for the maximum and minimum values of K_t. The lower limit, K_{tl}, is defined as a constant 0.05. The upper limit K_{tu}, is given a linear dependency on B/H_i and is determined by Equation 5.

$$K_{tu} = -0.006\frac{B}{H_i} + 0.93 \qquad \text{(Eq. 5)}$$

Utilizing alternative substrates and geometries such as oyster shell and precast concrete units in the construction of living shoreline breakwaters has not been thoroughly investigated, in comparison to traditional rubble mound structures. Literature investigating the wave attenuation properties of bagged oyster shell breakwaters is non-existent other than that previously published by the author and included in this study (Allen and Webb 2011). Other studies use methodologies such as Van der Meer et al.

(2005) for bagged oyster shell but have not produced evidence to prove these methodologies are a viable solution.

Quantitative information is published for precast concrete units but is exclusive to a specific geometry (Armono and Hall 2003; Douglass et al. 2012). An evaluation of wave attenuation for Reef Balls™ published by Armono and Hall (2003) looks at five configurations, including three configurations utilizing a rubble mound base. A multiple regression analysis is performed utilizing 112 unique tests from two of the five configurations, both consisting of a rubble mound base, resulting in Equation 6.

$$K_t = 1.616 - 31.322\frac{H_i}{gT^2} - 1.099\frac{h_c}{d} + 0.265\frac{h_c}{B} \qquad \text{(Eq. 6)}$$

Douglass et al. (2012) finds wave transmission coefficients for apex-truncated square concrete pyramids placed in single and double row configuration parallel and oblique to the incident wave crest in the range of $0.4 < K_t < 0.9$. The transmission coefficient values are obtained using physical laboratory modeling where the incident wave height is 5 cm < H_i < 8.6 cm having two wave periods of 1.34 s and 1.75 s. The wave depth is also varied such that $1.1 < h_c/d < 1.69$.

Data associated with the attenuating properties of ReefBLKs℠ are restricted to specific case studies (Reed 2012; DeQuattro 2010), whose primary objective is the ecological factors, where the attenuating properties are only briefly noted and rarely provide significant technical data. An exception to this is a recent unpublished report by Digital Engineering, Inc., September 2012, where incident and transmitted wave heights are measured at a site near Bayou la Batre, Alabama. Results from this study show wave transmission coefficients for incident significant wave heights of 0.11 to 0.40 m are $0.44 < K_t < 0.77$ for $0.57 < h_c/d < 1.0$ and $0.73 < K_t < 0.81$ for $0.44 < h_c/d < 0.57$. The report by Digital Engineering, Inc. (2012) concludes that wave attenuation is most efficient when the water depth, d, is within 0.1 m of the structure height, h_c, based on the low values of the wave transmission coefficient, $0.44 < K_t < 0.56$. Explanation of the symbols is given in the List of Symbols on page *xiii*.

OBJECTIVE

The wave attenuation capabilities of engineered reefs, specifically bagged oyster shell breakwaters, apex truncated square concrete pyramid units, and ReefBLKs℠ was determined through physical modeling using the wave basin at the University of South Alabama. The results obtained were compared to published literature for traditional rubble mound breakwaters. Relationships between the incident wave properties, structure dimensions, and measured wave transmission coefficients are described. The relationships developed are used to describe the effectiveness of each unit in terms of wave characteristics when applied to a living shoreline and design wave climate.

METHODOLOGY

Experimental Setup

The tests in this study were conducted using the University of South Alabama's wave basin. The wave basin is 6.09 m (20 ft) wide and 9.14 m (30 ft) long. Waves were generated in the basin by a unidirectional bulkhead capable of producing monochromatic waves, which propagated across the basin to a sloping sand beach. To simplify testing and analysis, and to minimize experimental errors, the incident wave height was measured as the wave height produced by the wave generator prior to the placement of any attenuating structure at the same location as used for measuring the transmitted wave height. The transmission coefficient obtained using this method is sometimes referred to as the influence coefficient, since the value is representative of all interactions the structure has on the incident wave. The influence coefficient term is presented in Douglass et al. (2012) and Murakami and Maki (2011), who reference Takayama et al. (1985). The Takayama et al. (1985) paper is written in Japanese, so the origin of the term is not certain.

Bagged Oyster Shell

The bagged oyster shell tests were conducted using a splitter wall and a single wave gage. The splitter wall served to eliminate the effects of diffraction around the bagged oyster shell breakwater. The wall was built 0.76 m (2.5 ft) from the side of the basin, 4.88 m (16 ft) in length, beginning 0.61 m (2.0 ft) from the bulkhead's maximum stroke. The wall was constructed from timber and held in place using high-density armor stone. The upright portion of the wall was supported by triangular stanchions, which were placed 0.61 m (2.0 ft) on center along the outboard side (Figure 1). Data collection was accomplished by placing the wave gage centered between the splitter wall and the basin side wall on the leeward side of the testing area.

Figure 1: University of South Alabama wave basin with splitter wall installed and graded beach face in preparation for testing the bagged oyster shell.

The composite breakwater structure was made up of oyster shell bags 0.76 m (30 in) in length having a nominal diameter of 0.076 m (3 in) (Figure 2). The bags were constructed using a 0.76 m (30 in) section of 0.10 m (4 in) PVC pipe. An empty bag was placed in the pipe and tied on one end. Oyster shells were then scooped into the assemblage and shaken/compacted until full, then the open end was closed using a cable tie. A total of 120 bags were produced for testing. The oyster shells and the netting material used in the project were obtained from the Alabama Department of Conservation and Natural Resources (ADCNR)-Coastal Section. The netting material was distributed by Atlantic Aquaculture Supply, LLC. It is described as “Oyster Setting Bag Net” with openings of 0.017 m (5/8 in) and is manufactured as a tube with a diameter of 0.123 m (4.5 in) (Atlantic Aquaculture 2010).

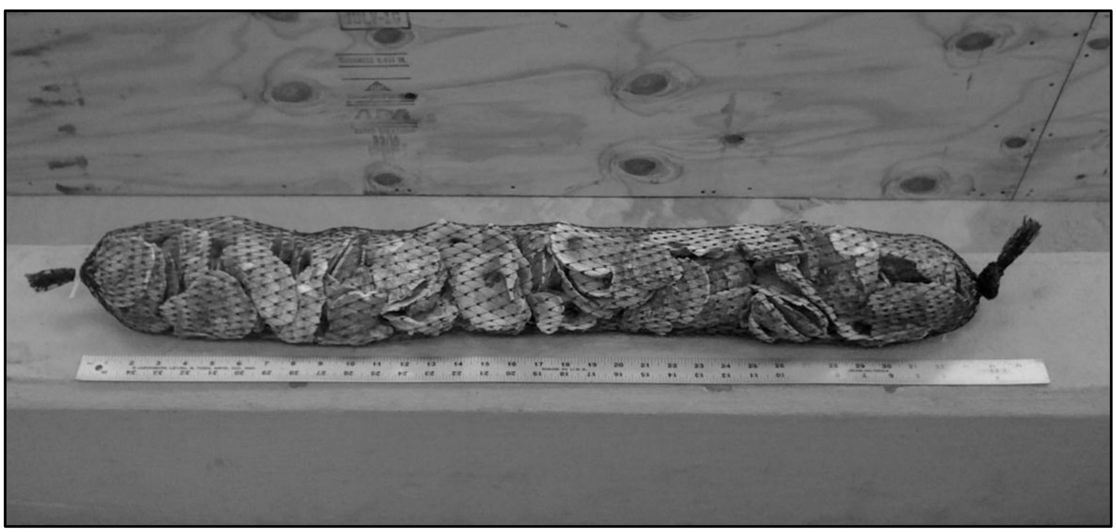

Figure 2: Completed oyster shell bag having a nominal diameter of 0.076 m (3 in) and 0.76 m (30 in) in length.

The oyster shells obtained from ADCNR were mature eastern oyster, *Crassostrea virginica*, shells recovered from the extinct reefs located along the shores of Mobile Bay in Alabama. A sample of the oyster shells were supplied to Southern Earth Sciences to determine grain size distribution using ASTM Standard C33. A summary of the findings is provided in Figure 3.

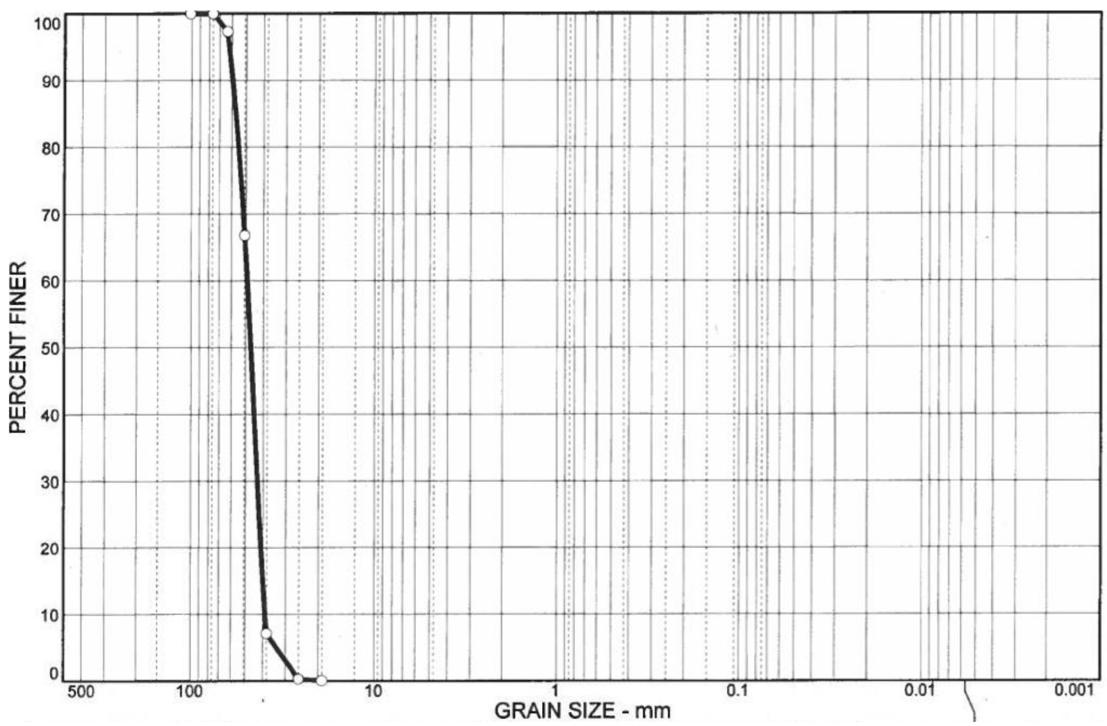

Figure 3: Grain size distribution findings for oyster shell used in the bagged oyster shell breakwater provided by Southern Earth Sciences.

The bagged oyster shell testing matrix was constructed to produce a range of values, which were adequate to describe the attenuation of a wave height (H_i = 0.10 m) and period (T = 1.34 s). The matrix contained 36 unique combinations of structure height and crest width. The height of the structure was varied from one bag high to six bags high

(0.08 - 0.45 m), which yielded a structure height 1.5 times greater than the still water depth. The crest width was also varied for each structure height. Structure crest widths varied from four bags to 19 bags (0.38 - 1.96 m), yielding a total of six unique crest widths. The largest crest width was proportional to the incident wavelength, where the wavelength was calculated using small amplitude wave theory. Seven additional tests were conducted using a larger wave height (H_i = 0.16 m) and period (T = 2.03 s), for selected experiments where the freeboard was greater than zero. The larger wave provided additional data of the variation between wave heights for a similar structure. A structure side slope of 1:1.5 (H:V) was kept constant throughout testing. A water depth of 0.30 m (12 in) remained constant throughout the experiment as well. A tabular form of the experimental setup is provided in Table 1 and detailed information pertaining to the incident wave characteristics can be found in Table B1 in Appendix B. A graphical representation of the terms used is shown in Figure 4. The root-mean-square wave height was used for each experiment.

Table 1: Bagged oyster shell breakwater experimental setup.

Experimental Setup	
Configuration	Trapezoidal Profile
Water Depth	0.30 m
Structure Height	1 - 6 bags (0.08 - 0.45 m)
Structure Crest Width	4 - 19 bags (0.38 - 1.96 m)
Control Waves (2)	H_i = 0.10 m, T = 1.34 s
	H_i = 0.16 m, T = 2.03 s
# of Experiments	(43) 36 w/ small wave
	7 w/ large wave

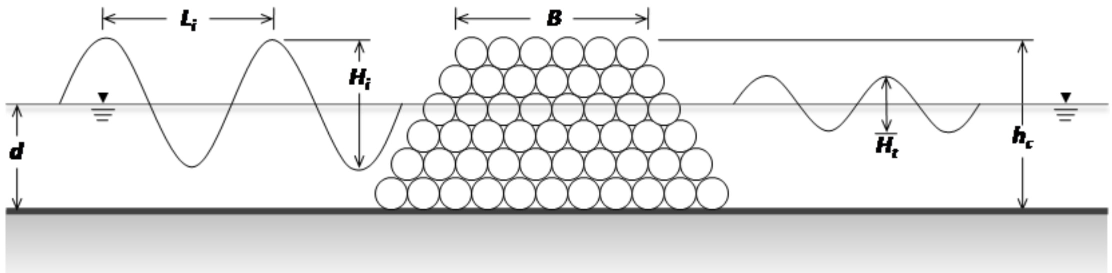

Figure 4: Cross-section of the bagged oyster shell breakwater with pertinent variables defined.

Concrete Pyramids

The concrete pyramid tests were conducted using the same splitter wall as is used in the bagged oyster shell testing. The splitter wall was placed 2.44 m (8.0 ft) from the side wall of the basin, and was 4.88 m (16 ft) in length, beginning 0.61 m (2 ft) from the bulkhead's maximum stroke length. Two wave gages were placed between the splitter wall and the basin side wall for data collection. The gages were placed such that one gage was in the lee of the pyramid crest and the other was centered between two crests. The basin setup is shown in Figure 5.

Figure 5: University of South Alabama wave basin setup for conducting experimental testing of the concrete pyramids.

The structures tested were four-sided pyramids with flat tops, which are known as apex-truncated square pyramids, but are referred to as concrete pyramids for simplicity in this document. The concrete pyramids were 1:5 (model: prototype) scale models of units for a project in Portersville Bay, Alabama (Douglass et al. 2012). The concrete pyramids were constructed with a hollow core, producing a side and top wall thickness of 0.05 m (2 in) and an open base. Two 0.06 m (2.5 in) holes were on three sides and five 0.06 (2.5 in) holes were on the fourth side, with a single 0.06 (2.5 in) hole on the top (Figure 6 and 7). The base of the pyramid was 0.61 m (24 in) with a nominal height of 0.30 m (12 in) and a crest width of 0.25 m (10 in), creating a side slope of 1:1.79 (H:V). The average weight of a pyramid was 64.4 kg (142 lbs).

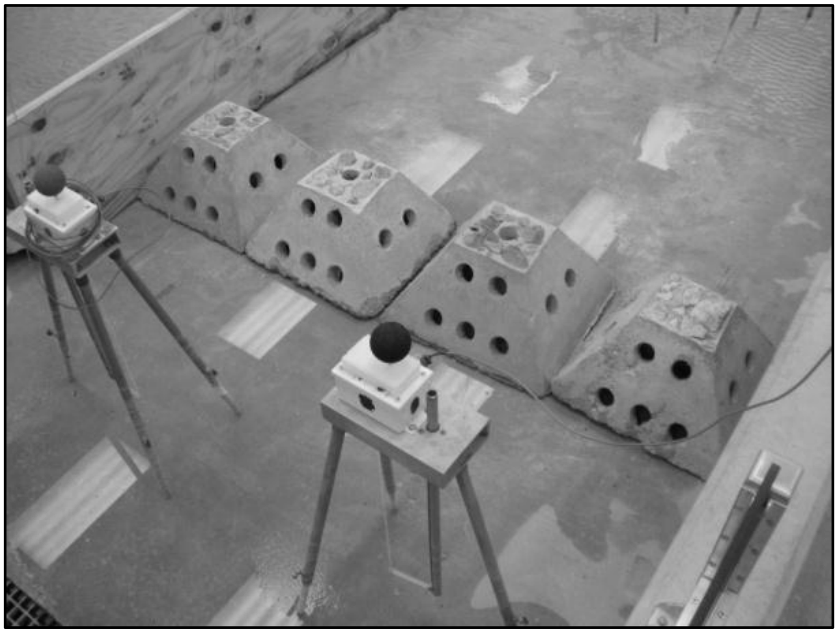

Figure 6: Single row configuration of model concrete pyramids in the University of South Alabama wave basin.

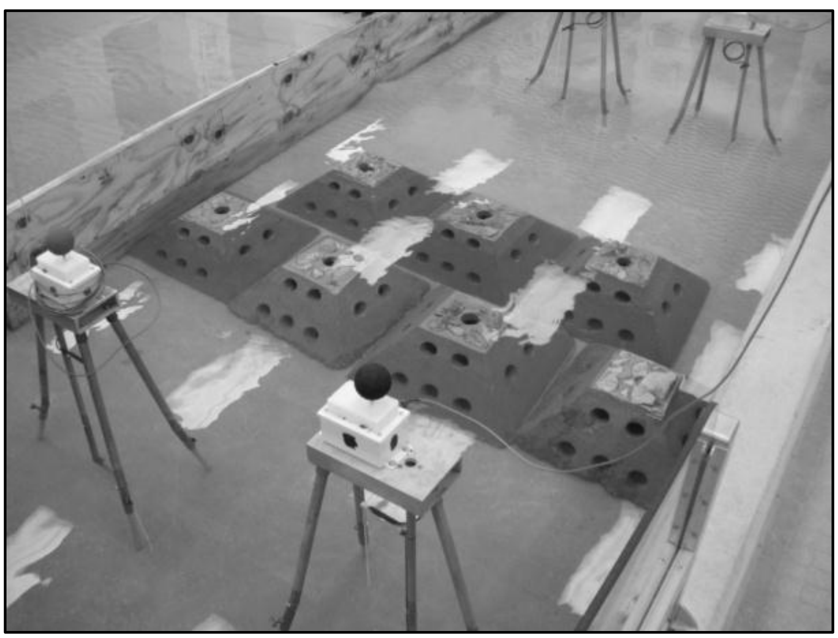

Figure 7: Offset double row configuration of model concrete pyramids in the University of South Alabama wave basin.

A testing matrix was developed to yield a comprehensive data set sufficient for describing the wave height attenuation characteristics of the concrete pyramids. The matrix contained 40 experiments for two configurations of the concrete pyramids and consisted of five water depths (0.20 - 0.41 m) and eight wave height and period combinations, for a total of 80 unique experiments. The testing matrix is provided in Table A1 and Table A2 of Appendix A. The control wave heights ranged from 0.05 m (2 in) to 0.20 m (8 in) with periods ranging from 1 to 3 s. A summary of the experimental setup is provided in Table 2 and detailed incident wave heights are provided in Table B2 and B3 in Appendix B. The control for these experiments was achieved by performing the testing matrix of 40 unique configurations before the concrete pyramid units were installed. The average of the incident wave height, H_i, and transmitted wave height, H_t, for each unique experiment was used in the analysis.

Table 2: Summary of the experimental setup for the concrete pyramids.

Experimental Setup	
Configurations	(1) Single Row
	(2) Offset Double Row
Water Depths	0.20, 0.25, 0.30, 0.36, 0.41 m
Wave Heights	0.05 - 0.20 m
Wave Periods	1 - 3 s
Total Experiments	80

The two configurations were constructed, comprised of a single row of units and a double row of units, where an additional row of units was placed leeward of the single row. The single row of concrete pyramids was placed parallel to the wave crest with the bases of the units in contact (Figure 6). In the double row configuration, the second row of units was offset from the first row such that the crest of a unit in the second row was centered between two crests of the first row (Figure 7). Additionally, the concrete pyramid bases of the second row were in contact with the first row for all the double row configuration testing. The crest width of the units was measured as shown in the cross-sectional diagram in Figure 8 and all other parameters were as those described in Figure 4.

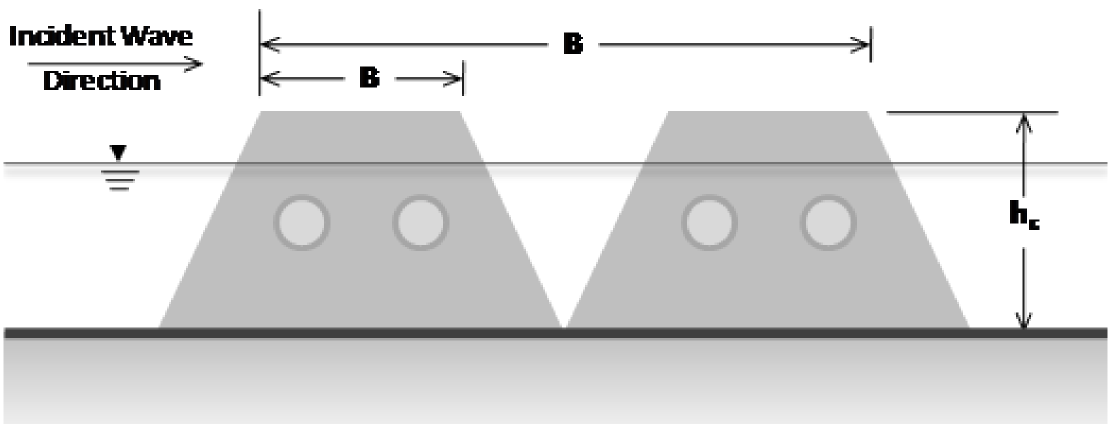

Figure 8: Cross-sectional diagram of the concrete pyramids showing the dimensional measurements used for analysis. The different measurements for the crest width, B, correspond to the single row and double row configurations. Measurements of wave characteristics and other applicable terms are the same as presented in Figure 5.

ReefBLK^{SM}

The ReefBLK^{SM} tests utilized the entire width of the wave basin and three wave gages. The ReefBLKs^{SM} were placed in an alternating point row across the basin a distance of 1.22 m (4.0 ft) from the maximum stroke of the bulkhead, as shown in Figure

9. The crest width, *B*, for the ReefBLK^{SM} breakwater was defined as the width measured perpendicular to the incident wave crest from the point closest to the incident wave direction on one unit to the point farthest from the incident wave direction of an adjacent unit and graphically shown in Figure 10. Three wave gages were placed in the lee of the structure to record the transmitted wave height. The ReefBLKs^{SM} were anchored to the basin floor to prevent movement.

Figure 9: The University of South Alabama wave basin setup for conducting the experimental testing of the ReefBLK^{SM} units.

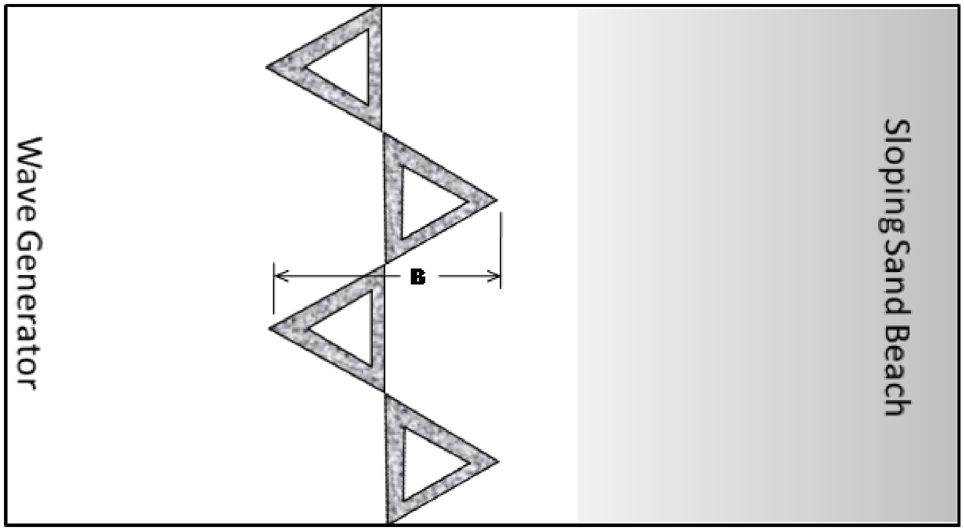

Figure 10: Plan view of the ReefBLK^{SM} breakwater configuration with the crest width measurement defined. All other measurements for the ReefBLK^{SM} testing follow those provided in the bagged oyster shell cross-section (Figure 4).

The ReefBLK^{SM} units are 1:2 (model: prototype) models of those developed by Coastal Environments, Inc. The model units have sides that measure 0.76 m (30 in) and a height of 0.30 m (12 in). The core of the unit, where the substrate is place, has a width of 0.073 m (2.88 in) (Figure 11). Netting material was supplied by Atlantic Aquaculture and described as "Rigid Polyethylene Diamond Shape Netting" with a mesh size of 13 mm (0.51 in) (Atlantic Aquaculture, 2013). The netting material was secured to the frame using black cable ties. The frame was constructed of 0.61 cm (0.25 in) round stock steel. Fabrication of the frame was performed in the University of South Alabama fabrication shop with the assistance of John Lyon (Figure 12). All the bending was performed by hand using a jig and all connections were welded.

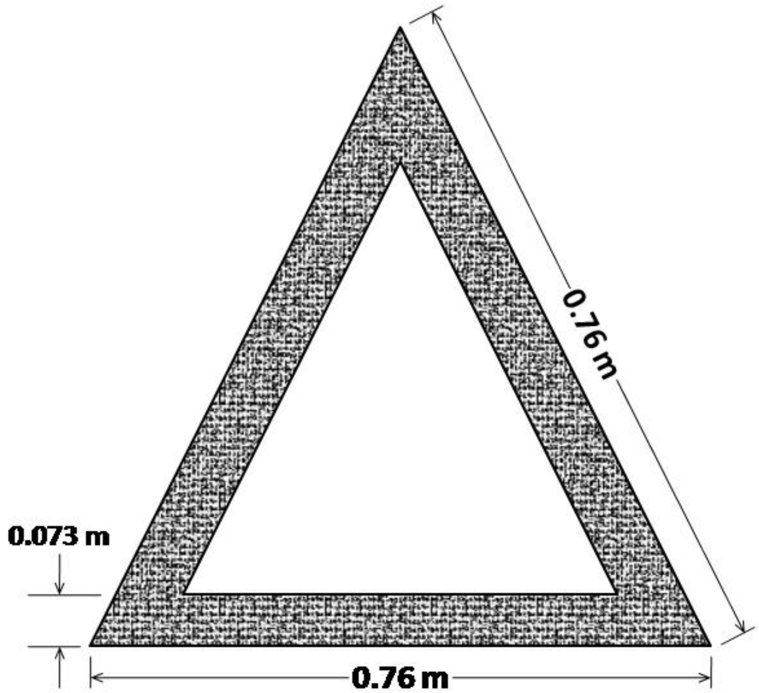

Figure 11: Plan view of model ReefBLK^{SM} with dimensions. (Figure not to scale)

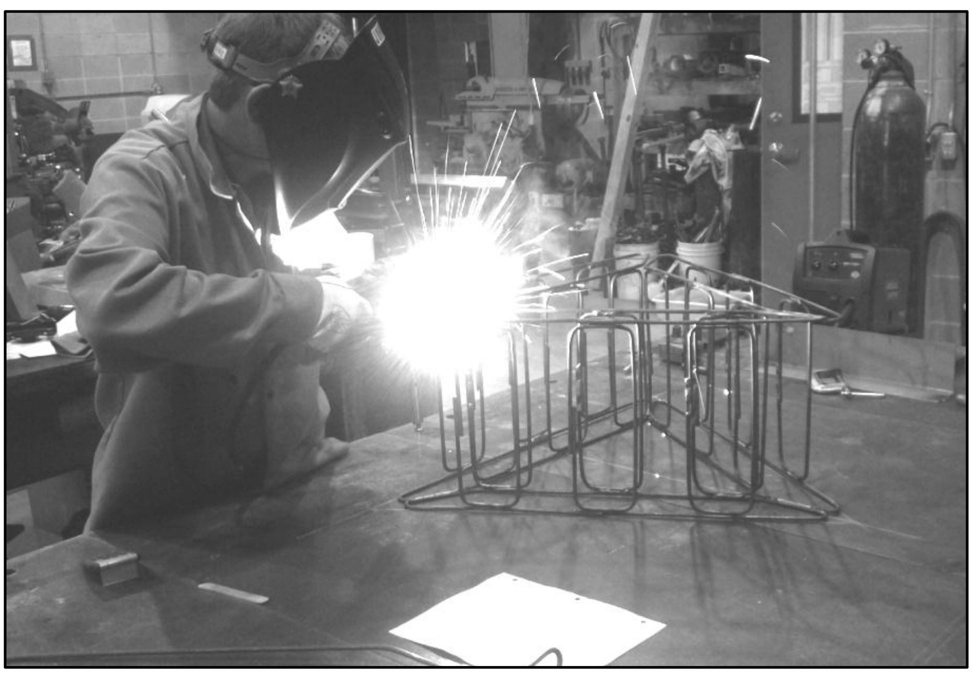

Figure 12: Construction of the ReefBLK^{SM} frame with the help of John Lyon using the University of South Alabama fabrication shop.

Once the frames were completed and painted to prevent oxidation, the netting material was installed (Figure 13). The netting material installation was performed in such a way as to allow the maximum amount of substrate. This style was not replicated in the prototypes. The prototype units used a tube-type netting design where three vertical tubes of netting were placed in each side of the unit. However, in the model a single continuous area was formed. The variation was due to the narrow width of the core where substrate was placed and the size of the oyster shells in the model unit. If the netting design of the prototypes was replicated, the oyster shell would not have been able to completely fill the area as it does in the prototype design.

Figure 13: Model ReefBLK^{SM} with netting material installed.

Oyster shell was used as the substrate in the ReefBLK^{SM} units. The oyster shell was obtained from the Auburn Shellfish Laboratory. The Auburn Shellfish Laboratory provided juvenile eastern oyster, *Crassostrea virginica*, shell which is better suited for filling the narrow space of the model ReefBLK^{SM}. A majority of the oyster shell was preprocessed at the Auburn Shellfish Laboratory by Scott Rickard using a trammel- type sorter obtained from the Chesapeake Bay Oyster Company (Figure 14). The sorter provided oyster shell larger than 1.91 cm (0.75 in) and smaller than 3.81 cm (1.5 in).

Figure 14: Oyster shell being processed through the Chesapeake Bay Oyster Company sorter at the Auburn Shellfish Laboratory.

The ReefBLKs^{SM} were filled with the juvenile oyster shell by placing the unit on a vibratory table and scooping/shoveling the shell into the unit as shown in Figure 15. The ReefBLKs^{SM} were filled in three lifts and additional compacting and shaking was performed between the lifts to ensure the oyster shell did not settle during testing. The average weight of a model ReefBLK^{SM} was 28.6 kg (63.1 lbs) once completed.

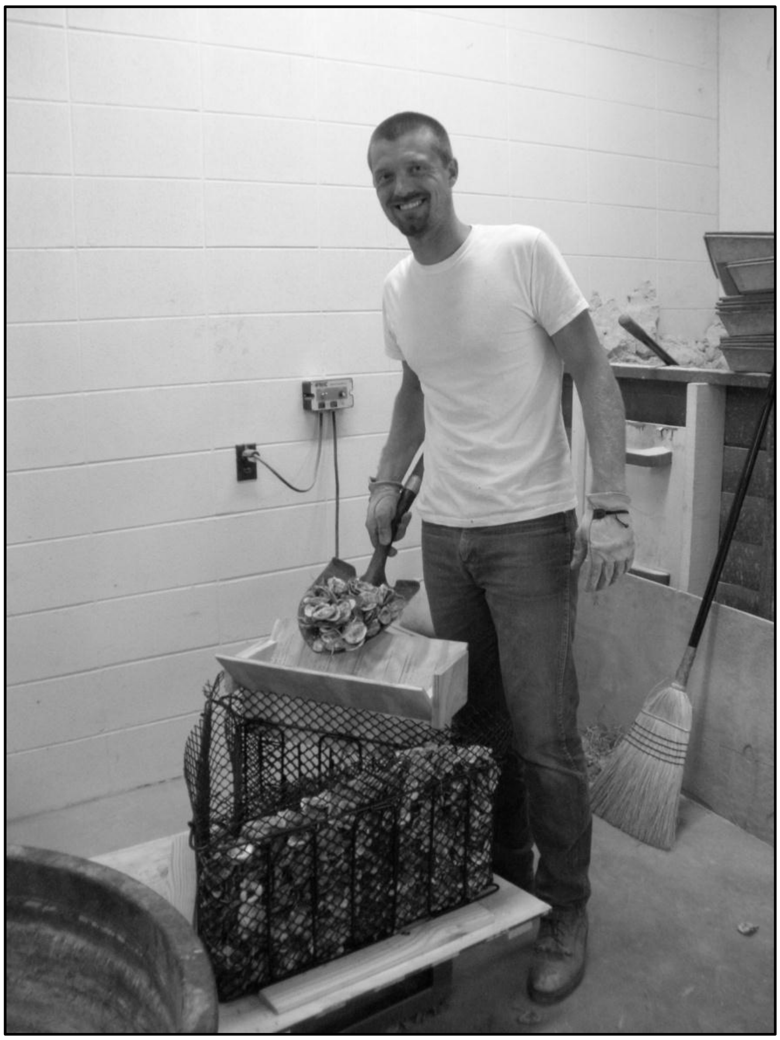

Figure 15: ReefBLK^{SM} being filled with oyster shell using a vibratory table.

ASTM International standard testing was performed on the material to describe the density properties and size distribution. ASTM Standard C 127 was used to calculate the apparent density, which is the density of the solid portion of the oyster shell, and was found to be 2479 kg/m^3 (155 lbs/ft^3). ASTM Standard C 29 was used to determine the bulk density or unit weight of the oyster shell, which was found to be 596 kg/m^3 (37.2 lbs/ft^3). A tabular form of these and additional oyster shell properties is given in Table A3 in Appendix A. Additionally, ASTM Standard C 33 was used to create a gradation curve (Figure 16), to describe the size distribution of the oyster shell. Figure A5 in Appendix A is provided as well to show a visual representation of the variation and shape of the oyster shell tested.

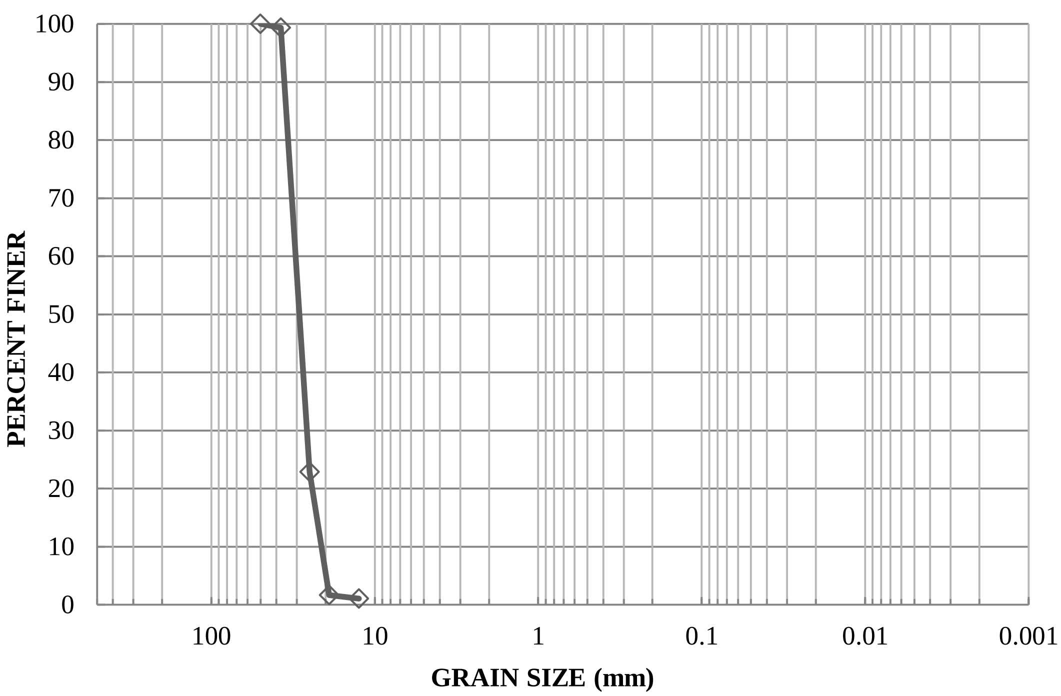

Figure 16: Gradation curve of oyster shell used in model ReefBLK^{SM}.

Testing the ReefBLK^{SM} structure in the wave basin followed a similar testing matrix as the concrete pyramids. Eight combinations of wave height and period (same as those for the concrete pyramids) were tested at five unique water depths producing a total of 40 unique experiments (Table A4 in Appendix A). A summary of the experimental setup is provided in Table 3 and a list of incident wave heights is provided in Table B4 in Appendix B. The control for the ReefBLK^{SM} testing was performed by conducting the 40 unique combinations of water depth and wave characteristics prior to the placement of the structure in the basin; where the average incident wave height, H_i, was measured at the same location as the corresponding average transmitted wave height, H_t.

Table 3: Summary of experimental setup for ReefBLKs^{SM}.

Experimental Setup	
Configurations	Alternating Point
Water Depths	0.20, 0.25, 0.30, 0.36, 0.41 m
Wave Heights	0.05 - 0.20 m
Wave Periods	1 - 3 s
Total Experiments	40

Data Collection

Data collection was conducted in "bursts" to reduce contamination from the reflection of wave energy from the shoreline. Each unique experiment from the testing matrices was performed in three "bursts" After each "burst" the basin was allowed to return to rest. The data used from each “burst” consisted of the first three or four waves that reached the wave gage before the first wave transmitted was able to reach the shore and return to the wave gage. A single factor ANOVA was performed on three of the controls from the ReefBLK℠ testing to verify that running in a burst mode produces statistically similar results. The cases were: wave 1 (H = 0.04 m) at a depth of 0.30 m (12 in), wave 4 (H = 0.10 m) at a depth of 0.30 m (12 in) and wave 7 (H = 0.17 m) at a depth of 0.30 m (12 in). The data input to the ANOVA were obtained from a zero downcrossing routine performed on one gage from each burst. The program provided the wave height of the first three waves. The data from each burst was then compared using an ANOVA. The results from each case showed there was no statistical difference at a 95% confidence interval for all three cases based on $p > 0.05$ and $F \ll F_{critical}$.

Results obtained in all the experiments were facilitated by using two-wire capacitance gages, which measured the water surface elevation (Figure 17). Prior to any testing and controls the gages were calibrated per the manufacturer's instructions. The gages were mounted on a three-legged base capable of being raised and lowered, based on the water level in the wave basin. The wave gages had a 0.51 m (20 in) range and, when placed in the wave basin, the base was adjusted so that the still water level was located at half the range. A sampling rate of 10 Hz was used for all tests and was digitally recorded using a program created by National Instruments called LabView. All data recorded by the program was exported to Microsoft Excel for analysis.

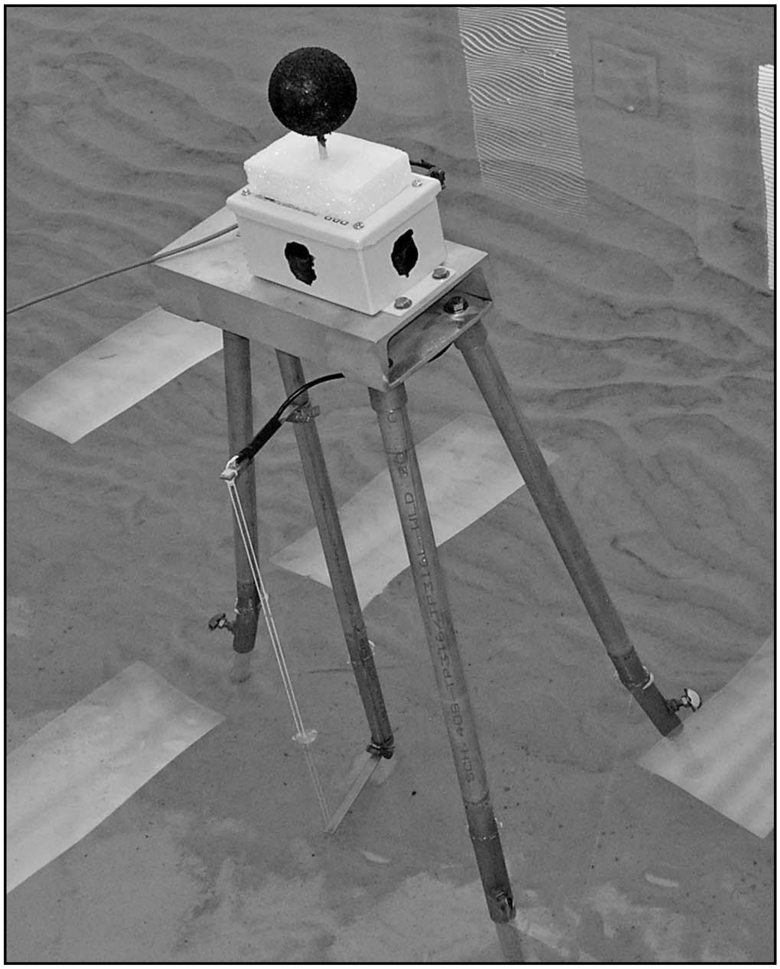

Figure 17: Two-wire capacitance gage used for measuring the water surface elevation within a range of 0.51 m (20 in).

The data for each "burst" was visually inspected and cropped to include three to five consecutive waves after the first wave propagated past the wave gage. The resulting time series was analyzed using a zero downcrossing technique, which provided the root-mean-square wave height, H_{rms}, average wave height, H_{avg}, average wave period, T_z, and number of waves analyzed, N. This data was filtered to remove any discrepancies due to outputs containing less than three waves and wave profiles containing external noise.

RESULTS

The testing objective was to determine the transmission coefficient for oyster shell bag breakwaters, concrete pyramids, and ReefBLKs^{SM} ,which is provided in the following section and all the raw testing data is provided in Appendix B. The results shown are given in meters, where applicable, and follow the testing matrix experiment numbers provided for each technology from the methodology.

Bagged Oyster Shell

Bagged oyster shell results are presented in the following two tables with respect to the incident wave height. Transmission coefficients for a RMS incident wave height of 0.10 m (0.301 ft), a period of 1.34 sec, and a wave length of 2.17 m (6.60 ft) are presented in Table 4; providing a total of 36 unique experiments. Transmission coefficients for a RMS incident wave height of 0.17 m (0.524 ft), a period of 2.03 sec, and a wave length of 3.51 m (10.7 ft) are given in Table 5; providing a total of seven unique experiments.

Table 4: Bagged oyster shell wave transmission coefficients for a RMS incident wave height of 0.10 m (0.30 ft) and a wave period of 1.34 sec. Physical dimensions are in meters and water depth is a constant 0.30 m (12 in).

Crest Width, B	Structure Height, h_c	Transmission Coefficient, K_t
0.38	0.08	0.97
0.84	0.09	0.92
1.30	0.08	0.89
1.62	0.09	0.84
1.89	0.09	0.78
0.60	0.09	0.91
0.41	0.17	0.87
0.83	0.16	0.85
1.30	0.16	0.78
1.62	0.17	0.72
1.93	0.16	0.61
0.61	0.17	0.88
0.41	0.24	0.78
0.84	0.24	0.59
1.30	0.23	0.60
1.60	0.23	0.47
1.93	0.23	0.34
0.61	0.23	0.63

Crest Width, B	Structure Height, h_c	Transmission Coefficient, K_t
0.41	0.29	0.46
0.89	0.31	0.11
1.30	0.30	0.05
1.61	0.29	0.02
1.96	0.30	0.11
0.61	0.30	0.16
0.43	0.36	0.15
0.89	0.37	0.06
1.30	0.36	0.39
1.60	0.37	0.24
1.96	0.37	0.01
0.61	0.36	0.09
0.42	0.43	0.12
0.89	0.45	0.05
1.32	0.42	0.31
1.62	0.42	0.14
1.96	0.45	0.06
0.61	0.43	0.08

Table 5: Bagged oyster shell wave transmission coefficients for a RMS incident wave height of 0.17 m (0.52 ft) and a wave period of 2.03 sec. Physical dimensions are in meters and water depth is a constant 0.30 m (12 in).

Crest Width, *B*	**Structure Height, h_c**	**Transmission Coefficient, K_t**
1.96	0.30	0.09
0.61	0.30	0.36
1.96	0.37	0.02
0.61	0.36	0.14
1.62	0.42	0.06
1.96	0.45	0.03
0.61	0.43	0.10

The results from Table 3 and Table 4 are applied to the graph in Figure 18 which shows the relationship between the non-dimensional height, h_c/d, the ratio of the structure height to the water depth, and the experimental transmission coefficient, K_t. Furthermore, the bagged oyster shell experimental K_t values obtained from all the unique experiments in Table 4 and Table 5 are shown in Figure 19 utilizing a two-dimensional space as a function of the non-dimensional height, h_c/d, and the non-dimensional length, B/L_i, which is the ratio of the crest width to incident wave length.

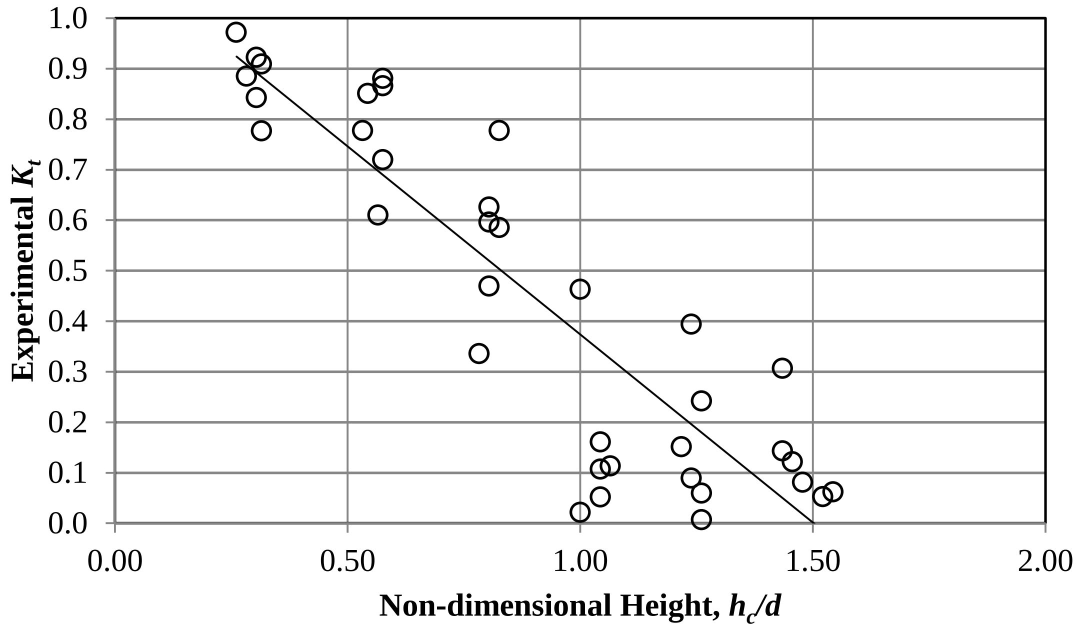

Figure 18: Relationship of non-dimensional height, h_c/d, versus the measured wave transmission coefficient, K_t, for all unique experiments tested with the bagged oyster shell.

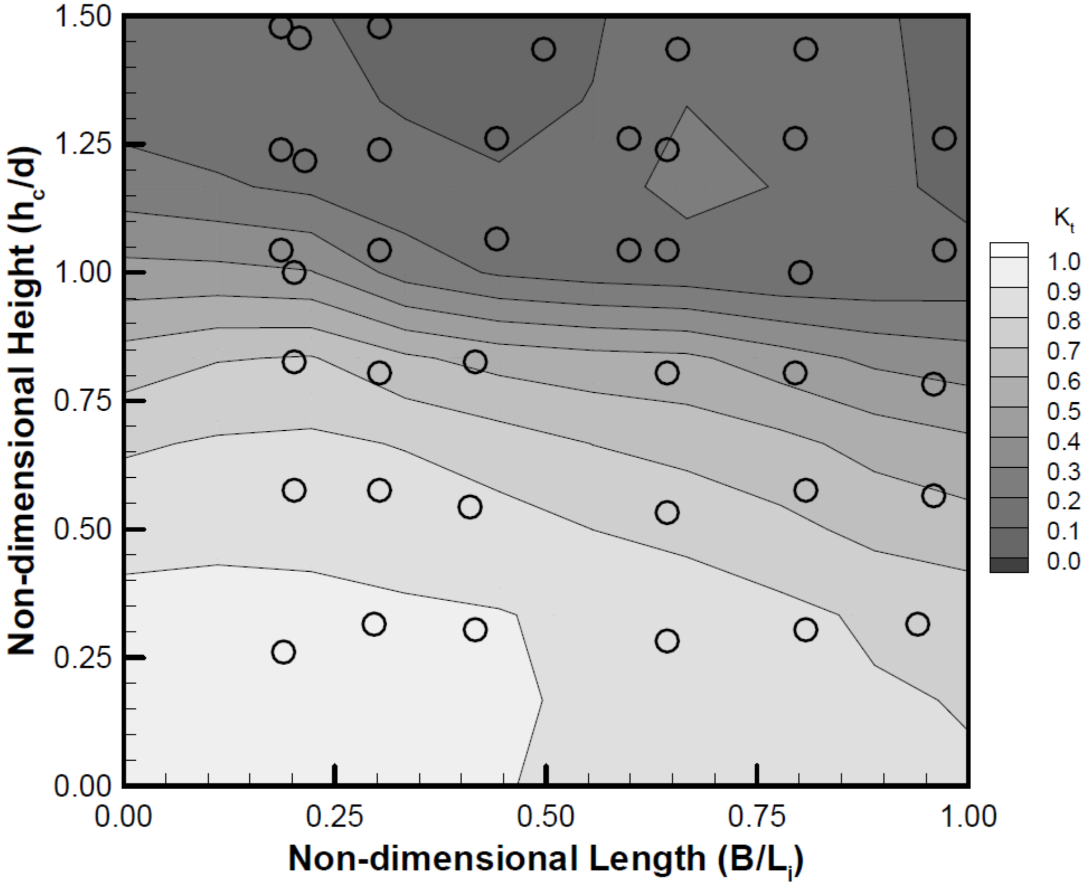

Figure 19: Two-dimensional graph showing the variation of the bagged oyster shell experimental K_t values as a function of the non-dimensional structure height and length. Open symbols (○) represent discrete data points used for interpolating contours.

Concrete Pyramids

Concrete pyramid wave transmission coefficients are provided in Table 6 and Table 7. Experimental results with "N/A" indicate that test data is insufficient due to lack of data or inconsistent values. Experimental transmission coefficients for the single row configuration as a function of the water depth and incident wave properties are given in Table 6 and associated with the experiment number provided in Table A1 of Appendix A.

Experimental transmission coefficients obtained from the offset double row configuration of concrete pyramids as a function of the water depth and incident wave properties are given in Table 7 and associated with the experiment number provided in Table A2 of Appendix A.

Table 6: Concrete pyramid measured wave transmission coefficients obtained for the single row configuration as a function of the non-dimensional length and height. Structure crest width, *B*, is a constant 0.25 m (10 in) and structure height, h_c, is a constant 0.30 m (12 in). Wave length is calculated using small amplitude wave theory.

Experiment Number	B/L_i	h_c/d	K_t	Experiment Number	B/L_i	h_c/d	K_t
1	0.16	1.50	0.82	21	0.14	1.00	0.79
2	0.09	1.50	0.55	22	N/A	N/A	N/A
3	0.18	1.50	0.52	23	0.09	1.00	0.53
4	0.12	1.50	0.50	24	0.07	1.00	0.64
5	0.19	1.50	0.46	25	0.11	0.86	0.85
6	N/A	N/A	N/A	26	0.07	0.86	0.94
7	0.11	1.50	0.36	27	0.14	0.86	0.84
8	0.08	1.50	0.52	28	0.09	0.86	0.69
9	0.13	1.20	0.56	29	0.13	0.86	0.92
10	0.07	1.20	0.59	30	N/A	N/A	N/A
11	0.15	1.20	0.71	31	0.08	0.86	0.69
12	0.10	1.20	0.56	32	0.06	0.86	0.71
13	0.15	1.20	0.70	33	0.11	0.75	0.91
14	N/A	N/A	N/A	34	0.07	0.75	0.92
15	0.10	1.20	0.42	35	0.12	0.75	0.95
16	0.07	1.20	0.63	36	0.08	0.75	0.78
17	0.12	1.00	0.75	37	0.13	0.75	1.05
18	0.08	1.00	0.74	38	N/A	N/A	N/A
19	0.15	1.00	0.72	39	0.08	0.75	0.84
20	0.09	1.00	0.69	40	0.06	0.75	0.79

Table 7: Concrete pyramid measured wave transmission coefficients obtained for the offset double row configuration as a function of the non-dimensional length and height. Structure crest width, *B*, is a constant 1.04 m (41 in) and structure height, h_c, is a constant 0.30 m (12 in). Wave length is calculated using small amplitude wave theory.

Experiment Number	B/L_i	h_c/d	K_t	Experiment Number	B/L_i	h_c/d	K_t
41	0.64	1.50	0.46	61	0.58	1.00	0.72
42	0.38	1.50	0.49	62	N/A	N/A	N/A
43	0.76	1.50	0.47	63	0.37	1.00	0.48
44	0.48	1.50	0.37	64	0.28	1.00	0.53
45	0.77	1.50	0.27	65	0.47	0.86	0.95
46	N/A	N/A	N/A	66	0.29	0.86	0.65
47	0.44	1.50	0.35	67	0.56	0.86	0.72
48	0.33	1.50	0.25	68	0.36	0.86	0.66
49	0.55	1.20	0.55	69	0.53	0.86	0.87
50	0.30	1.20	0.62	70	N/A	N/A	N/A
51	0.62	1.20	0.66	71	0.34	0.86	0.62
52	0.42	1.20	0.49	72	0.26	0.86	0.61
53	0.60	1.20	0.61	73	0.45	0.75	0.92
54	N/A	N/A	N/A	74	0.27	0.75	0.88
55	0.40	1.20	0.44	75	0.51	0.75	1.10
56	0.30	1.20	0.39	76	0.34	0.75	0.85
57	0.50	1.00	0.62	77	0.54	0.75	1.10
58	0.31	1.00	0.51	78	N/A	N/A	N/A
59	0.60	1.00	0.67	79	0.33	0.75	0.77
60	0.39	1.00	0.54	80	0.25	0.75	0.67

From the data presented in Table 6 and Table 7 for the concrete pyramids, the graph in Figure 20 was produced showing the non-dimensional height, h_c/d, versus the measured transmission coefficient, K_t. The non-dimensional length, B/L_i, versus the measured transmission coefficient, K_t, with respect to the individual wave characteristics tested for the single row and offset double row configuration of concrete pyramids is plotted in Figures 21 and 22. Additionally, the variation of the measured transmission coefficient, K_t, as a function of the non-dimensional height, h_c/d, and the non-dimensional length, B/L_i, is shown in Figure 23 and 24 as a two-dimensional graph for the single row and offset double row configurations, respectively.

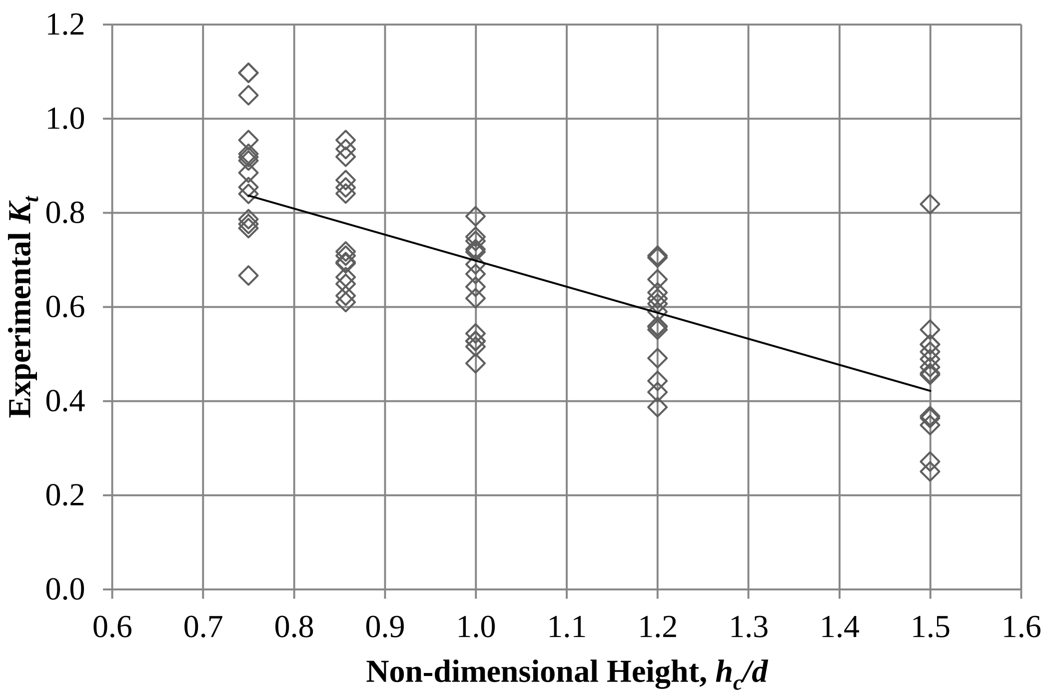

Figure 20: Relationship of the non-dimensional height, h_c/d, to wave transmission coefficients, K_t, obtained for the concrete pyramid single row and offset double row configurations.

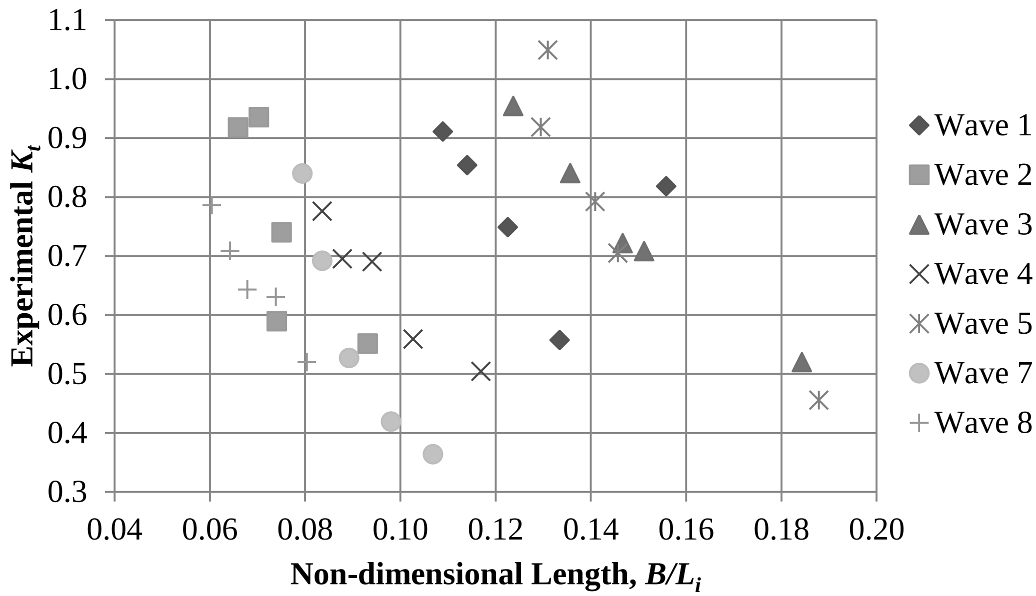

Figure 21: Non-dimensional length, B/L_i, versus measured wave transmission coefficients, K_t, for single row configuration of concrete pyramids.

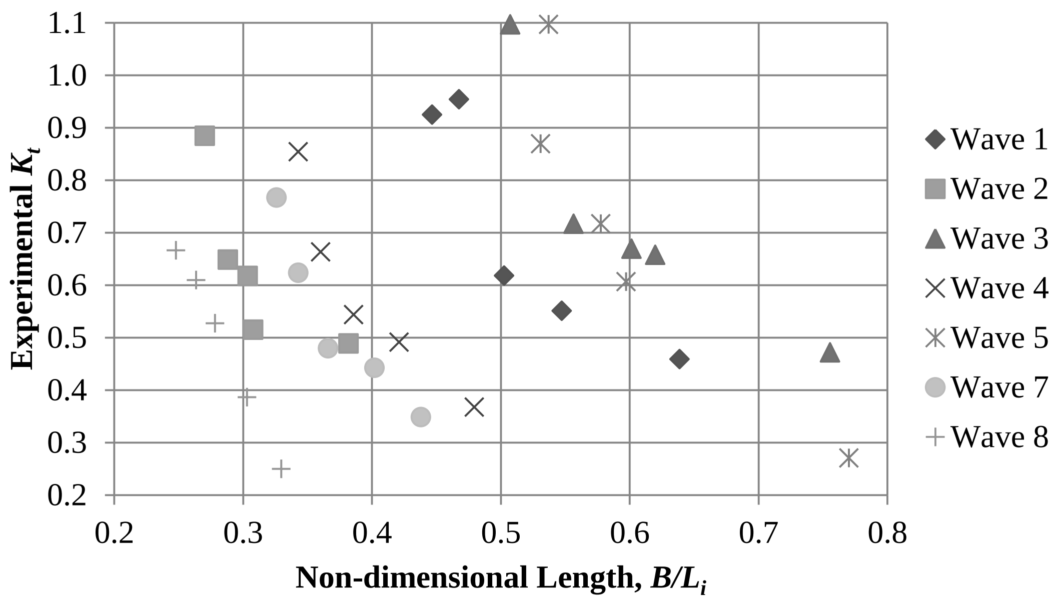

Figure 22: Non-dimensional length, B/L_i, as a function of measured wave transmission coefficients, K_t, for offset double row configuration of concrete pyramids.

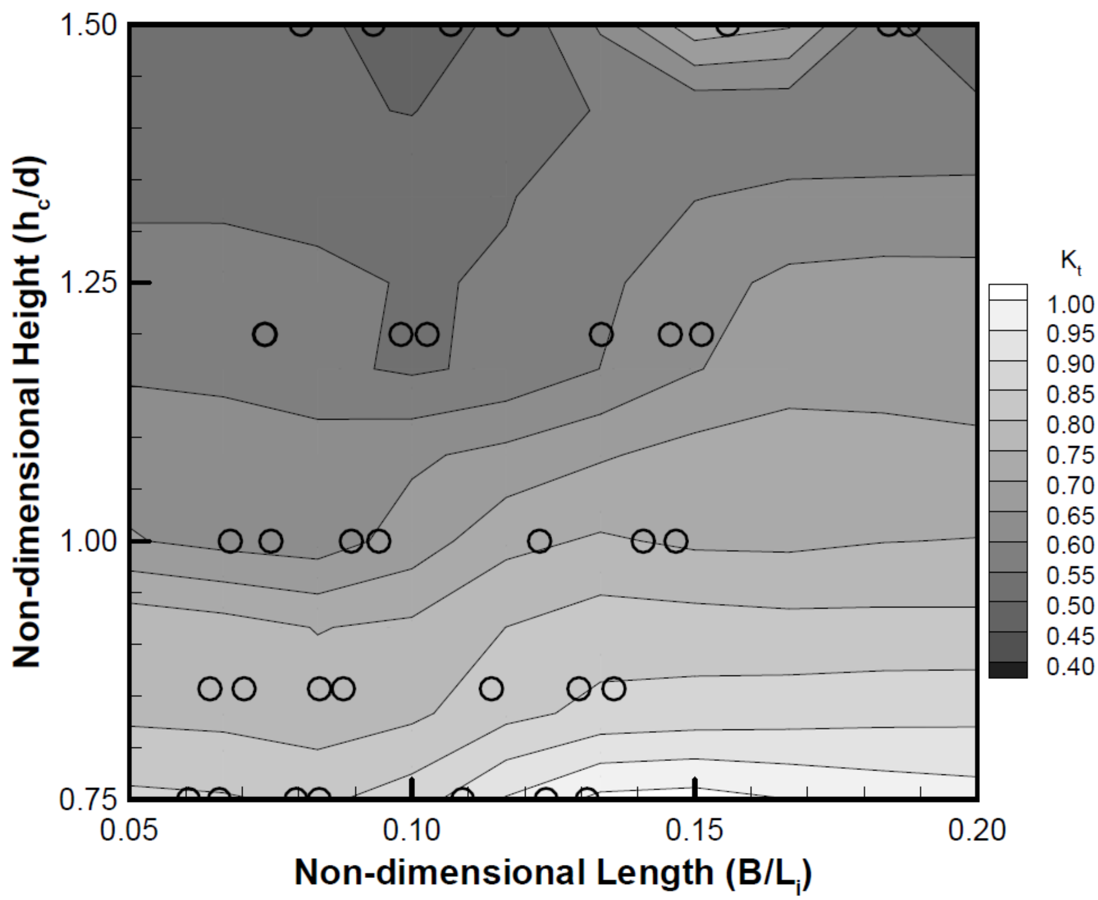

Figure 23: Two-dimensional plot of measured wave transmission coefficients, as a function of the non-dimensional height and length, for concrete pyramids in a single row configuration. Open symbols (○) represent discrete data points used for interpolating contours.

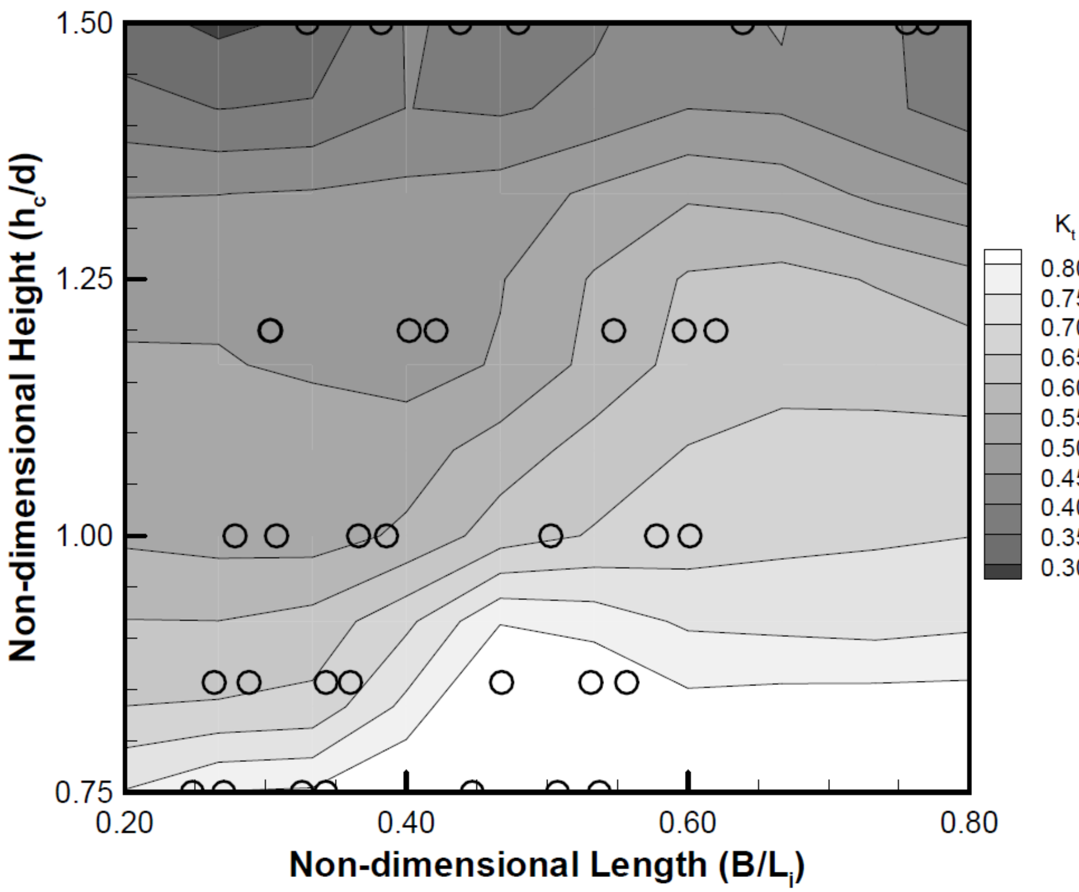

Figure 24: Two-dimensional plot of measured wave transmission coefficients, as a function of the non-dimensional height and length, for concrete pyramids in an offset double row configuration. Open symbols (○) represent discrete data points used for interpolating contours.

<u>ReefBLK^{SM}</u>

ReefBLK^{SM} measured wave transmission coefficient results are presented in Table 8. Experimental results with "N/A" indicate that test data is insufficient due to lack of data or inconsistent values. The values are organized by experiment number referenced from the testing matrix provided in Table A4 in Appendix A. Additionally, the non-dimensional length, B/L_i, and height, h_c/d, associated with the experimental K_t values are given.

Table 8: ReefBLK^{SM} measured wave transmission coefficients as a function of the non-dimensional length and height, organized by experiment number. Structure crest width, *B*, is a constant 1.32 m (52 in) and structure height, h_c, is a constant 0.30 m (12 in). Wave length is calculated using small amplitude wave theory.

Experiment Number	B/L_i	h_c/d	K_t
81	0.75	1.50	0.62
82	0.44	1.50	0.61
83	1.03	1.50	0.46
84	0.58	1.50	0.49
85	0.97	1.50	0.48
86	N/A	N/A	N/A
87	N/A	N/A	N/A
88	N/A	N/A	N/A
89	0.69	1.20	0.62
90	0.39	1.20	0.69
91	0.90	1.20	0.46
92	0.53	1.20	0.45
93	0.92	1.20	0.45
94	N/A	N/A	N/A
95	N/A	N/A	N/A
96	0.37	1.20	0.62
97	0.64	1.00	0.62
98	0.36	1.00	0.68
99	0.83	1.00	0.54
100	0.50	1.00	0.55

Experiment Number	B/L_i	h_c/d	K_t
101	0.88	1.00	0.58
102	N/A	N/A	N/A
103	0.47	1.00	0.72
104	0.34	1.00	0.70
105	0.61	0.86	0.74
106	0.35	0.86	0.77
107	0.76	0.86	0.67
108	0.46	0.86	0.69
109	0.84	0.86	0.64
110	N/A	N/A	N/A
111	0.43	0.86	0.73
112	0.33	0.86	0.64
113	0.57	0.75	0.83
114	0.34	0.75	0.82
115	0.78	0.75	0.61
116	0.43	0.75	0.81
117	0.79	0.75	0.73
118	N/A	N/A	N/A
119	0.41	0.75	0.80
120	0.31	0.75	0.79

Using the data presented in Table 8 the graph in Figure 25 was produced showing the relationship of the non-dimensional height, h_c/d, and the measured transmission coefficient, K_t. A plot of the non-dimensional length, B/L_i, versus the measured wave transmission coefficient, K_t, produced from the data given in Table 8 with respect to each unique wave characteristic is provided in Figure 26. Additionally, the data from Table 8 are used to produce a two-dimensional plot, which shows the measured transmission coefficient, K_t, as a function of the non-dimensional height, h_c/d, and the non-dimensional length, B/L_i (Figure 27).

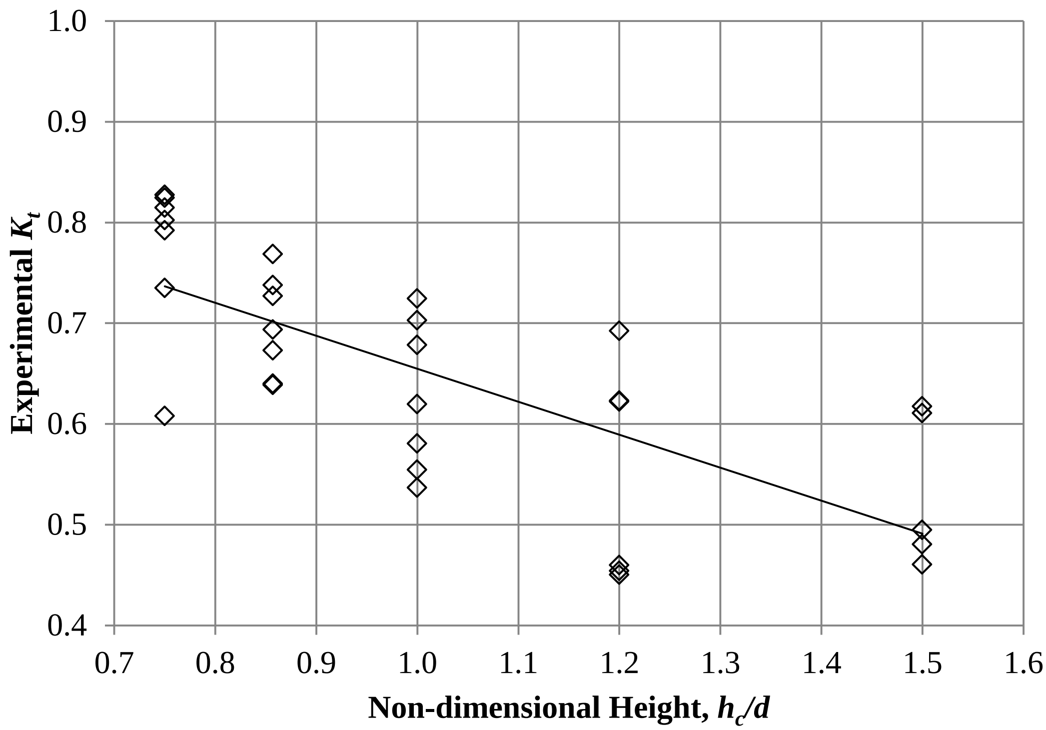

Figure 25: Graph showing the non-dimensional height, h_c/d, versus the measured transmission coefficient, K_t, for all tests performed on the ReefBLK^{SM} units. The solid line is a linear regression of the data.

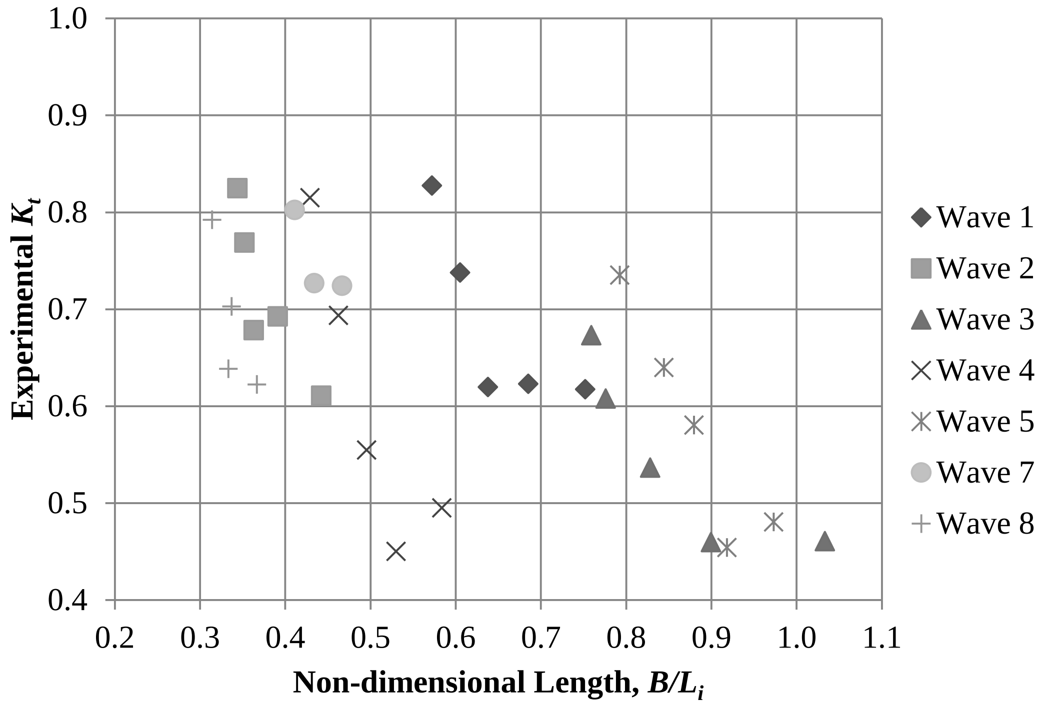

Figure 26: Graph showing the non-dimensional length, B/L_i, as a function of the measured transmission coefficient, K_t, for all tests performed on the ReefBLK^{SM} units with respect to each unique wave characteristic.

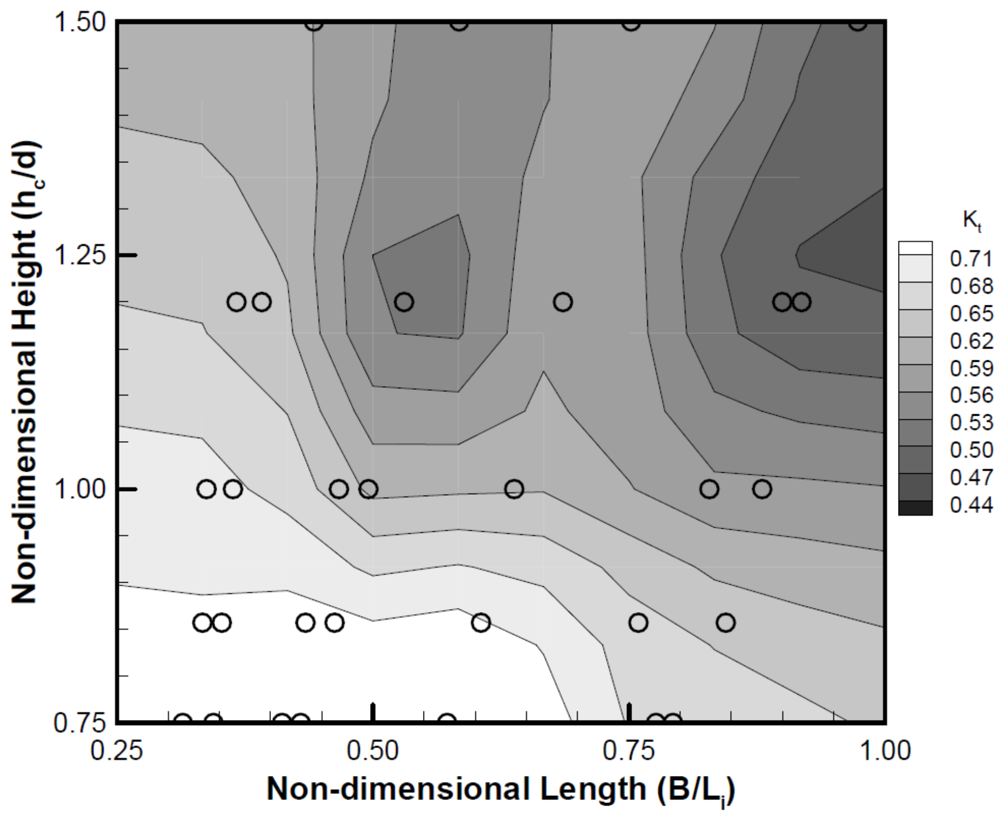

Figure 27: Two-dimensional plot of the measured wave transmission coefficient, K_t, for the ReefBLK^{SM} units as a function of the non-dimensional length and height. Open symbols (○) represent discrete data points used for interpolating contours.

Additional Testing Observations

In addition to the results obtained for the objective, other notable observations were made during testing. When performing the concrete pyramid testing for the offset double row configuration, the second row of units moved approximately 0.10 m (4 in) during experiment 80 and 0.03 m (1.5 in) during experiment 79. The units were relocated after every burst to minimize bias. Before anchoring the ReefBLK^{SM} units to the basin floor the units shifted by as much as 0.91 m (36 in) during all tests conducted in 0.41 m (16 in) of water. All ReefBLK^{SM} experiments performed before anchoring the units were discarded and re-run after anchoring.

DISCUSSION

Bagged Oyster Shell

The results obtained from testing were compared to published methodologies for estimating transmission coefficients of rubble mound breakwaters. The transmission coefficients of the structures tested were calculated using the formulae described by Van der Meer et al. (2005) and summarized in the literature review section. These coefficients were then compared to the transmission coefficients determined from the test data in Table 4 and Table 5 by using a one-to-one graph (Figure 28).

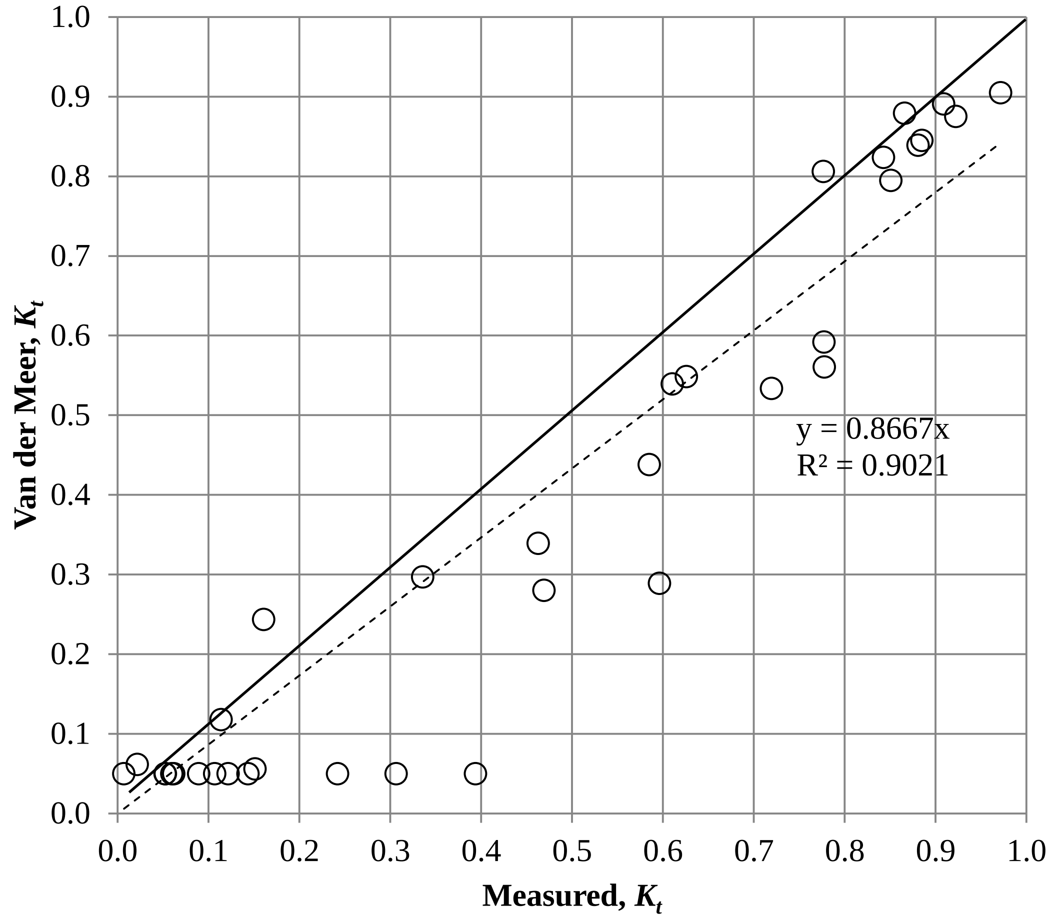

Figure 28: A comparison of measured and predicted transmission coefficients using the predictive equations of Van der Meer et al. (2005) for bagged oyster shell. Open symbols (o) represent measured data, the dashed line is a linear regression with a zero intercept, and the dark solid line represents perfect agreement.

There are similarities in the comparison of the measured and predicted values of the transmission coefficient (Figure 28). With a slope of approximately one, the Van der Meer et al. (2005) equation is shown to be adequate in estimating the wave height attenuation of a bagged oyster shell breakwater. However, the predicted K_t values from Van der Meer et al. (2005) are an under estimate from the measured values obtained through testing (Figure 28). This could be a result of the porosity of the bagged oyster shell breakwaters being different than the rubble breakwaters used in the Van der Meer et al. (2005) tests. Implications of the Van der Meer et al. (2005) formulae underestimating the transmission coefficients can result in designs that do not meet the expected goals. Also shown in the graph is the product of the forced lower limit of the Van der Meer et al. (2005) equations. Based on the research performed by Van der Meer et al. (2005), the equations are no longer valid for predicting K_t, once the freeboard of the structure becomes positive. Through the limited testing performed during this research it is also obvious that predicting K_t becomes difficult once the freeboard becomes positive (Figure 19). As the dimensionless freeboard, h_c/d, becomes larger the data become skewed. The skew is likely due to outside variables affecting the transmissive properties of the structure. As the freeboard becomes larger, the transmissive properties of the structure become more reliant on factors such as run up and overtopping which are not accounted for in the predictive equations given by Van der Meer et al. (2005).

Concrete Pyramids

The results obtained for the concrete pyramids do not show any inclusive resemblance to published methodologies. A one-to-one graph of the transmission coefficients for the single row concrete pyramid configuration results in Table 6 and the transmission coefficients obtained from the Van der Meer et al. (2005) formulae is shown in Figure 29.

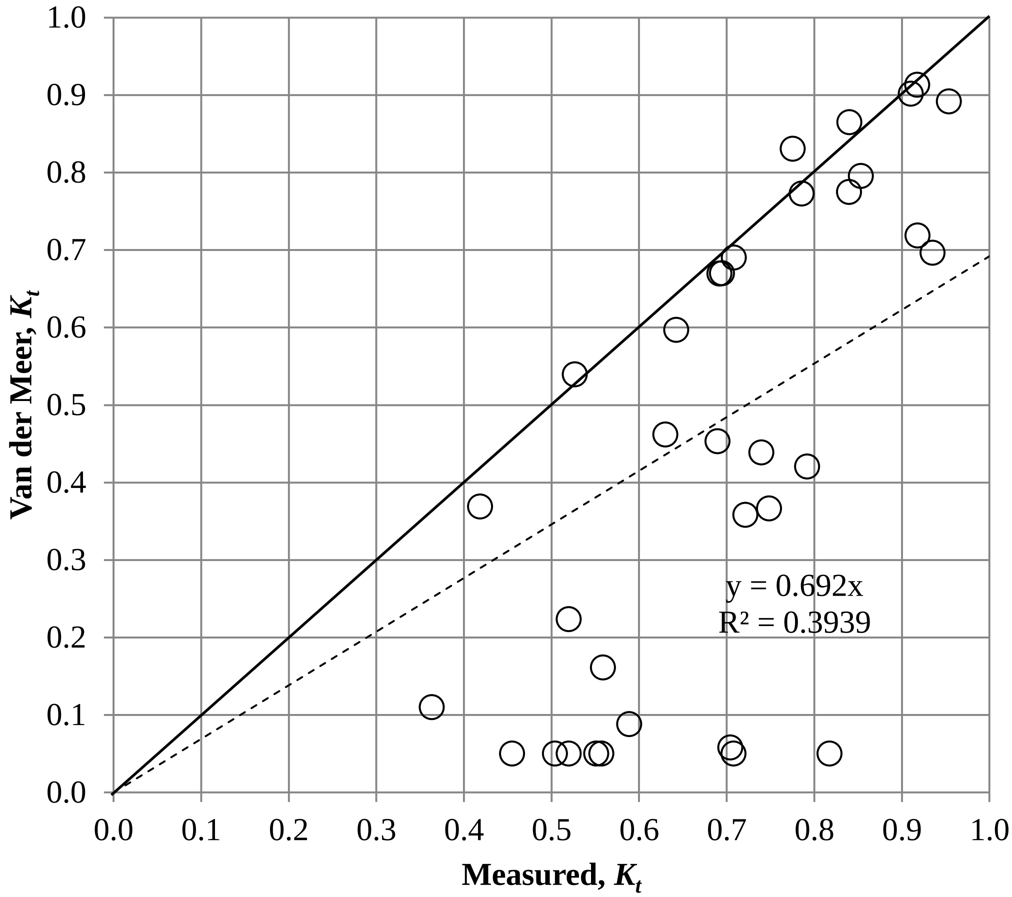

Figure 29: Graph showing the single row concrete pyramid transmission coefficient results compared to the transmission coefficients obtained using the Van der Meer et al. (2005) formulae. Open symbols (o) represent measured data, the dashed line is a linear regression with a zero intercept, and the solid line represents perfect one-to-one agreement.

The Van der Meer et al. (2005) formulae are not sufficient for predicting the wave transmission coefficients of the single row concrete pyramid configuration, based on the slope and distribution of the data points (Figure 29). However, the Van der Meer et al. (2005) formulae do show agreement for cases where the ratio of the incident wave height, H_i, to incident wave length, L_i, is greater than 0.04, (Figure 30).

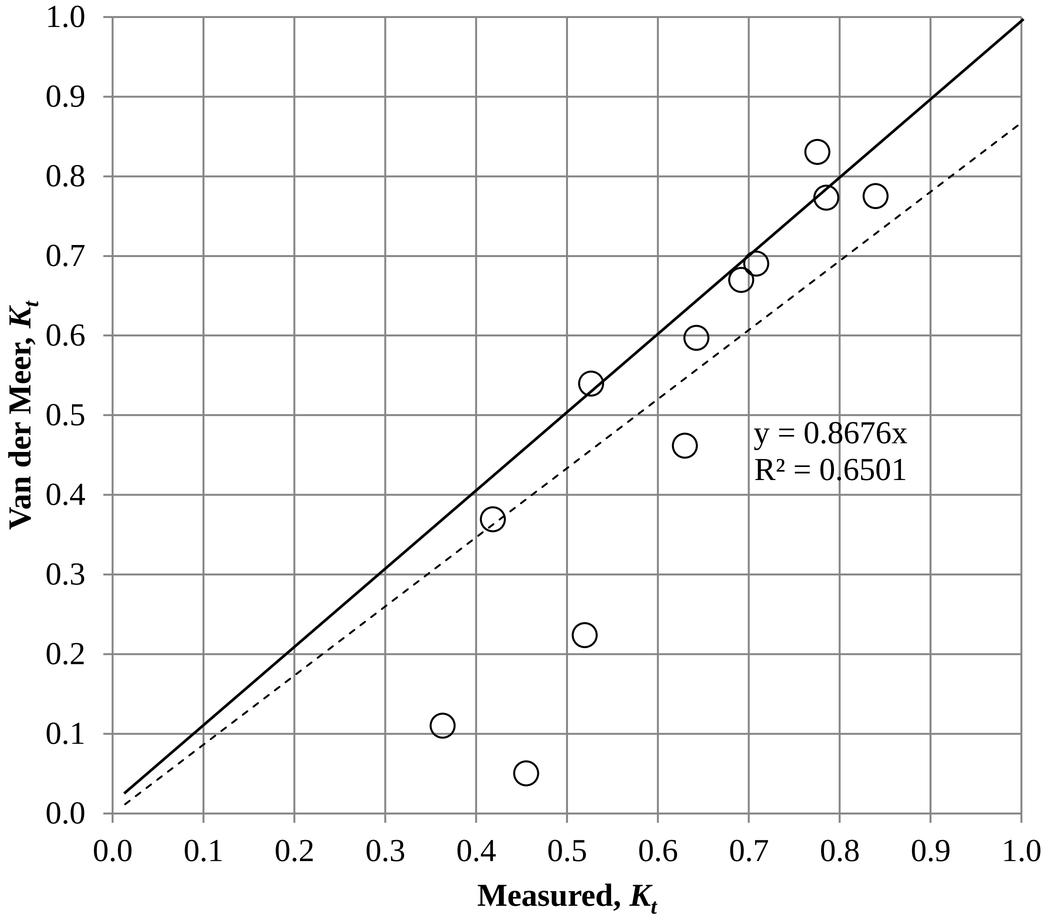

Figure 30: One-to-one comparison of measured transmission coefficients to transmission coefficients computed using the Van der Meer et al. (2005) formulae for cases where H_i/L_i is greater than 0.04 for the single row concrete pyramids. The dashed line is a linear regression with a zero intercept, and the solid line represents perfect one-to-one agreement.

With the slope of the linear regression line approximately one, the predictive equations published by Van der Meer et al. (2005) are sufficient in estimating the transmissive properties of the single row configuration of concrete pyramids for incident waves where H_i/L_i is greater than 0.04 (Figure 30). The variations observed for the cases of $H_i/L_i < 0.04$ is due to the wave interaction with the crests of the structures, based on observations made during testing.

Observations made during testing show the waves diffracting as they contact the structure, leading to reflection of the waves off the side of the structure, and ultimately steepening the subsequent wave as it passes between the crests of the structures resulting in a transmitted wave greater than that predicted by the Van der Meer et al. (2005) formulae. This is confirmed by the comparison made in Figure 29 where the measured wave transmission coefficient in all cases is greater than the wave transmission coefficient calculated using the Van der Meer et al. (2005) formulae. However, the interaction of the incident wave and the structure geometry is lessened as the freeboard decreases and is not identifiable once the freeboard becomes less than zero (e.g. the structure is fully submerged), resulting in the Van der Meer et al. (2005) formulae being valid for cases of $H_i/L_i > 0.04$ and cases where the freeboard is less than zero.

The comparison of Van der Meer et al. (2005) computed transmission coefficients and measured transmission coefficients from Table 7 for the offset double row configuration is shown in Figure 31. Based on the slope of the linear regression line being much less than one, the Van der Meer et al. (2005) formulae are not accurate and, furthermore, are over predictive of the wave attenuation for offset double row concrete pyramid breakwaters. However, segmented data for cases where $H_i/L_i > 0.04$, as done for the single row configuration, shows similarity between the measured wave transmission coefficients and wave transmission coefficients computed using the Van der Meer et al. (2005) formulae (Figure 32). Contrary to the single row configuration, when the freeboard is less than zero the Van der Meer et al. (2005) are not valid. Based on observations during testing of the offset double row configuration of concrete pyramids for freeboards less than zero, the incident wave broke over the first row and crashed into the second row. The interaction with the second row of units is not accounted for in the Van der Meer et al. (2005) formulae since they are based on a trapezoidal profile.

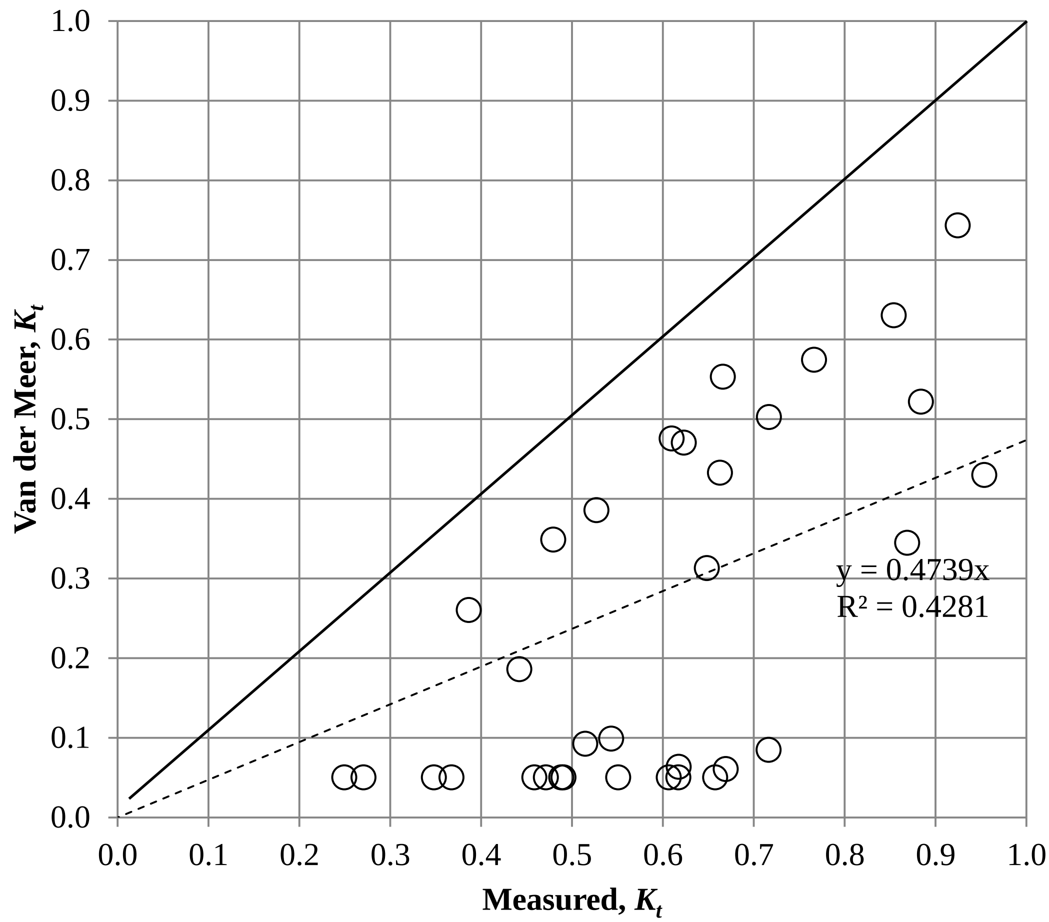

Figure 31: Graph showing a one-to-one comparison of the measured wave transmission coefficients and the computed wave transmission coefficients using the Van der Meer et al. (2005) formulae for the offset double row configuration of concrete pyramids. Open symbols (o) represent measured data, the dashed line is a linear regression with a zero intercept, and the solid line represents perfect one-to-one agreement.

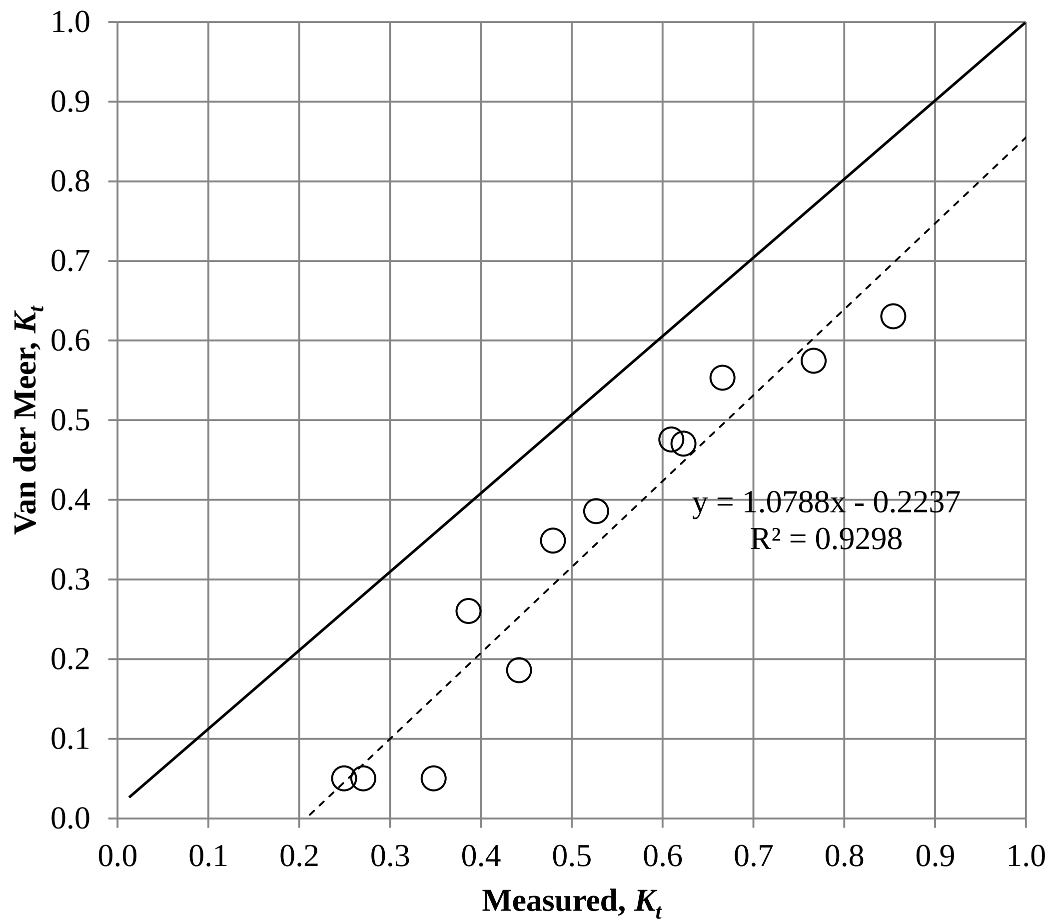

Figure 32: Segmented wave transmission coefficient data for H_i/L_i > 0.04 showing a one-to-one agreement with the computed wave transmission coefficients using Van der Meer et al. (2005) formulae for the offset double row configuration of concrete pyramids. Open symbols (o) represent measured data, the dashed line is a linear regression, and the solid line represents perfect one-to-one agreement.

The slope of the linear regression line is approximately one in Figure 32; however, the linear regression line is offset from the line representing the perfect one-to-one agreement by 0.22. In other terms the predictive formulae of Van der Meer et al. (2005) results in a value of 0.22 less than the measured transmission coefficient.

The relationship between the measured transmission coefficient, K_t, as a function of the non-dimensional height, h_c/d, and width, B/L_i, for the single row (Figure 23) and offset double row (Figure 24) configuration of concrete pyramids shows a distinguishable increase in wave energy dissipation as the non-dimensional height, h_c/d, increases. The trend of transmitted wave height reduction is non-linear with respect to the non-dimensional height, h_c/d. When h_c/d is less than one, the rate of change of the transmission coefficient is higher than when h_c/d is greater than one. However, an exception to this trend is when the non-dimensional length, B/L_i, is greater than 0.45. As B/L_i increases greater than 0.45 the non-dimensional height, h_c/d, must increase at a higher rate to achieve the same wave attenuating properties.

The transmission coefficient is directly related to the dimensionless width, unlike the bagged oyster shell two-dimensional relationship (Figure 19) and the common conception that wave energy dissipation increases with dimensionless width for traditional rubble mound breakwaters as shown in the body of knowledge (Seelig 1980; Seebrook and Hall 1998; Van der Meer et al. 2005). The decrease in wave height reduction with respect to dimensionless width (Figures 23 and 24) is a function of the processes within the composite structure as previously mentioned. The incident wave diffraction and reflection within the structure steepens the wave resulting in an increase in wave height on the leeward side of the structure, based on observations made during testing. The amount of reflected wave energy transferred to the subsequent incident wave decreases as the wave length increases. In other terms, the wave energy stored in the structure has time to dissipate before the next wave reaches the structure. The trend of the wave transmission coefficient, K_t, increasing as the non-dimensional length, B/L_i, increases is true for the single row and the offset double row configuration of concrete pyramids.

ReefBLK℠

The wave transmission results obtained for the ReefBLKs℠ cannot be compared to the same published methodologies as used for the bagged oyster shell and the concrete pyramids due to the unique cross-sectional profile of the composite structure. Additionally, comparison to other published literature for Reef Balls™ (Armono and Hall 2003) and Jeffreys (1944) formulae for rectangular profiles obtained from Rageh (2009) failed to produce any definitive correlation. However, when modifying the Armono and Hall (2003) formula (Equation 6) from the literature review, a weak agreement is produced.

To modify the equation for ReefBLKs℠, the ratio of the structure height to crest width is removed since it is a constant when using the standard prototype ReefBLK℠ units in the common design alternating point configuration, as used in the testing performed in this study. The final equation developed for the ReefBLKs℠ is shown in Equation 7.

$$K_t = 1.3 - 25\frac{H_i}{gT^2} - \frac{{h_c}^{1.5}}{d} \qquad \text{(Eq. 7)}$$

Applying the modified Armono and Hall (2003) equation to the 40 experiments performed in this study produces a R^2 value of 0.621 when forcing a y-intercept of zero for the linear regression line (Figure 33).

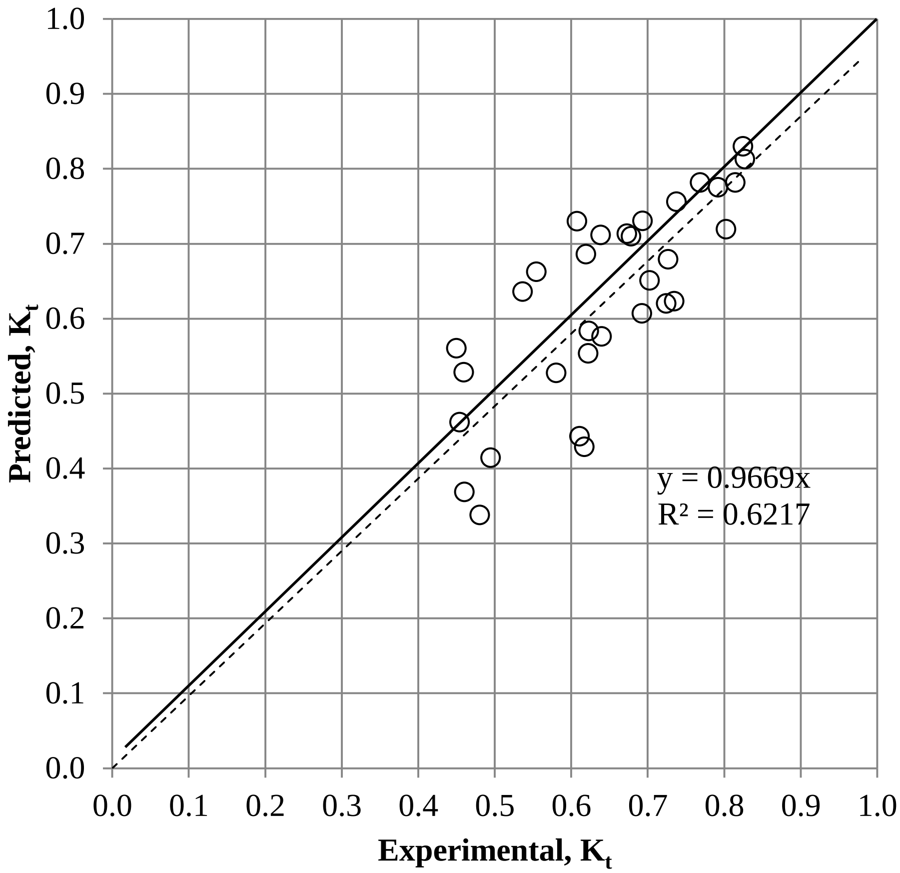

Figure 33: Comparison of the experimental wave transmission coefficient with the predicted wave transmission coefficient in a one-to-one graph using modified Armono and Hall (2003) formula. Open symbols (o) represent measured data, the dotted line represents a linear regression line of the data and the solid line represents a perfect one-to-one agreement.

Predicting the wave transmission coefficient for the ReefBLKs^{SM} using Equation 7 provides an adequate approximation of the wave attenuation characteristics for a breakwater composed of model ReefBLKs^{SM} in the typical design configuration based on the comparison with experimental results (Figure 33). However, the application of this equation to prototype designs has not been confirmed and should be used with caution.

The non-dimensional length, B/L_i, as a function of the experimental transmission coefficient, K_t, with respect to each unique wave characteristic performed (Figure 26) shows that as the water depth, d, decreases the rate of decrease in the wave transmission coefficient is high; however, once the water depth becomes greater than the structure height the rate of decrease becomes much less. More simply stated a small change in water depth, d, has more effect on the wave transmission coefficient when the water depth is greater than the structure height than when the water depth is less than the structure height.

Some general observations can be made as to the behavior of K_t as a function of the non-dimensional height, h_c/d, and length, B/L_i (Figure 27). As the non-dimensional length, B/L_i, increases the transmission coefficient decreases. Considering the structure geometry is constant, essentially as the incident wave length, L_i, decreases, the wave attenuating properties of the structure increase. In the vertical plane, the wave transmission coefficient decreases as the non-dimensional height, h_c/d, increases. Since the structure geometry is constant, the variable in the non-dimensional height is the water depth, d. Hence, as the water depth, d, increases the wave attenuation coefficient, K_t, increases.

Also, for non-dimensional heights less than one, the attenuating capabilities of the structure are less affected by the non-dimensional length (Figure 27). When the non-dimensional length is less than 0.45, the variation of the wave transmission coefficient varies linearly with respect to the non-dimensional height. However, once the non-dimensional height becomes greater than one and the non-dimensional length becomes greater than 0.45, the variation of the wave transmission coefficient does not follow a discernible pattern, but is representative of wave transmission coefficients smaller than 0.60.

Laboratory Scaling

The experiments performed in this study did not follow a specific scale, with respect to the hydrodynamic properties. Hydrodynamic scaling is not necessary due to the dimensionless presentation of the results. Furthermore, the scaling could not be performed given that Froude and Reynolds number scaling would be required. Froude scaling is a function of the gravitational forces which, in water, corresponds to the free surface. Reynolds number scaling is controlled by the viscous forces of the water. Since the structures have forcing components changing from above to below the water line, the scaling would have to be dynamic and would have to change as the water level changed, which is impossible. The only scaling used is the physical dimensions of the units, as stated in the methodology, due to size limitations on the wave basin.

The oyster shell substrate used in the ReefBLKs℠ is reduced from the size used in the prototype units but does not follow any specific scale. Changing the size of the oyster shell substrate affects the porosity of the unit. The porosity of the unit affects the transmissive properties, and the significance of the porosity is a function of the freeboard. As the freeboard decreases (i.e. larger water depth or smaller structure height) the wave transmission due to porosity decreases (Ting et al. 2004; Mizutani and Mostafa 2001). When the transmitted wave height becomes a function of overtopping, the significance of the structure porosity becomes negligible (Ting et al. 2004; Mizutani and Mostafa 2001). Since the majority of engineered reefs are designed to have a structure crest at or below the still wave level, the effects of porosity will be negligible. A comparison of wave transmission coefficients obtained from a project site on the east side of Coffee Island south of Bayou la Batre, Alabama (Digital Engineering, Inc., unpublished report, September 2012) with measured transmission coefficients in the laboratory (Figure 34) confirms the porosity of the ReefBLKs℠ is negligible when the non-dimensional height, h_c/d, is small.

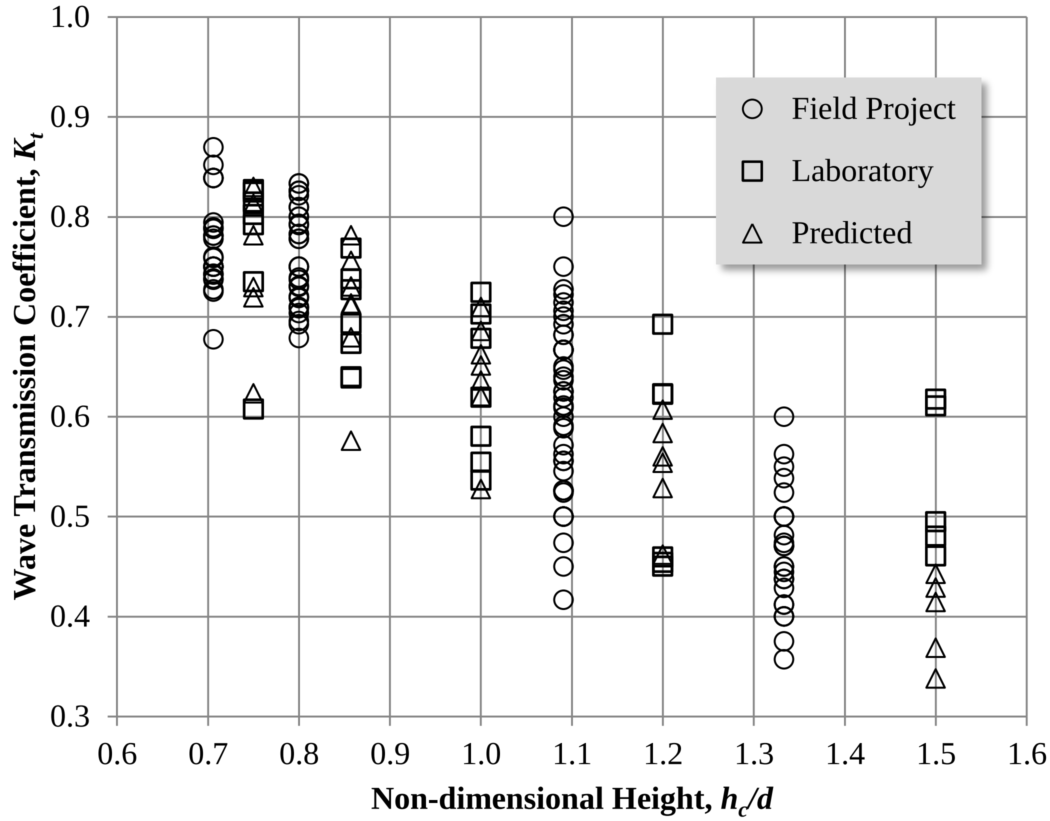

Figure 34: Plot showing the comparison of measured, predicted, and field project wave transmission coefficients, K_t, as a function of non-dimensional height, h_c/d, for the ReefBLK^{SM}.

The laboratory results are similar to the data collected from the field project for h_c/d less than 1.3 (Figure 34). The variance in the h_c/d values greater than 1.3 can be attributed to the porosity; however, field data with h_c/d values greater than 1.33 are not available so the magnitude of the variance cannot be determined. Additionally, the wave transmission coefficients computed using the modified Armono and Hall (2003) equation, applied to the laboratory cases, as a function of the non-dimensional height are shown in Figure 34. Based on the agreement of the computed wave transmission coefficients with those measured in the laboratory and field, application of the modified Armono and Hall (2003) equation to the laboratory scale and prototype design scale is valid within the range tested. An exception to the agreement is when $h_c/d = 1.5$ the computed wave transmission coefficient is less than the measured. The variance of the computed and laboratory wave transmission coefficient values is likely due to the porosity, since the modified equation does not account for porosity. The implications of using the modified Armono and Hall (2003) equation when $h_c/d = 1.5$ could lead to the structure not achieving the design transmitted wave height, ultimately leading to a design failure to stabilize or accrete a leeward shoreline.

CONCLUSIONS

The wave attenuating capabilities of bagged oyster shell, apex-truncated square concrete pyramids, and ReefBLKs^{SM} have distinct characteristics which make each superior for different wave climates and site characteristics. Testing performed in the University of South Alabama wave basin showed that wave attenuation properties for bagged oyster shell, and some cases of concrete pyramids, can be estimated using formulae developed by Van der Meer et al. (2005), while estimating transmissive properties for ReefBLKs^{SM} follows Equation 7. The trends of wave attenuation with respect to the non-dimensional height, h_c/d, and length, B/L_i, are similar to those of rubble mound structures for the bagged oyster shell and ReefBLKs^{SM}; however, the concrete pyramids violate the common conception for wave attenuation with respect to the non-dimensional length.

The attenuating properties for the bagged oyster shell and ReefBLKs^{SM} are most efficient when the structure height is equal to the water depth. As the structure height increases or water depth decreases, for fully submerged structures, an appreciable amount of wave attenuation is achieved; however, once the structure height is greater than the water depth a larger increase in structure height is needed to gain a small increase in wave attenuation. The wave attenuation properties of the concrete pyramids follow more of a linear pattern as the water depth decreases. While similar to the ratio of attenuating properties to non-dimensional height, h_c/d, as the bagged oyster shell and ReefBLKs^{SM}, they differ in that a near-linear relationship of attenuating properties and non-dimensional height is observed for h_c/d greater than one; however, the rate is still less than that observed for h_c/d less than one.

The wave attenuating capacity of the bagged oyster shell and ReefBLKs^{SM} increases as the non-dimensional length, B/L_i, increases. When B/L_i is less than 0.45, little to no appreciable wave attenuation is observed; however, once B/L_i becomes greater than 0.45, the rate of change increases. The concrete pyramids follow an opposite pattern. As B/L_i increases the structures become less effective at attenuating the wave height. The rate of decreasing wave attenuation is nearly exponential. The decrease in wave attenuation as B/L_i increases is valid from $0.10 < B/L_i < 0.60$.

The wave attenuation of all the engineered reefs tested was found to be substantial if properly designed. However, while wave attenuation is the primary goal in the engineering design, other design factors such as placement, wave climate, and bathymetry should not be overlooked. The following list is a summary of all the pertinent results found in this study to consider when designing engineered reefs in terms of wave attenuation.

- Bagged oyster shell breakwaters and concrete pyramids can be designed based on the formulae presented by Van der Meer et al. (2005).
- Estimating wave attenuation for ReefBLKs^{SM} follows Equation 7 modified from Armono and Hall (2003).
- The bagged oyster shell and ReefBLKs^{SM} are better at attenuating short wave lengths.

- The concrete pyramids are more efficient in attenuating long wave lengths
- Anomalies in wave attenuation are present in all engineered reefs when B/L_i is 0.75 and h_c/d is greater than one.
- In general, the primary factor in the success of engineered reefs, used for wave attenuation, is the freeboard of the structure.

RECOMMENDATIONS

While the research presented is adequate for general design estimations, further research should look at the anomalies discovered when B/L_i is equal to 0.75. Additional testing should include more variations in the wave properties, especially for the bagged oyster shell. The trend of B/L_i with respect to the wave transmission coefficient for the concrete pyramids should be investigated to include configurations of more than two rows and the effects of spacing between the rows. Variations in spacing could lead to a "tuning" system for specific wave properties based on design site conditions (e.g. the distance between the rows becomes most effective for a specified wave length). The equation developed for the ReefBLKs℠ should undergo further investigation. Application of this equation to prototype scale has not been confirmed.

REFERENCES

REFERENCES

Adams, M. A. (2002). “Shoreline Structures Environmental Design: A Guide for Structures along Estuaries and Large Rivers.” *Fisheries and Oceans Canada*, Vancouver, BC and *Environment Canada*, Delta, BC.

Ahmadian, A. S. and Simons, R. (2012). “3-D Wave Field around Submerged Breakwaters.” *33rd International Conference on Coastal Engineering*. ASCE, Reston, VA.

Ahmed, M. and Anwar, R. (2011). “Experimental Study on the Performance of Submerged Breakwater as Shore Protection Structure.” International Conference on Environment and BioScience, IACSIT Press, Singapore, 156-160

Ahrens, J. (1984). ”Reef Type Breakwaters.” *19th International Conference on Coastal Engineering*, ASCE, Reston, VA, 2648-2662.

Airoldi, L., Abbiati, M., Beck, M. W., Hawkins, S. J., Jonsson, P. R., Martin, D., Moschella, P. S., Sundelof, A., Thompson, R. C., Aberg, P. (2005). “An Ecological Perspective on the Development and Design of Low-Crested and other Hard Defense Structures.” Journal of Coastal Engineering, 52, 1073-1087.

Allen, R. J. and Webb, B. M. (2011). “Determination of Wave Transmission Coefficients for Oyster Shell Bag Breakwaters.” *Conference on Coastal Engineering Pratice*, American Society of Civil Engineers, Reston, VA.

Armono, H. D. and Hall, K. (2003). Wave Transmission on Submerged Breakwaters Made of Hollow Hemispherical Shape Artificial Reefs. *Proceeding of 31st Annual Conference of the Canadian Society for Civil Engineering* Canadian Society for Civil Engineering, New Brunswick, Canada.

ASTM Standard C29. (2009). “Standard Test Method for Bulk Density (unit Weight) and Voids in Aggregate.” *ASTM International*, West Conshohocken, PA. DOI: 10.1520/C0029_C0029M-07.

ASTM Standard C33. (2003). “Specification for Concrete Aggregates.” *ASTM International*, West Conshohocken, PA. DOI: 10.1520/C0033-03.

ASTM Standard C127. (2007). "Standard Method for Density, Relative Density (Specific Gravity), and Absorption of Coarse Aggregates." *ASTM International*, West Conshohocken, PA. DOI: 10.1520/C0127-12.

Atlantic Aquaculture. (2010). “Soft Mesh Polyethylene Netting.” *Atlantic Aquaculture*, http://www.atlanticaquaculture.com/soft_mesh_polyethylene_netting.htm (Nov. 2010).

Atlantic Aquaculture. (2013). “Rigid Polyethylene Netting.” *Atlantic Aquaculture*, http://www.atlanticaquaculture.com/Rigid%20netting.htm (Jan. 2013).

Bendell, B. (2006). “Recommended Appropriate Shoreline Stabilization Methods for Diffeerent Estuarine Shoreline Types in North Carolina.” *Management, Policy, Science and Engineering of Nonstructural Erosion Control in the Chesapeake Bay: Proceedings of the 2006 Living Shoreline Summit*, Chesapeake Bay National Estuarine Research Reserve, Williamsburg, VA, 19-24.

Benoit, J., Hardaway, S. C., Hernandez, D., Holman, R., Koch, E., McLellan, N., Peterson, S., Reed, D., Suman, D. (2007). *Mitigating Shore Erosion Along Sheltered Coasts*. The National Academic Press, Washington, D.C.

Borsje, B. W., van Wesenbeeck, B. K., Dekker, F., Paalvast, P., Bouma, T. J., van Katwijk, M. M., de Vries, M. B. (2010). “How Ecological Engineering can Serve in Coastal Protection.” *Journal of Ecological Engineering*, 37, 113-122.

Dahl, T. (2006). *Status and Trends of Wetlands in the Conterminous United States 1998-2004.* U.S. Fish and Wildlife Service, Washington, D.C.

d'Angremond, K. V., Van der Meer, J. W., De Jong, R. J. (1996). ”Wave Transmission at Low Crested Stuctures.” *25th International Conference on Coastal Engineering*, ASCE, Reston, VA, 3305-3318.

Dattatri, J., Raman, H., Shankar, J. N. (1978). "Performance Characteristics of Submerged Breakwaters." *16th International Conference on Coastal Engineering*, ASCE, Reston, VA, 2153-2171.

Davis, J. L., Takacs, R. L., Schnabel, R. (2006). “Evaluating Ecological Impacts of Living Shorelines and Shoreline Habitat Elements: An Example from the Upper Western Cheapeake Bay.” *Management, Policy, Science, and Engineering of Nonstructural Erosion Control in the Chesapeake Bay*, Chesapeake Bay National Estuarine Research Reserve, Williamsburg, VA, 55-61.

DeQuattro, J. (2010). “Coastal Restoration at Work: Coastal Alabama Restoration.” *5th National Conference on Coastal and Estuarine Habitat Restoration*. Restore America's Estuaries. Galveston, Texas. (Presentation)

Dick, T. M. and Brebner, A. (1968). "Solid and Permeable Submerged Structures." *11th International Conference on Coastal Engineering*, ASCE, Reston, VA, 1141-1158.

Douglass, S. L. and Pickel, B. H. (1999). "The Tide Doesn't go Out Anymore: The Effects of Bulkheads on Urban Bay Shorelines." *Shore & Beach* 67(2&3), 19-25.

Douglass, S. L., Ferraro, C., Dixon, C. R., Oliver, L., Pitts, L. (2012). "A Gulf of Mexico March Restoration and Protection Project." *33rd International Conference on Coastal Engineering*. ASCE, Reston, VA, management.76.

Duhring, K. A. (2006). "Overview of Living Shoreline Design Options for Erosion Protection on tidal Shorelines." *Management, Policy, Science and Engineering of Nonstructural Erosion Control in the Chesapeake Bay: Proceedings of the 2006 Living Shoreline Summit,* Chesapeake Bay National Estuarine Research Reserve, Williamsburg, VA, 13-18

Goda, Y., Takeda, H., Moriya, Y. (1967). "*Laboratory Investigation on Wave Transmission over Breakwaters*." Port and Harbour Technical Research Institute, Report No. 13, Ministry of Transport, Yokosuka, Japan.

Golshani, A., Mizutani, N., Hur, D. S., Shimizu, H. (2002). "Three-Dimensional Experimental Study of Wave-Induced Flow Around a Permeable Breakwater." *Proceedings of the 12th International Offshore and Polar Engineering Conference*. International Society of Offshore and Polar Engineers, Kitakyushu, Japan, 744-751.

Hardaway, S. C., Milligan, D. A., Hobbs, C. H., Wilcox, C. A., O'Brien, K. P., Varnell, L. (2010a). "*Mathews County Shoreline Management Plan*." Virginia Institute of Marine Science, Gloucester Point, VA

Hardaway, S. C., Milligan, D. A., Duhring, K. (2010b). "*Living Shoreline Design Guidelines for Shore Protection in Virginia's Estuarine Environments*." Virginia Institute of Marine Sciences, Gloucester Point, VA.

Hall, W. C. and Hall, J. V. (1940). "*A Model Study of the Effect of Submerged Breakwaters on Wave Action*" (TM-1). Beach Erosion Board, U.S. Army Corps of Engineers, Washington, D.C.

Jeffreys, H. (1944). *Note on the Offshore Bar Problem and Reflection from a Bar*. Great Britain. Ministry of Supply, Wave Report 3.

Kramer, M., Zanuttigh, B., Van der Meer, J., Vidal, C., Gironella, F. (2005). "Laboratory Experiments on Low-Crested Breakwaters." *Journal of Coastal Engineering, 52*, 867-885.

Lynett, P., Liu, P., Losada, I. J., Vidal, C. (2000). "Solitary Wave Interaction with Porous Breakwaters." *Journal of Waterway, Port, Coastal, and Ocean Engineering* , 314-322.

Mizutani, N. and Mostafa, A. M. (2001). "Porous Flow in a Vertical Breakwater Induced by Nonlinear Waves." *Journal of Offshore and Polar Engineering,* 11(3).

Murakami, K. and Maki, D. (2011). "Wave Breaking and Wave Setup of Artificial Reef with Inclined Crown." *32nd International Conference on Coastal Engineering*, ASCE, Reston, VA, waves.18.

National Oceanic and Atmospheric Administration (NOAA). (2013). "A Guide to National Shoreline Data and Terms: Glossary." *National Oceanic and Atmospheric Administration*, http://shoreline.noaa.gov/glossary.html#partj (Feb. 2013)

Perez-Romero, D. M., Ortega-Sanchez, M., Monino, A., Losada, M. (2009). "Characteristic Friction Coefficient and Scale Effects in Oscillatory Porous Flow." *Journal of Coastal Engineering*, 56, 931-939

Rageh, O. S. (2009). "Hydrodynamic Efficiency of Vertical Thick Porous Breakwaters." *Proceedings of the 13th International Water Technology Conference*. International Water Technology, El-Mansoura, Egypt, 1659-1671.

Reed, H. (2012). "A Comparison of Breakwater Effectiveness in Various Types of Designs in Relation to the High Wave Impact Area of Deadman's Island, Gulf Breeze Florida." *Mississippi-Alabama Bays and Bayous Symposium*, Mississippi-Alabama Sea Grant Consortium, Biloxi, MS. (Presentation)

Roland, R. M. and Douglass, S. L. (2005). "Estimating Wave Tolerance of Spartina Alterniflora in Coastal Alabama." *Journal of Coastal Research*, 21(3) , 453-463.

Seebrook, S. R. and Hall, K. R. (1998). "Wave Transmission at Submerged Rubblemound Breakwaters." *26th International Conference on Coastal Engineering,* ASCE, Reston, VA, 2000-2013.

Seelig, W. (1980). *Two-Dimensional Tests of Wave Transmission and Reflection Characteristics of Laboratory Breakwaters.* U.S. Army Corps of Engineers Waterways Experiment Station, Vicksburg, MS.

Stout, J. P. (1990). *Suggestions for Planting and Maintaining Wetlands in Coastal Alabama*. Alabama Department of Environmental Management, Montgomery, AL.

Swann, L. (2008). "The Use of Living Shorelines to Mitigate the Effects of Strom Events on Dauphin Island, Alabama, USA." *American Fisheries Society Symposium. 64.* American Fisheries Society.

Takayama, T., Nagai, K., Sekiguchi, T. (1985). "Irregular wave experiments on wave dissipation function of submerged breakwater with wide crown." *Proceeding of the 32nd Conference on Coastal Engineering*, Japanese Society of Civil Engineers, 545-549. (Japanese Text)

Ting, C. L., Lin, M. C., Cheng, C. Y. (2004). "Porosity effects on non-breaking surface waves over permeable submerged breakwaters." *Journal of Coastal Engineering*, 50 , 213-224.

U.S. Army Corps of Engineers. (2002). *Coastal Engineering Manual*. Engineering Manual 1110-2-1100, U.S. Army Corps of Engineers, Washington D.C. (in 6 volumes)

Van der Meer, J. W., Briganti, R., Zanuttigh, B., Wang, B. (2005). "Wave Transmission and Reflection at Low-Crested Structures: Design Formulae, Oblique Wave Attack, and Spectral Change." *Journal of Coastal Engineering*, 52, 915-929.

Van der Meer, J. and d'Angremond, K. (1991). "Wave Transmission at Low Crested Stuctures." *Coastal Stuctures and Breakwaters*. Institution of Civil Engineers, London, England, 25-42.

Vanneste, D. and Troch, P. (2010). "Experimental Research on Pore Pressure Attenuation in Rubble-Mound Breakwaters." *31st International Conference on Coastal Engineering*. ASCE, Reston, VA.

Walker, R., Bendell, B., Wallendorf, L. (2011). "Defining Engineering Guidance for Living Shoreline Projects." *Conference on Coastal Engineering Pratice*, American Society of Civil Engineers, Reston, VA.

Yozzo, D. J., Davis, J. E., Cagney, P. T. (2003). "Shore Protection Projects." *Coastal Engineering Manual, Chapter V-3.* U.S. Army Corps of Engineers, Washington, D.C.

APPENDICES

APPENDIX A: ADDITIONAL FIGURES AND GRAPHS

Figure A1: ReefBLK^{SM} installed at Coffee Island, Alabama (Photo Courtesy: Beth Maynor Young, 2010).

Figure A2: Construction of Reef Balls to be placed along Alabama shorelines under the American Recovery and Reinvestment Act (Photo Courtesy: Jeff DeQuattro/The Nature Conservancy).

Figure A3: Composition of a bagged oyster shell breakwater to be used at Helen Wood Park, Alabama.

Figure A4: Concrete pyramids installed at Little Bay, Alabama.

Table A1: Single row configuration testing matrix of concrete pyramids.

Incident Wave	Water Depth (m)				
	0.203	**0.254**	**0.305**	**0.356**	**0.406**
1	1	9	17	25	33
2	2	10	18	26	34
3	3	11	19	27	35
4	4	12	20	28	36
5	5	13	21	29	37
6	6	14	22	30	38
7	7	15	23	31	39
8	8	16	24	32	40

Table A2: Offset double row configuration testing matrix of concrete pyramids.

Incident Wave	Water Depth (m)				
	0.203	**0.254**	**0.305**	**0.356**	**0.406**
1	41	49	57	65	73
2	42	50	58	66	74
3	43	51	59	67	75
4	44	52	60	68	76
5	45	53	61	69	77
6	46	54	62	70	78
7	47	55	63	71	79
8	48	56	64	72	80

Table A3: Oyster shell substrate properties used in ReefBLK^SM units.

Oyster Shell Properties	
Bulk Density (kg/m³)	596
Bulk Specific Gravity	2.28
Bulk Specific Gravity (SSD)	2.36
Apparent Specific Gravity	2.49
Absorption Capacity	4%

Figure A5: Oyster shell distribution with scale used in the ReefBLK^SM construction.

Table A4: ReefBLK^{SM} testing matrix.

Incident Wave	Water Depth (m)				
	0.203	0.254	0.305	0.356	0.406
1	81	89	97	105	113
2	82	90	98	106	114
3	83	91	99	107	115
4	84	92	100	108	116
5	85	93	101	109	117
6	86	94	102	110	118
7	87	95	103	111	119
8	88	96	104	112	120

APPENDIX B: RAW DATA

Table B1: Summary of results for bagged oyster shell testing. All dimensions are in meters. Wave length calculated using small amplitude wave theory. Water depth is a constant 0.30 m (12 in).

Crest Width, B	Structure Height, h_c	Incident Wave Height, H_i	Wave Period, T	Wave Length, L	Transmitted Wave Height, H_t	Transmission Coefficient, K_t
0.36	0.07	0.09	1.34	1.90	0.22	0.97
0.79	0.08	0.09	1.34	1.90	0.44	0.92
1.22	0.08	0.09	1.34	1.90	0.65	0.89
1.53	0.08	0.09	1.34	1.90	0.81	0.84
1.78	0.09	0.09	1.34	1.90	0.94	0.78
0.56	0.09	0.09	1.34	1.90	0.32	0.91
0.38	0.16	0.09	1.34	1.90	0.27	0.87
0.78	0.15	0.09	1.34	1.90	0.46	0.85
1.22	0.15	0.09	1.34	1.90	0.68	0.78
1.53	0.16	0.09	1.34	1.90	0.85	0.72
1.82	0.16	0.09	1.34	1.90	0.99	0.61
0.57	0.16	0.09	1.34	1.90	0.37	0.88
0.38	0.23	0.09	1.34	1.90	0.31	0.78
0.79	0.23	0.09	1.34	1.90	0.51	0.59
1.22	0.22	0.09	1.34	1.90	0.72	0.60
1.51	0.22	0.09	1.34	1.90	0.86	0.47
1.82	0.22	0.09	1.34	1.90	1.02	0.34
0.57	0.22	0.09	1.34	1.90	0.40	0.63
0.38	0.28	0.09	1.34	1.90	0.33	0.46
0.84	0.29	0.09	1.34	1.90	0.57	0.11
1.22	0.29	0.09	1.34	1.90	0.75	0.05
1.52	0.28	0.09	1.34	1.90	0.90	0.02
1.84	0.29	0.09	1.34	1.90	1.07	0.11
0.57	0.29	0.09	1.34	1.90	0.43	0.16
0.41	0.34	0.09	1.34	1.90	0.37	0.15
0.84	0.35	0.09	1.34	1.90	0.59	0.06
1.22	0.34	0.09	1.34	1.90	0.78	0.39
1.51	0.35	0.09	1.34	1.90	0.93	0.24
1.84	0.35	0.09	1.34	1.90	1.10	0.01
0.57	0.34	0.09	1.34	1.90	0.46	0.09
0.40	0.40	0.09	1.34	1.90	0.40	0.12
0.84	0.42	0.09	1.34	1.90	0.63	0.05
1.24	0.40	0.09	1.34	1.90	0.82	0.31
1.53	0.40	0.09	1.34	1.90	0.96	0.14
1.84	0.42	0.09	1.34	1.90	1.13	0.06
0.57	0.41	0.09	1.34	1.90	0.49	0.08
1.84	0.29	0.15	2.03	3.08	1.07	0.09
0.57	0.29	0.15	2.03	3.08	0.43	0.36
1.84	0.35	0.15	2.03	3.08	1.10	0.02
0.57	0.34	0.15	2.03	3.08	0.46	0.14
1.53	0.40	0.15	2.03	3.08	0.96	0.06
1.84	0.42	0.15	2.03	3.08	1.13	0.03
0.57	0.41	0.15	2.03	3.08	0.49	0.10

Table B2: Summary of results for single row of concrete pyramids. All dimensions are in meters. Wave length calculated using small amplitude wave theory. Structure crest width, *B*, is a constant 0.25 m (10 in) and structure height, h_c, is a constant 0.30 m (12 in).

Experiment Number	Water Depth, d	Incident Wave Height, H_i	Incident Wave Period, T	Incident Wave Length, L	Transmitted Wave Height, H_t	Transmission Coefficient, K_t
1	0.20	0.02	1.26	1.63	0.02	0.82
2	0.20	0.04	2.00	2.73	0.02	0.55
3	0.20	0.03	1.10	1.38	0.02	0.52
4	0.20	0.07	1.62	2.17	0.03	0.50
5	0.20	0.07	1.08	1.35	0.03	0.46
6	0.20	N/A	N/A	N/A	N/A	N/A
7	0.20	0.11	1.76	2.38	0.04	0.36
8	0.20	0.14	2.29	3.16	0.07	0.52
9	0.25	0.04	1.33	1.90	0.02	0.56
10	0.25	0.06	2.25	3.43	0.04	0.59
11	0.25	0.03	1.21	1.68	0.02	0.71
12	0.25	0.07	1.67	2.47	0.04	0.56
13	0.25	0.06	1.24	1.74	0.04	0.70
14	0.25	N/A	N/A	N/A	N/A	N/A
15	0.25	0.14	1.74	2.59	0.06	0.42
16	0.25	0.19	2.25	3.44	0.12	0.63
17	0.30	0.04	1.35	2.07	0.03	0.75
18	0.30	0.08	2.06	3.38	0.06	0.74
19	0.30	0.04	1.18	1.73	0.03	0.72
20	0.30	0.09	1.68	2.70	0.06	0.69
21	0.30	0.07	1.21	1.80	0.05	0.79
22	0.30	N/A	N/A	N/A	N/A	N/A
23	0.30	0.16	1.76	2.84	0.08	0.53
24	0.30	0.23	2.25	3.74	0.15	0.64
25	0.36	0.05	1.37	2.23	0.04	0.85
26	0.36	0.08	2.05	3.61	0.08	0.94
27	0.36	0.04	1.20	1.87	0.03	0.84
28	0.36	0.11	1.69	2.89	0.08	0.69
29	0.36	0.07	1.24	1.96	0.06	0.92
30	0.36	N/A	N/A	N/A	N/A	N/A
31	0.36	0.19	1.76	3.04	0.13	0.69
32	0.36	0.24	2.22	3.95	0.17	0.71
33	0.41	0.05	1.37	2.33	0.05	0.91
34	0.41	0.09	2.06	3.85	0.08	0.92
35	0.41	0.04	1.25	2.05	0.04	0.95
36	0.41	0.12	1.68	3.04	0.10	0.78
37	0.41	0.07	1.20	1.94	0.08	1.05
38	0.41	N/A	N/A	N/A	N/A	N/A
39	0.41	0.19	1.76	3.19	0.16	0.84
40	0.41	0.27	2.23	4.20	0.21	0.79

Table B3: Summary of results for offset double row of concrete pyramids. All dimensions are in meters. Wave length calculated using small amplitude wave theory. Structure crest width, *B*, is a constant 1.04 m (43 in) and structure height, h_c, is a constant 0.30 m (12 in).

Experiment Number	Water Depth, d	Incident Wave Height, H_i	Incident Wave Period, T	Incident Wave Length, L	Transmitted Wave Height, H_t	Transmission Coefficient, K_t
41	0.20	0.02	1.26	1.63	0.01	0.46
42	0.20	0.04	2.00	2.73	0.02	0.49
43	0.20	0.03	1.10	1.38	0.02	0.47
44	0.20	0.07	1.62	2.17	0.02	0.37
45	0.20	0.07	1.08	1.35	0.02	0.27
46	0.20	N/A	N/A	N/A	N/A	N/A
47	0.20	0.11	1.76	2.38	0.04	0.35
48	0.20	0.14	2.29	3.16	0.03	0.25
49	0.25	0.04	1.33	1.90	0.02	0.55
50	0.25	0.06	2.25	3.43	0.04	0.62
51	0.25	0.03	1.21	1.68	0.02	0.66
52	0.25	0.07	1.67	2.47	0.04	0.49
53	0.25	0.06	1.24	1.74	0.04	0.61
54	0.25	N/A	N/A	N/A	N/A	N/A
55	0.25	0.14	1.74	2.59	0.06	0.44
56	0.25	0.19	2.25	3.44	0.07	0.39
57	0.30	0.04	1.35	2.07	0.03	0.62
58	0.30	0.08	2.06	3.38	0.04	0.51
59	0.30	0.04	1.18	1.73	0.03	0.67
60	0.30	0.09	1.68	2.70	0.05	0.54
61	0.30	0.07	1.21	1.80	0.05	0.72
62	0.30	N/A	N/A	N/A	N/A	N/A
63	0.30	0.16	1.76	2.84	0.08	0.48
64	0.30	0.23	2.25	3.74	0.12	0.53
65	0.36	0.05	1.37	2.23	0.05	0.95
66	0.36	0.08	2.05	3.61	0.05	0.65
67	0.36	0.04	1.20	1.87	0.03	0.72
68	0.36	0.11	1.69	2.89	0.07	0.66
69	0.36	0.07	1.24	1.96	0.06	0.87
70	0.36	N/A	N/A	N/A	N/A	N/A
71	0.36	0.19	1.76	3.04	0.12	0.62
72	0.36	0.24	2.22	3.95	0.15	0.61
73	0.41	0.05	1.37	2.33	0.05	0.92
74	0.41	0.09	2.06	3.85	0.08	0.88
75	0.41	0.04	1.25	2.05	0.04	1.10
76	0.41	0.12	1.68	3.04	0.11	0.85
77	0.41	0.07	1.20	1.94	0.08	1.10
78	0.41	N/A	N/A	N/A	N/A	N/A
79	0.41	0.19	1.76	3.19	0.15	0.77
80	0.41	0.27	2.23	4.20	0.18	0.67

Table B4: Summary of results for ReefBLK[SM]. All dimensions are in meters. Wave length calculated using small amplitude wave theory. Structure crest width, *B*, is a constant 1.32 m (52 in) and structure height, h_c, is a constant 0.30 m (12 in).

Experiment Number	Water Depth, d	Incident Wave Height, H_i	Incident Wave Period, T	Incident Wave Length, L	Transmitted Wave Height, H_t	Transmission Coefficient, K_t
81	0.20	0.03	1.34	1.75	0.02	0.62
82	0.20	0.05	2.18	2.98	0.03	0.61
83	0.20	0.04	1.04	1.28	0.02	0.46
84	0.20	0.06	1.68	2.26	0.03	0.49
85	0.20	0.06	1.09	1.36	0.03	0.48
86	0.20	N/A	N/A	N/A	N/A	N/A
87	0.20	N/A	N/A	N/A	N/A	N/A
88	0.20	N/A	N/A	N/A	N/A	N/A
89	0.25	0.04	1.35	1.93	0.02	0.62
90	0.25	0.06	2.23	3.37	0.04	0.69
91	0.25	0.05	1.09	1.47	0.02	0.46
92	0.25	0.09	1.68	2.49	0.04	0.45
93	0.25	0.08	1.07	1.44	0.04	0.45
94	0.25	N/A	N/A	N/A	N/A	N/A
95	0.25	N/A	N/A	N/A	N/A	N/A
96	0.25	0.18	2.35	3.60	0.11	0.62
97	0.30	0.04	1.35	2.07	0.03	0.62
98	0.30	0.07	2.19	3.63	0.05	0.68
99	0.30	0.05	1.11	1.59	0.03	0.54
100	0.30	0.09	1.66	2.66	0.05	0.55
101	0.30	0.10	1.06	1.50	0.06	0.58
102	0.30	N/A	N/A	N/A	N/A	N/A
103	0.30	0.15	1.75	2.83	0.11	0.72
104	0.30	0.21	2.35	3.91	0.15	0.70
105	0.36	0.05	1.34	2.18	0.04	0.74
106	0.36	0.08	2.12	3.75	0.06	0.77
107	0.36	0.06	1.14	1.74	0.04	0.67
108	0.36	0.11	1.67	2.85	0.07	0.69
109	0.36	0.11	1.06	1.56	0.07	0.64
110	0.36	N/A	N/A	N/A	N/A	N/A
111	0.36	0.18	1.76	3.04	0.13	0.73
112	0.36	0.22	2.23	3.96	0.14	0.64
113	0.41	0.05	1.36	2.31	0.04	0.83
114	0.41	0.09	2.05	3.83	0.08	0.82
115	0.41	0.07	1.10	1.70	0.04	0.61
116	0.41	0.12	1.70	3.07	0.10	0.81
117	0.41	0.12	1.08	1.66	0.09	0.73
118	0.41	N/A	N/A	N/A	N/A	N/A
119	0.41	0.20	1.76	3.21	0.16	0.80
120	0.41	0.22	2.23	4.20	0.17	0.79

Table B5: Bagged oyster shell breakwater raw data for incident wave heights. Physical dimensions are in meters.

Incident Wave Height, H_i					
a	**b**	**c**	**Average**	**Std. Dev.**	**Variance**
0.089	0.095	0.091	0.092	0.003	0.000
0.169	0.153	0.158	0.160	0.009	0.000

Table B6: Bagged oyster shell breakwater raw data for incident wave periods.

Incident Wave Period, T_z					
a	**b**	**c**	**Average**	**Std. Dev.**	**Variance**
1.35	1.33	1.33	1.34	0.013	0.000
2.05	2.03	2.00	2.03	0.025	0.001

Table B7: Transmitted wave height of bagged oyster shell breakwater raw experimental data for an incident wave height of 0.10 m (0.30 ft) and a period of 1.34 sec as a function of structure geometry. All physical dimensions are in meters.

Crest Width, B	Structure Height, z	Transmitted Wave Height, H_t					
		a	b	c	Average	Std. Dev.	Variance
0.381	0.076	0.088	0.092	0.088	0.089	0.002	0.000
0.838	0.089	0.084	0.086	0.084	0.085	0.001	0.000
1.295	0.083	0.081	0.079	0.083	0.081	0.002	0.000
1.626	0.089	0.078	0.078	0.076	0.077	0.001	0.000
1.892	0.092	0.070	0.071	0.072	0.071	0.001	0.000
0.597	0.092	0.086	0.082	0.082	0.083	0.002	0.000
0.406	0.168	0.080	0.078	0.081	0.079	0.001	0.000
0.826	0.159	0.078	0.078	0.078	0.078	0.000	0.000
1.295	0.156	0.071	0.072	0.071	0.071	0.001	0.000
1.626	0.168	0.066	0.066	0.066	0.066	0.000	0.000
1.930	0.165	0.057	0.054	0.056	0.056	0.001	0.000
0.610	0.168	0.080	0.081	0.081	0.081	0.000	0.000
0.406	0.241	0.071	0.072	0.071	0.071	0.001	0.000
0.838	0.241	0.050	0.056	0.056	0.054	0.003	0.000
1.295	0.235	0.053	0.054	0.057	0.055	0.002	0.000
1.600	0.235	0.043	0.041	0.045	0.043	0.002	0.000
1.930	0.229	0.032	0.030	0.030	0.031	0.001	0.000
0.610	0.235	0.056	0.060	0.055	0.057	0.003	0.000
0.406	0.292	0.044	0.041	0.042	0.042	0.001	0.000
0.889	0.311	0.011	0.009	0.011	0.010	0.001	0.000
1.295	0.305	0.005	0.005	0.005	0.005	0.000	0.000
1.613	0.292	0.002	0.002	0.002	0.002	0.000	0.000
1.956	0.305	0.012	0.009	0.009	0.010	0.002	0.000
0.610	0.305	0.013	0.012	0.019	0.015	0.004	0.000
0.432	0.356	0.014	0.014	0.014	0.014	0.000	0.000
0.889	0.368	0.006	0.005	0.005	0.005	0.000	0.000
1.295	0.362	0.038	0.035	0.036	0.036	0.002	0.000
1.600	0.368	0.018	0.029	0.019	0.022	0.006	0.000
1.956	0.368	0.001	0.000	0.001	0.001	0.000	0.000
0.610	0.362	0.008	0.008	0.008	0.008	0.000	0.000
0.419	0.425	0.011	0.011	0.011	0.011	0.000	0.000
0.889	0.445	0.005	0.005	0.005	0.005	0.000	0.000
1.321	0.419	0.028	0.026	0.030	0.028	0.002	0.000
1.626	0.419	0.013	0.015	0.012	0.013	0.002	0.000
1.956	0.451	0.005	0.005	0.006	0.006	0.000	0.000
0.610	0.432	0.008	0.008	0.006	0.007	0.001	0.000

Table B8: Transmitted wave period of bagged oyster shell breakwater raw experimental data for an incident wave height of 0.10 m (0.30 ft) and a period of 1.34 sec as a function of structure geometry. All physical dimensions are in meters.

Crest Width, B	Structure Height, z	Transmitted Wave Period, T_z					
		a	b	c	Average	Std. Dev.	Variance
0.381	0.076	1.33	1.33	1.33	1.33	0.005	0.000
0.838	0.089	1.33	1.35	1.33	1.34	0.013	0.000
1.295	0.083	1.33	1.33	1.33	1.33	0.005	0.000
1.626	0.089	1.35	1.35	1.35	1.35	0.000	0.000
1.892	0.092	1.35	1.33	1.35	1.34	0.014	0.000
0.597	0.092	1.33	1.33	1.33	1.33	0.005	0.000
0.406	0.168	1.35	1.35	1.33	1.34	0.010	0.000
0.826	0.159	1.35	1.35	1.33	1.34	0.014	0.000
1.295	0.156	1.35	1.38	1.35	1.36	0.014	0.000
1.626	0.168	1.35	1.35	1.35	1.35	0.000	0.000
1.930	0.165	1.35	1.38	1.35	1.36	0.014	0.000
0.610	0.168	1.33	1.35	1.35	1.34	0.014	0.000
0.406	0.241	1.33	1.33	1.35	1.33	0.014	0.000
0.838	0.241	1.06	1.35	1.33	1.25	0.161	0.026
1.295	0.235	1.33	1.33	1.37	1.34	0.020	0.000
1.600	0.235	0.87	0.98	1.33	1.06	0.244	0.059
1.930	0.229	0.77	0.77	0.77	0.77	0.000	0.000
0.610	0.235	1.30	1.33	1.33	1.32	0.019	0.000
0.406	0.292	1.30	1.35	1.30	1.32	0.029	0.001
0.889	0.311	1.40	0.93	1.40	1.24	0.270	0.073
1.295	0.305	1.40	1.50	1.50	1.47	0.058	0.003
1.613	0.292	1.50	1.40	1.40	1.43	0.058	0.003
1.956	0.305						
0.610	0.305	0.80	0.80	1.37	0.99	0.327	0.107
0.432	0.356	1.45	1.40	1.40	1.42	0.029	0.001
0.889	0.368	1.45	1.45	1.40	1.43	0.029	0.001
1.295	0.362						
1.600	0.368						
1.956	0.368	1.40	0.73	1.47	1.20	0.410	0.168
0.610	0.362	1.40	1.35	1.30	1.35	0.050	0.002
0.419	0.425	1.40	1.40	1.40	1.40	0.000	0.000
0.889	0.445	1.50	1.45	1.45	1.47	0.029	0.001
1.321	0.419						
1.626	0.419						
1.956	0.451						
0.610	0.432	1.50	1.45	1.45	1.47	0.029	0.001

Table B9: Transmitted wave height of bagged oyster shell breakwater raw experimental data for an incident wave height of 0.16 m (0.52 ft) and a period of 2.03 sec as a function of structure geometry. All physical dimensions are in meters.

Crest Width, B	Structure Height, z	Transmitted Wave Height, H_t					
		a	b	c	Average	Std. Dev.	Variance
1.956	0.305	0.013	0.018	0.013	0.014	0.003	0.000
0.610	0.305	0.052	0.052	0.070	0.058	0.010	0.000
1.956	0.368	0.004	0.004	0.004	0.004	0.000	0.000
0.610	0.362	0.022	0.022	0.022	0.022	0.000	0.000
1.626	0.419	0.011	0.008	0.009	0.009	0.001	0.000
1.956	0.451	0.006	0.004	0.004	0.005	0.001	0.000
0.610	0.432	0.016	0.018	0.016	0.017	0.001	0.000

Table B10: Transmitted wave period of bagged oyster shell breakwater raw experimental data for an incident wave height of 0.16 m (0.52 ft) and a period of 2.03 sec as a function of structure geometry. All physical dimensions are in meters.

Crest Width, B	Structure Height, z	Transmitted Wave Period, T_z					
		a	b	c	Average	Std. Dev.	Variance
1.956	0.305	0.87	1.53	1.57	1.32	0.395	0.156
0.610	0.305	1.50	1.50	2.25	1.75	0.433	0.188
1.956	0.368	2.00	2.10	2.30	2.13	0.153	0.023
0.610	0.362	2.05	2.05	2.05	2.05	0.000	0.000
1.626	0.419	0.67	0.86	0.82	0.78	0.102	0.010
1.956	0.451	2.40	1.63	1.90	1.98	0.389	0.152
0.610	0.432	2.05	2.10	2.05	2.07	0.029	0.001

Table B11: Concrete pyramid control average wave properties. The burst values are the average of the gage data. Areas of omitted data are indicative of incomplete or inconsistent data. All physical dimensions are in meters.

Wave Number		1					
Burst/Variable		a	b	c	Average	St. Dev.	Variance
Water Depth	Value						
0.203	H_{rms}	0.026	0.022		0.024	0.003	0.000
	H_{avg}	0.024	0.017		0.020	0.005	0.000
	T_z	1.38	1.15		1.26	0.159	0.025
	N	2.5	4.0		3.3	1.061	1.125
0.254	H_{rms}	0.038		0.039	0.039	0.000	0.000
	H_{avg}	0.038		0.038	0.038	0.000	0.000
	T_z	1.33		1.33	1.33	0.000	0.000
	N	3.0		3.0	3.0	0.000	0.000
0.305	H_{rms}	0.043	0.042		0.043	0.000	0.000
	H_{avg}	0.043	0.042		0.042	0.000	0.000
	T_z	1.37	1.33		1.35	0.024	0.001
	N	3.00	3.00		3.0	0.000	0.000
.356	H_{rms}	0.049	0.052	0.050	0.050	0.001	0.000
	H_{avg}	0.048	0.051	0.049	0.049	0.001	0.000
	T_z	1.37	1.37	1.37	1.37	0.000	0.000
	N	3.0	3.0	3.0	3.0	0.000	0.000
.406	H_{rms}	0.054		0.055	0.054	0.000	0.000
	H_{avg}	0.053		0.053	0.053	0.000	0.000
	T_z	1.37		1.37	1.37	0.000	0.000
	N	3.0		3.0	3.0	0.000	0.000

Table B11: Cont.

Wave Number		2					
Burst/Variable		**a**	**b**	**c**	**Average**	**St. Dev.**	**Variance**
Water Depth	**Value**						
0.203	H_{rms}	0.043	0.047	0.043	0.044	0.002	0.000
	H_{avg}	0.041	0.047	0.042	0.043	0.003	0.000
	T_z	1.98	2.00	2.02	2.00	0.017	0.000
	N	2.5	2.0	2.5	2.3	0.289	0.083
0.254	H_{rms}	0.067		0.062	0.064	0.004	0.000
	H_{avg}	0.067		0.058	0.062	0.006	0.000
	T_z	2.14		2.35	2.25	0.147	0.022
	N	2.5		4.0	3.3	1.061	1.125
0.305	H_{rms}	0.077	0.075	0.076	0.076	0.001	0.000
	H_{avg}	0.077	0.075	0.076	0.076	0.001	0.000
	T_z	2.07	2.03	2.07	2.06	0.019	0.000
	N	3.00	3.00	3.00	3.0	0.000	0.000
.356	H_{rms}	0.082	0.084	0.083	0.083	0.001	0.000
	H_{avg}	0.081	0.083	0.082	0.082	0.001	0.000
	T_z	2.05	2.05	2.05	2.05	0.000	0.000
	N	3.0	3.0	3.0	3.0	0.000	0.000
.406	H_{rms}	0.088	0.088	0.091	0.089	0.002	0.000
	H_{avg}	0.088	0.088	0.091	0.089	0.002	0.000
	T_z	2.07	2.05	2.07	2.06	0.010	0.000
	N	3.0	3.0	3.0	3.0	0.000	0.000

Table B11: Cont.

Wave Number		3					
Burst/Variable		a	b	c	Average	St. Dev.	Variance
Water Depth	Value						
0.203	H_{rms}	0.037	0.037	0.036	0.037	0.000	0.000
	H_{avg}	0.035	0.035	0.034	0.035	0.000	0.000
	T_z	1.10	1.10	1.10	1.10	0.000	0.000
	N	2.0	2.0	2.0	2.0	0.000	0.000
0.254	H_{rms}	0.040	0.035	0.035	0.037	0.003	0.000
	H_{avg}	0.038	0.030	0.031	0.033	0.004	0.000
	T_z	1.10	1.23	1.28	1.21	0.095	0.009
	N	2.0	3.0	3.0	2.7	0.577	0.333
0.305	H_{rms}	0.041		0.041	0.041	0.000	0.000
	H_{avg}	0.039		0.040	0.039	0.000	0.000
	T_z	1.18		1.18	1.18	0.000	0.000
	N	2.00		2.00	2.0	0.000	0.000
.356	H_{rms}	0.042	0.042	0.042	0.042	0.000	0.000
	H_{avg}	0.041	0.040	0.040	0.040	0.000	0.000
	T_z	1.20	1.20	1.20	1.20	0.000	0.000
	N	2.0	2.0	2.0	2.0	0.000	0.000
.406	H_{rms}	0.042	0.042		0.042	0.000	0.000
	H_{avg}	0.040	0.039		0.040	0.001	0.000
	T_z	1.20	1.29		1.25	0.065	0.004
	N	2.0	2.5		2.3	0.354	0.125

Table B11: Cont.

Wave Number		4					
Burst/Variable		**a**	**b**	**c**	**Average**	**St. Dev.**	**Variance**
Water Depth	**Value**						
0.203	H_{rms}	0.069	0.063	0.072	0.068	0.005	0.000
	H_{avg}	0.069	0.061	0.072	0.068	0.006	0.000
	T_z	1.67	1.53	1.68	1.62	0.084	0.007
	N	3.0	3.5	4.0	3.5	0.500	0.250
0.254	H_{rms}	0.078		0.073	0.076	0.003	0.000
	H_{avg}	0.078		0.071	0.074	0.005	0.000
	T_z	1.67		1.67	1.67	0.003	0.000
	N	3.0		3.5	3.3	0.354	0.125
0.305	H_{rms}	0.095	0.082	0.088	0.088	0.007	0.000
	H_{avg}	0.095	0.076	0.086	0.086	0.009	0.000
	T_z	1.70	1.66	1.68	1.68	0.019	0.000
	N	3.00	4.00	3.50	3.5	0.500	0.250
.356	H_{rms}	0.114	0.115	0.110	0.113	0.003	0.000
	H_{avg}	0.114	0.115	0.110	0.113	0.003	0.000
	T_z	1.70	1.70	1.67	1.69	0.019	0.000
	N	3.0	3.0	3.0	3.0	0.000	0.000
.406	H_{rms}	0.124	0.127	0.122	0.124	0.003	0.000
	H_{avg}	0.124	0.126	0.122	0.124	0.002	0.000
	T_z	1.67	1.68	1.70	1.68	0.017	0.000
	N	3.0	3.0	3.0	3.0	0.000	0.000

Table B11: Cont.

Wave Number		5					
Burst/Variable		a	b	c	Average	St. Dev.	Variance
Water Depth	Value						
0.203	H_{rms}	0.067	0.067	0.077	0.071	0.006	0.000
	H_{avg}	0.063	0.063	0.073	0.067	0.006	0.000
	T_z	1.08	1.08	1.10	1.08	0.014	0.000
	N	2.0	2.0	3.0	2.3	0.577	0.333
0.254	H_{rms}	0.071		0.065	0.068	0.004	0.000
	H_{avg}	0.063		0.055	0.059	0.005	0.000
	T_z	1.25		1.23	1.24	0.012	0.000
	N	2.5		3.0	2.8	0.354	0.125
0.305	H_{rms}	0.086	0.076	0.070	0.077	0.008	0.000
	H_{avg}	0.079	0.067	0.058	0.068	0.010	0.000
	T_z	1.10	1.23	1.30	1.21	0.102	0.010
	N	2.00	2.50	3.00	2.5	0.500	0.250
.356	H_{rms}	0.081	0.082	0.074	0.079	0.005	0.000
	H_{avg}	0.071	0.073	0.061	0.068	0.007	0.000
	T_z	1.24	1.22	1.27	1.24	0.025	0.001
	N	2.5	2.5	3.0	2.7	0.289	0.083
.406	H_{rms}	0.086	0.080	0.085	0.083	0.003	0.000
	H_{avg}	0.079	0.067	0.076	0.074	0.007	0.000
	T_z	1.15	1.23	1.21	1.20	0.043	0.002
	N	2.0	3.0	2.5	2.5	0.500	0.250

Table B11: Cont.

Wave Number		6					
Burst/Variable		a	b	c	Average	St. Dev.	Variance
Water Depth	Value						
0.203	H_{rms}						
	H_{avg}						
	T_z						
	N						
0.254	H_{rms}						
	H_{avg}						
	T_z						
	N						
0.305	H_{rms}						
	H_{avg}						
	T_z						
	N						
.356	H_{rms}						
	H_{avg}						
	T_z						
	N						
.406	H_{rms}						
	H_{avg}						
	T_z						
	N						

Table B11: Cont.

Wave Number		7					
Burst/Variable		**a**	**b**	**c**	**Average**	**St. Dev.**	**Variance**
Water Depth	**Value**						
0.203	H_{rms}	0.110	0.109	0.109	0.109	0.001	0.000
	H_{avg}	0.110	0.108	0.108	0.108	0.001	0.000
	T_z	1.77	1.77	1.75	1.76	0.010	0.000
	N	3.0	3.0	3.0	3.0	0.000	0.000
0.254	H_{rms}	0.138	0.141	0.136	0.138	0.002	0.000
	H_{avg}	0.138	0.139	0.135	0.137	0.002	0.000
	T_z	1.73	1.73	1.75	1.74	0.010	0.000
	N	3.0	3.0	3.0	3.0	0.000	0.000
0.305	H_{rms}	0.164	0.157	0.162	0.161	0.003	0.000
	H_{avg}	0.164	0.157	0.162	0.161	0.004	0.000
	T_z	1.77	1.77	1.75	1.76	0.010	0.000
	N	3.00	3.00	3.00	3.0	0.000	0.000
.356	H_{rms}	0.191	0.193	0.187	0.190	0.003	0.000
	H_{avg}	0.191	0.193	0.187	0.190	0.003	0.000
	T_z	1.77	1.77	1.75	1.76	0.010	0.000
	N	3.0	3.0	3.0	3.0	0.000	0.000
.406	H_{rms}	0.191	0.197	0.195	0.195	0.003	0.000
	H_{avg}	0.191	0.197	0.195	0.194	0.003	0.000
	T_z	1.75	1.77	1.75	1.76	0.010	0.000
	N	3.0	3.0	3.0	3.0	0.000	0.000

Table B11: Cont.

Wave Number		8					
Burst/Variable		a	b	c	Average	St. Dev.	Variance
Water Depth	Value						
0.203	H_{rms}	0.135	0.140	0.136	0.137	0.003	0.000
	H_{avg}	0.134	0.140	0.136	0.136	0.003	0.000
	T_z	2.30	2.30	2.28	2.29	0.010	0.000
	N	3.0	3.0	3.0	3.0	0.000	0.000
0.254	H_{rms}	0.192	0.190	0.188	0.190	0.002	0.000
	H_{avg}	0.191	0.188	0.187	0.189	0.002	0.000
	T_z	2.23	2.25	2.27	2.25	0.017	0.000
	N	3.0	3.0	3.0	3.0	0.000	0.000
0.305	H_{rms}	0.230	0.227	0.226	0.228	0.002	0.000
	H_{avg}	0.229	0.226	0.225	0.227	0.002	0.000
	T_z	2.26	2.25	2.25	2.25	0.005	0.000
	N	3.50	4.00	4.00	3.8	0.289	0.083
.356	H_{rms}	0.244	0.240	0.248	0.244	0.004	0.000
	H_{avg}	0.242	0.239	0.247	0.243	0.004	0.000
	T_z	2.21	2.23	2.23	2.22	0.009	0.000
	N	3.5	3.5	4.0	3.7	0.289	0.083
.406	H_{rms}	0.263	0.272	0.267	0.268	0.004	0.000
	H_{avg}	0.262	0.270	0.265	0.266	0.004	0.000
	T_z	2.23	2.23	2.23	2.23	0.000	0.000
	N	4.0	4.0	4.0	4.0	0.000	0.000

Table B12: Concrete pyramid single row test data average of all gages. The burst values are the average of the gage data. Areas of omitted data are indicative of incomplete or inconsistent data. All physical dimensions are in meters.

Wave Number		**1**					
Burst/Variable		**a**	**b**	**c**	**Average**	**St. Dev.**	**Variance**
Water Depth	**Value**						
0.203	H_{rms}	0.017	0.016	0.018	0.017	0.001	0.000
	H_{avg}	0.017	0.015	0.018	0.017	0.001	0.000
	T_z	1.35	1.35	1.40	1.37	0.029	0.001
	N	2.0	2.0	2.0	2.0	0.000	0.000
0.254	H_{rms}	0.023	0.024	0.020	0.022	0.002	0.000
	H_{avg}	0.022	0.023	0.018	0.021	0.002	0.000
	T_z	1.33	1.30	1.39	1.34	0.047	0.002
	N	2.0	2.0	2.5	2.2	0.289	0.083
0.305	H_{rms}	0.032	0.034	0.032	0.032	0.001	0.000
	H_{avg}	0.031	0.033	0.031	0.032	0.001	0.000
	T_z	1.36	1.40	1.35	1.37	0.027	0.001
	N	2.50	3.00	2.50	2.7	0.289	0.083
.356	H_{rms}	0.044	0.042		0.043	0.002	0.000
	H_{avg}	0.044	0.041		0.042	0.002	0.000
	T_z	1.42	1.40		1.41	0.012	0.000
	N	3.0	3.0		3.0	0.000	0.000
.406	H_{rms}	0.050	0.050	0.049	0.049	0.001	0.000
	H_{avg}	0.049	0.049	0.048	0.048	0.001	0.000
	T_z	1.37	1.38	1.37	1.37	0.010	0.000
	N	3.0	3.0	3.0	3.0	0.000	0.000

Table B12: Cont.

Wave Number		2					
Burst/Variable		a	b	c	Average	St. Dev.	Variance
Water Depth	**Value**						
0.203	H_{rms}	0.025		0.027	0.026	0.002	0.000
	H_{avg}	0.023		0.024	0.024	0.001	0.000
	T_z	1.61		1.34	1.48	0.193	0.037
	N	4.0		5.0	4.5	0.707	0.500
0.254	H_{rms}	0.041	0.035	0.035	0.037	0.004	0.000
	H_{avg}	0.041	0.035	0.035	0.037	0.003	0.000
	T_z	2.15	2.20	2.20	2.18	0.029	0.001
	N	3.0	3.0	3.0	3.0	0.000	0.000
0.305	H_{rms}	0.056	0.057	0.056	0.056	0.000	0.000
	H_{avg}	0.056	0.057	0.056	0.056	0.000	0.000
	T_z	2.10	2.08	2.08	2.09	0.010	0.000
	N	3.00	3.00	3.00	3.0	0.000	0.000
.356	H_{rms}	0.079	0.073	0.080	0.077	0.003	0.000
	H_{avg}	0.079	0.073	0.079	0.077	0.003	0.000
	T_z	2.07	2.07	2.03	2.06	0.019	0.000
	N	3.0	3.0	3.0	3.0	0.000	0.000
.406	H_{rms}	0.083	0.082	0.081	0.082	0.001	0.000
	H_{avg}	0.082	0.082	0.081	0.082	0.001	0.000
	T_z	2.07	2.07	2.07	2.07	0.000	0.000
	N	3.0	3.0	3.0	3.0	0.000	0.000

Table B12: Cont.

Wave Number		3					
Burst/Variable		a	b	c	Average	St. Dev.	Variance
Water Depth	Value						
0.203	H_{rms}		0.020	0.018	0.019	0.001	0.000
	H_{avg}		0.019	0.017	0.018	0.001	0.000
	T_z		1.08	1.05	1.06	0.018	0.000
	N		2.0	2.0	2.0	0.000	0.000
0.254	H_{rms}	0.024	0.025		0.024	0.001	0.000
	H_{avg}	0.023	0.024		0.023	0.001	0.000
	T_z	1.13	1.10		1.11	0.018	0.000
	N	2.0	2.0		2.0	0.000	0.000
0.305	H_{rms}	0.030	0.029		0.030	0.000	0.000
	H_{avg}	0.029	0.028		0.028	0.000	0.000
	T_z	1.13	1.15		1.14	0.018	0.000
	N	2.00	2.00		2.0	0.000	0.000
.356	H_{rms}	0.035	0.036	0.035	0.035	0.001	0.000
	H_{avg}	0.034	0.034	0.034	0.034	0.000	0.000
	T_z	1.15	1.15	1.20	1.17	0.029	0.001
	N	2.0	2.0	2.0	2.0	0.000	0.000
.406	H_{rms}	0.041	0.042	0.037	0.040	0.003	0.000
	H_{avg}	0.039	0.040	0.034	0.038	0.003	0.000
	T_z	1.20	1.20	1.33	1.24	0.072	0.005
	N	2.0	2.0	2.5	2.2	0.289	0.083

Table B12: Cont.

Wave Number		4					
Burst/Variable		a	b	c	Average	St. Dev.	Variance
Water Depth	Value						
0.203	H_{rms}	0.036	0.033	0.034	0.035	0.001	0.000
	H_{avg}	0.035	0.033	0.034	0.034	0.001	0.000
	T_z	1.23	1.48	1.45	1.38	0.137	0.019
	N	4.0	3.5	3.5	3.7	0.289	0.083
0.254	H_{rms}	0.042	0.042	0.042	0.042	0.000	0.000
	H_{avg}	0.042	0.041	0.041	0.042	0.000	0.000
	T_z	1.63	1.45	1.46	1.51	0.105	0.011
	N	3.0	3.5	3.5	3.3	0.289	0.083
0.305	H_{rms}	0.059	0.062	0.058	0.060	0.002	0.000
	H_{avg}	0.059	0.062	0.057	0.059	0.003	0.000
	T_z	1.67	1.67	1.62	1.65	0.026	0.001
	N	3.00	3.00	3.50	3.2	0.289	0.083
.356	H_{rms}	0.075	0.082	0.080	0.079	0.004	0.000
	H_{avg}	0.073	0.082	0.080	0.078	0.005	0.000
	T_z	1.71	1.70	1.67	1.69	0.024	0.001
	N	3.5	3.0	3.0	3.2	0.289	0.083
.406	H_{rms}	0.095	0.102	0.095	0.098	0.004	0.000
	H_{avg}	0.095	0.101	0.092	0.096	0.005	0.000
	T_z	1.73	1.72	1.72	1.72	0.010	0.000
	N	3.0	3.0	3.5	3.2	0.289	0.083

Table B12: Cont.

Wave Number		5					
Burst/Variable		a	b	c	Average	St. Dev.	Variance
Water Depth	**Value**						
0.203	H_{rms}	0.030	0.033	0.032	0.032	0.001	0.000
	H_{avg}	0.029	0.032	0.031	0.030	0.001	0.000
	T_z	1.10	1.10	1.10	1.10	0.000	0.000
	N	2.0	2.0	2.0	2.0	0.000	0.000
0.254	H_{rms}	0.044	0.046	0.043	0.044	0.002	0.000
	H_{avg}	0.041	0.043	0.040	0.041	0.001	0.000
	T_z	1.10	1.13	1.10	1.11	0.014	0.000
	N	2.0	2.0	2.0	2.0	0.000	0.000
0.305	H_{rms}	0.057	0.058	0.058	0.058	0.001	0.000
	H_{avg}	0.054	0.054	0.053	0.054	0.000	0.000
	T_z	1.10	1.08	1.10	1.09	0.014	0.000
	N	2.00	2.00	2.00	2.0	0.000	0.000
.356	H_{rms}	0.068	0.066	0.069	0.068	0.001	0.000
	H_{avg}	0.063	0.061	0.064	0.063	0.001	0.000
	T_z	1.10	1.10	1.08	1.09	0.014	0.000
	N	2.0	2.0	2.0	2.0	0.000	0.000
.406	H_{rms}	0.085	0.082	0.083	0.083	0.002	0.000
	H_{avg}	0.078	0.077	0.078	0.078	0.001	0.000
	T_z	1.10	1.13	1.13	1.12	0.014	0.000
	N	2.0	2.0	2.0	2.0	0.000	0.000

Table B12: Cont.

Wave Number		6					
Burst/Variable		a	b	c	Average	St. Dev.	Variance
Water Depth	Value						
0.203	H_{rms}						
	H_{avg}						
	T_z						
	N						
0.254	H_{rms}						
	H_{avg}						
	T_z						
	N						
0.305	H_{rms}						
	H_{avg}						
	T_z						
	N						
.356	H_{rms}						
	H_{avg}						
	T_z						
	N						
.406	H_{rms}						
	H_{avg}						
	T_z						
	N						

Table B12: Cont.

Wave Number		7					
Burst/Variable		**a**	**b**	**c**	**Average**	**St. Dev.**	**Variance**
Water Depth	**Value**						
0.203	H_{rms}	0.041	0.041	0.040	0.040	0.000	0.000
	H_{avg}	0.040	0.040	0.039	0.039	0.001	0.000
	T_z	1.05	1.04	1.04	1.04	0.006	0.000
	N	5.5	5.5	5.5	5.5	0.000	0.000
0.254	H_{rms}	0.059	0.058	0.062	0.060	0.002	0.000
	H_{avg}	0.057	0.056	0.059	0.057	0.002	0.000
	T_z	1.21	1.21	1.21	1.21	0.000	0.000
	N	5.0	5.0	5.0	5.0	0.000	0.000
0.305	H_{rms}	0.088	0.087	0.088	0.088	0.001	0.000
	H_{avg}	0.085	0.084	0.085	0.085	0.001	0.000
	T_z	1.51	1.53	1.51	1.52	0.010	0.000
	N	4.00	4.00	4.00	4.0	0.000	0.000
.356	H_{rms}	0.130	0.131	0.134	0.132	0.002	0.000
	H_{avg}	0.130	0.131	0.134	0.132	0.002	0.000
	T_z	1.77	1.78	1.77	1.77	0.010	0.000
	N	3.0	3.0	3.0	3.0	0.000	0.000
.406	H_{rms}	0.159	0.165	0.165	0.163	0.003	0.000
	H_{avg}	0.159	0.165	0.165	0.163	0.003	0.000
	T_z	1.75	1.77	1.77	1.76	0.010	0.000
	N	3.0	3.0	3.0	3.0	0.000	0.000

Table B12: Cont.

Wave Number		8					
Burst/Variable		a	b	c	Average	St. Dev.	Variance
Water Depth	**Value**						
0.203	H_{rms}	0.077	0.073	0.069	0.073	0.004	0.000
	H_{avg}	0.077	0.071	0.065	0.071	0.006	0.000
	T_z	2.37	2.03	1.70	2.03	0.333	0.111
	N	3.0	3.5	4.0	3.5	0.500	0.250
0.254	H_{rms}	0.121	0.120	0.116	0.119	0.003	0.000
	H_{avg}	0.121	0.119	0.116	0.119	0.003	0.000
	T_z	2.27	2.30	2.28	2.28	0.017	0.000
	N	3.0	3.0	3.0	3.0	0.000	0.000
0.305	H_{rms}	0.138	0.145	0.156	0.146	0.009	0.000
	H_{avg}	0.138	0.144	0.155	0.146	0.009	0.000
	T_z	2.28	2.28	2.30	2.29	0.013	0.000
	N	4.00	3.00	3.00	3.3	0.577	0.333
.356	H_{rms}		0.172	0.173	0.173	0.001	0.000
	H_{avg}		0.171	0.173	0.172	0.001	0.000
	T_z		2.27	2.32	2.29	0.035	0.001
	N		3.0	3.5	3.3	0.354	0.125
.406	H_{rms}	0.205	0.211	0.212	0.210	0.004	0.000
	H_{avg}	0.205	0.210	0.211	0.209	0.003	0.000
	T_z	2.26	2.28	2.27	2.27	0.006	0.000
	N	4.0	4.0	3.5	3.8	0.289	0.083

Table B13: Concrete pyramid offset double row experimental test data. The burst values are the average of the gage data. Areas of omitted data are indicative of incomplete or inconsistent data. All physical dimensions are in meters.

Wave Number		1					
Burst/Variable		a	b	c	Average	St. Dev.	Variance
Water Depth	Value						
0.203	H_{rms}		0.012	0.011	0.011	0.000	0.000
	H_{avg}		0.010	0.009	0.009	0.001	0.000
	T_z		1.34	1.22	1.28	0.083	0.007
	N		3.5	4.0	3.8	0.354	0.125
0.254	H_{rms}	0.022	0.021	0.021	0.021	0.001	0.000
	H_{avg}	0.022	0.021	0.020	0.021	0.001	0.000
	T_z	1.38	1.35	1.38	1.37	0.014	0.000
	N	2.0	2.0	2.0	2.0	0.000	0.000
0.305	H_{rms}	0.028	0.025	0.028	0.027	0.001	0.000
	H_{avg}	0.027	0.024	0.028	0.026	0.002	0.000
	T_z	1.40	1.43	1.40	1.41	0.014	0.000
	N	2.00	2.50	2.00	2.2	0.289	0.083
.356	H_{rms}		0.048	0.048	0.048	0.000	0.000
	H_{avg}		0.047	0.047	0.047	0.000	0.000
	T_z		1.43	1.40	1.42	0.024	0.001
	N		3.0	3.0	3.0	0.000	0.000
.406	H_{rms}	0.050	0.050	0.051	0.050	0.001	0.000
	H_{avg}	0.048	0.049	0.050	0.049	0.001	0.000
	T_z	1.40	1.40	1.37	1.39	0.019	0.000
	N	3.0	3.0	3.0	3.0	0.000	0.000

Table B13: Cont.

Wave Number		2					
Burst/Variable		a	b	c	Average	St. Dev.	Variance
Water Depth	Value						
0.203	H_{rms}	0.022	0.023	0.024	0.023	0.001	0.000
	H_{avg}	0.020	0.021	0.021	0.021	0.001	0.000
	T_z	1.43	1.42	1.47	1.44	0.027	0.001
	N	4.5	4.5	4.5	4.5	0.000	0.000
0.254	H_{rms}	0.039	0.040	0.040	0.040	0.001	0.000
	H_{avg}	0.037	0.039	0.039	0.039	0.001	0.000
	T_z	1.81	1.87	1.85	1.84	0.028	0.001
	N	4.0	3.5	3.5	3.7	0.289	0.083
0.305	H_{rms}	0.042	0.040	0.043	0.042	0.001	0.000
	H_{avg}	0.040	0.037	0.040	0.039	0.002	0.000
	T_z	1.29	1.23	1.33	1.28	0.047	0.002
	N	6.50	6.50	6.00	6.3	0.289	0.083
.356	H_{rms}	0.055	0.056	0.060	0.057	0.003	0.000
	H_{avg}	0.051	0.052	0.058	0.053	0.004	0.000
	T_z	1.30	1.31	1.25	1.29	0.034	0.001
	N	6.5	6.5	5.5	6.2	0.577	0.333
.406	H_{rms}	0.081	0.081	0.081	0.081	0.000	0.000
	H_{avg}	0.078	0.079	0.079	0.079	0.000	0.000
	T_z	1.85	1.81	1.72	1.80	0.066	0.004
	N	4.0	3.5	4.0	3.8	0.289	0.083

Table B13: Cont.

Wave Number		3					
Burst/Variable		a	b	c	Average	St. Dev.	Variance
Water Depth	Value						
0.203	H_{rms}	0.017			0.017		
	H_{avg}	0.016			0.016		
	T_z	1.13			1.13		
	N	2.0			2.0		
0.254	H_{rms}	0.023	0.023	0.021	0.022	0.001	0.000
	H_{avg}	0.022	0.022	0.021	0.022	0.001	0.000
	T_z	1.13	1.18	1.18	1.16	0.029	0.001
	N	2.0	2.0	2.0	2.0	0.000	0.000
0.305	H_{rms}	0.027	0.027	0.028	0.027	0.000	0.000
	H_{avg}	0.026	0.026	0.027	0.026	0.000	0.000
	T_z	1.15	1.15	1.15	1.15	0.000	0.000
	N	2.00	2.00	2.00	2.0	0.000	0.000
.356	H_{rms}	0.033	0.034	0.033	0.033	0.000	0.000
	H_{avg}	0.029	0.029	0.029	0.029	0.000	0.000
	T_z	1.37	1.30	1.23	1.30	0.067	0.004
	N	3.0	3.0	3.0	3.0	0.000	0.000
.406	H_{rms}	0.046	0.047	0.045	0.046	0.001	0.000
	H_{avg}	0.044	0.044	0.043	0.043	0.001	0.000
	T_z	1.23	1.23	1.23	1.23	0.000	0.000
	N	2.0	2.0	2.0	2.0	0.000	0.000

Table B13: Cont.

Wave Number		4					
Burst/Variable		**a**	**b**	**c**	**Average**	**St. Dev.**	**Variance**
Water Depth	**Value**						
0.203	H_{rms}	0.026	0.026	0.025	0.026	0.001	0.000
	H_{avg}	0.025	0.025	0.024	0.025	0.001	0.000
	T_z	1.29	1.28	1.34	1.30	0.033	0.001
	N	4.0	4.0	3.5	3.8	0.289	0.083
0.254	H_{rms}	0.038	0.039	0.037	0.038	0.001	0.000
	H_{avg}	0.037	0.037	0.035	0.036	0.001	0.000
	T_z	1.14	1.13	1.14	1.13	0.001	0.000
	N	4.5	4.5	4.5	4.5	0.000	0.000
0.305	H_{rms}	0.047	0.048	0.048	0.048	0.001	0.000
	H_{avg}	0.046	0.047	0.047	0.046	0.001	0.000
	T_z	1.02	1.02	1.02	1.02	0.000	0.000
	N	5.00	5.00	5.00	5.0	0.000	0.000
.356	H_{rms}	0.072	0.078	0.077	0.076	0.003	0.000
	H_{avg}	0.072	0.076	0.076	0.075	0.002	0.000
	T_z	1.70	1.35	1.52	1.52	0.175	0.031
	N	3.0	4.0	3.5	3.5	0.500	0.250
.406	H_{rms}	0.106	0.106		0.106	0.000	0.000
	H_{avg}	0.106	0.106		0.106	0.000	0.000
	T_z	1.68	1.68		1.68	0.000	0.000
	N	3.0	3.0		3.0	0.000	0.000

Table B13: Cont.

Wave Number		5					
Burst/Variable		**a**	**b**	**c**	**Average**	**St. Dev.**	**Variance**
Water Depth	**Value**						
0.203	H_{rms}	0.019	0.020	0.016	0.018	0.002	0.000
	H_{avg}	0.019	0.019	0.016	0.018	0.002	0.000
	T_z	1.15	1.20	1.25	1.20	0.050	0.002
	N	1.5	1.5	1.0	1.3	0.289	0.083
0.254	H_{rms}	0.038	0.038	0.037	0.038	0.001	0.000
	H_{avg}	0.036	0.036	0.035	0.036	0.000	0.000
	T_z	1.10	1.10	1.10	1.10	0.000	0.000
	N	2.0	2.0	2.0	2.0	0.000	0.000
0.305	H_{rms}	0.051	0.053	0.054	0.053	0.002	0.000
	H_{avg}	0.047	0.049	0.050	0.049	0.001	0.000
	T_z	1.08	1.08	1.05	1.07	0.014	0.000
	N	2.00	2.00	2.00	2.0	0.000	0.000
.356	H_{rms}	0.063	0.063	0.064	0.064	0.000	0.000
	H_{avg}	0.059	0.059	0.060	0.060	0.000	0.000
	T_z	1.10	1.13	1.08	1.10	0.025	0.001
	N	2.0	2.0	2.0	2.0	0.000	0.000
.406	H_{rms}	0.090	0.088	0.085	0.088	0.002	0.000
	H_{avg}	0.083	0.081	0.080	0.081	0.002	0.000
	T_z	1.13	1.10	1.13	1.12	0.014	0.000
	N	2.0	2.0	2.0	2.0	0.000	0.000

Table B13: Cont.

Wave Number		6					
Burst/Variable		a	b	c	Average	St. Dev.	Variance
Water Depth	Value						
0.203	H_{rms}						
	H_{avg}						
	T_z						
	N						
0.254	H_{rms}						
	H_{avg}						
	T_z						
	N						
0.305	H_{rms}						
	H_{avg}						
	T_z						
	N						
.356	H_{rms}						
	H_{avg}						
	T_z						
	N						
.406	H_{rms}						
	H_{avg}						
	T_z						
	N						

Table B13: Cont.

Wave Number		7					
Burst/Variable		a	b	c	Average	St. Dev.	Variance
Water Depth	**Value**						
0.203	H_{rms}	0.035	0.042	0.040	0.039	0.004	0.000
	H_{avg}	0.033	0.041	0.039	0.038	0.004	0.000
	T_z	1.06	1.21	1.13	1.13	0.073	0.005
	N	5.0	4.5	5.0	4.8	0.289	0.083
0.254	H_{rms}	0.063	0.061	0.063	0.062	0.001	0.000
	H_{avg}	0.060	0.060	0.062	0.061	0.001	0.000
	T_z	1.18	1.18	1.25	1.20	0.038	0.001
	N	5.0	5.0	4.5	4.8	0.289	0.083
0.305	H_{rms}	0.088	0.074	0.080	0.081	0.007	0.000
	H_{avg}	0.086	0.069	0.077	0.077	0.008	0.000
	T_z	1.55	1.33	1.35	1.41	0.121	0.015
	N	3.50	4.00	4.00	3.8	0.289	0.083
.356	H_{rms}	0.118	0.118	0.119	0.119	0.001	0.000
	H_{avg}	0.118	0.118	0.119	0.118	0.001	0.000
	T_z	1.78	1.78	1.77	1.78	0.010	0.000
	N	3.0	3.0	3.0	3.0	0.000	0.000
.406	H_{rms}	0.150	0.147	0.151	0.149	0.002	0.000
	H_{avg}	0.149	0.147	0.150	0.149	0.002	0.000
	T_z	1.78	1.78	1.78	1.78	0.000	0.000
	N	3.0	3.0	3.0	3.0	0.000	0.000

Table B13: Cont.

Wave Number		8					
Burst/Variable		a	b	c	Average	St. Dev.	Variance
Water Depth	**Value**						
0.203	H_{rms}	0.038			0.038		
	H_{avg}	0.034			0.034		
	T_z	1.38			1.38		
	N	6.0			6.0		
0.254	H_{rms}		0.084	0.077	0.081	0.005	0.000
	H_{avg}		0.076	0.070	0.073	0.004	0.000
	T_z		1.70	1.55	1.63	0.104	0.011
	N		4.0	4.5	4.3	0.354	0.125
0.305	H_{rms}	0.117		0.122	0.120	0.003	0.000
	H_{avg}	0.117		0.122	0.120	0.003	0.000
	T_z	2.33		2.40	2.37	0.047	0.002
	N	3.00		3.00	3.0	0.000	0.000
.356	H_{rms}	0.152	0.154	0.145	0.151	0.005	0.000
	H_{avg}	0.152	0.154	0.139	0.148	0.008	0.000
	T_z	2.27	2.33	2.11	2.24	0.116	0.013
	N	3.0	3.0	3.5	3.2	0.289	0.083
.406	H_{rms}	0.182	0.177	0.175	0.178	0.004	0.000
	H_{avg}	0.180	0.176	0.174	0.177	0.003	0.000
	T_z	2.28	2.28	2.30	2.29	0.010	0.000
	N	3.0	3.0	3.0	3.0	0.000	0.000

Table B14: ReefBLK^{SM} raw experimental data for controls. The burst values are the average of the gage data. Areas of omitted data are indicative of incomplete or inconsistent data. All physical dimensions are in meters.

Wave Number		1					
Burst/Variable		a	b	c	Average	St. Dev.	Variance
Water Depth	Value						
0.203	H_{rms}	0.031	0.030	0.030	0.030	0.001	0.000
	H_{avg}	0.031	0.030	0.030	0.030	0.001	0.000
	T_z	1.36	1.33	1.34	1.34	0.011	0.000
	N	3.0	3.0	3.0	3.0	0.000	0.000
0.254	H_{rms}	0.038	0.038	0.039	0.039	0.001	0.000
	H_{avg}	0.038	0.038	0.039	0.038	0.001	0.000
	T_z	1.35	1.36	1.33	1.35	0.012	0.000
	N	3.0	3.0	3.0	3.0	0.000	0.000
0.305	H_{rms}	0.044	0.045	0.045	0.045	0.000	0.000
	H_{avg}	0.044	0.044	0.045	0.044	0.000	0.000
	T_z	1.34	1.34	1.36	1.35	0.006	0.000
	N	3.00	3.00	3.00	3.0	0.000	0.000
.356	H_{rms}	0.051	0.050	0.051	0.051	0.000	0.000
	H_{avg}	0.050	0.050	0.051	0.050	0.000	0.000
	T_z	1.34	1.34	1.34	1.34	0.000	0.000
	N	3.0	3.0	3.0	3.0	0.000	0.000
.406	H_{rms}	0.053	0.054	0.054	0.053	0.000	0.000
	H_{avg}	0.052	0.053	0.053	0.053	0.000	0.000
	T_z	1.37	1.37	1.33	1.36	0.019	0.000
	N	3.0	3.0	3.0	3.0	0.000	0.000

Table B14: Cont.

Wave Number		2					
Burst/Variable		a	b	c	Average	St. Dev.	Variance
Water Depth	Value						
0.203	H_{rms}	0.058	0.056	0.051	0.055	0.004	0.000
	H_{avg}	0.057	0.056	0.050	0.054	0.004	0.000
	T_z	2.17	2.18	2.18	2.18	0.008	0.000
	N	3.0	3.0	3.0	3.0	0.000	0.000
0.254	H_{rms}	0.059	0.059	0.060	0.059	0.000	0.000
	H_{avg}	0.059	0.059	0.060	0.059	0.000	0.000
	T_z	2.21	2.23	2.24	2.23	0.017	0.000
	N	3.0	3.0	3.0	3.0	0.000	0.000
0.305	H_{rms}	0.071	0.072	0.073	0.072	0.001	0.000
	H_{avg}	0.071	0.072	0.073	0.072	0.001	0.000
	T_z	2.20	2.19	2.19	2.19	0.006	0.000
	N	3.00	3.00	3.00	3.0	0.000	0.000
.356	H_{rms}	0.080	0.080	0.079	0.080	0.001	0.000
	H_{avg}	0.080	0.080	0.079	0.080	0.001	0.000
	T_z	2.09	2.09	2.18	2.12	0.050	0.002
	N	3.0	3.0	4.0	3.3	0.577	0.333
.406	H_{rms}	0.096	0.094	0.090	0.093	0.003	0.000
	H_{avg}	0.095	0.094	0.089	0.093	0.003	0.000
	T_z	2.05	2.06	2.05	2.05	0.005	0.000
	N	4.0	4.0	4.0	4.0	0.000	0.000

Table B14: Cont.

Wave Number		3					
Burst/Variable		a	b	c	Average	St. Dev.	Variance
Water Depth	Value	0.045	0.045	0.047	0.046	0.001	0.000
0.203	H_{rms}	0.043	0.043	0.044	0.043	0.001	0.000
	H_{avg}	1.03	1.05	1.03	1.04	0.013	0.000
	T_z	2.0	2.0	2.0	2.0	0.000	0.000
	N	0.055	0.051	0.055	0.054	0.002	0.000
0.254	H_{rms}	0.051	0.048	0.052	0.050	0.002	0.000
	H_{avg}	1.08	1.10	1.08	1.09	0.013	0.000
	T_z	2.0	2.0	2.0	2.0	0.000	0.000
	N	0.057	0.059	0.056	0.057	0.002	0.000
0.305	H_{rms}	0.053	0.055	0.053	0.054	0.001	0.000
	H_{avg}	1.10	1.10	1.12	1.11	0.010	0.000
	T_z	2.00	2.00	2.00	2.0	0.000	0.000
	N	0.060	0.063	0.061	0.061	0.002	0.000
.356	H_{rms}	0.056	0.059	0.058	0.058	0.002	0.000
	H_{avg}	1.12	1.15	1.15	1.14	0.019	0.000
	T_z	2.0	2.0	2.0	2.0	0.000	0.000
	N	0.082	0.084	0.075	0.080	0.004	0.000
.406	H_{rms}	0.075	0.077	0.070	0.074	0.004	0.000
	H_{avg}	1.08	1.10	1.11	1.10	0.017	0.000
	T_z	3.0	3.0	2.7	2.9	0.192	0.037
	N	0.045	0.045	0.047	0.046	0.001	0.000

Table B14: Cont.

Wave Number		4					
Burst/Variable		**a**	**b**	**c**	**Average**	**St. Dev.**	**Variance**
Water Depth	**Value**						
0.203	H_{rms}	0.065	0.065	0.061	0.064	0.003	0.000
	H_{avg}	0.065	0.065	0.061	0.064	0.003	0.000
	T_z	1.69	1.69	1.67	1.68	0.013	0.000
	N	3.0	3.0	3.0	3.0	0.000	0.000
0.254	H_{rms}	0.086	0.085	0.085	0.086	0.000	0.000
	H_{avg}	0.086	0.085	0.085	0.085	0.000	0.000
	T_z	1.68	1.68	1.68	1.68	0.000	0.000
	N	3.0	3.0	3.0	3.0	0.000	0.000
0.305	H_{rms}	0.093	0.092	0.093	0.093	0.001	0.000
	H_{avg}	0.093	0.092	0.093	0.093	0.001	0.000
	T_z	1.64	1.68	1.67	1.66	0.017	0.000
	N	3.00	3.00	3.00	3.0	0.000	0.000
.356	H_{rms}	0.106	0.106	0.106	0.106	0.000	0.000
	H_{avg}	0.106	0.106	0.106	0.106	0.000	0.000
	T_z	1.68	1.67	1.67	1.67	0.006	0.000
	N	3.0	3.0	3.0	3.0	0.000	0.000
.406	H_{rms}	0.117	0.120	0.118	0.118	0.001	0.000
	H_{avg}	0.117	0.120	0.118	0.118	0.001	0.000
	T_z	1.70	1.70	1.70	1.70	0.000	0.000
	N	3.0	3.0	3.0	3.0	0.000	0.000

Table B14: Cont.

Wave Number		5					
Burst/Variable		a	b	c	Average	St. Dev.	Variance
Water Depth	Value						
0.203	H_{rms}	0.066	0.067	0.063	0.065	0.002	0.000
	H_{avg}	0.064	0.063	0.059	0.062	0.002	0.000
	T_z	1.05	1.12	1.09	1.09	0.034	0.001
	N	2.0	2.3	2.5	2.3	0.255	0.065
0.254	H_{rms}	0.081	0.083	0.083	0.082	0.001	0.000
	H_{avg}	0.078	0.079	0.079	0.079	0.001	0.000
	T_z	1.07	1.08	1.07	1.07	0.005	0.000
	N	2.0	2.0	2.0	2.0	0.000	0.000
0.305	H_{rms}	0.103	0.100	0.100	0.101	0.002	0.000
	H_{avg}	0.099	0.096	0.096	0.097	0.002	0.000
	T_z	1.07	1.06	1.06	1.06	0.006	0.000
	N	3.00	3.00	2.67	2.9	0.192	0.037
.356	H_{rms}	0.113	0.119	0.112	0.115	0.004	0.000
	H_{avg}	0.108	0.116	0.107	0.110	0.005	0.000
	T_z	1.04	1.07	1.07	1.06	0.013	0.000
	N	3.0	3.0	3.0	3.0	0.000	0.000
.406	H_{rms}	0.121	0.120	0.132	0.124	0.007	0.000
	H_{avg}	0.116	0.117	0.129	0.121	0.008	0.000
	T_z	1.07	1.07	1.11	1.08	0.026	0.001
	N	3.0	3.0	3.0	3.0	0.000	0.000

Table B14: Cont.

Wave Number		6					
Burst/Variable		a	b	c	Average	St. Dev.	Variance
Water Depth	Value						
0.203	H_{rms}						
	H_{avg}						
	T_z						
	N						
0.254	H_{rms}						
	H_{avg}						
	T_z						
	N						
0.305	H_{rms}						
	H_{avg}						
	T_z						
	N						
.356	H_{rms}						
	H_{avg}						
	T_z						
	N						
.406	H_{rms}						
	H_{avg}						
	T_z						
	N						

Table B14: Cont.

Wave Number		7					
Burst/Variable		**a**	**b**	**c**	**Average**	**St. Dev.**	**Variance**
Water Depth	**Value**						
0.203	H_{rms}						
	H_{avg}						
	T_z						
	N						
0.254	H_{rms}	0.126	0.116	0.128	0.123	0.006	0.000
	H_{avg}	0.125	0.116	0.127	0.123	0.006	0.000
	T_z	1.76	1.75	1.77	1.76	0.009	0.000
	N	3.0	3.0	3.0	3.0	0.000	0.000
0.305	H_{rms}	0.152	0.156	0.155	0.154	0.002	0.000
	H_{avg}	0.151	0.155	0.155	0.154	0.002	0.000
	T_z	1.77	1.73	1.76	1.75	0.017	0.000
	N	3.00	3.00	3.00	3.0	0.000	0.000
.356	H_{rms}	0.177	0.181	0.182	0.180	0.003	0.000
	H_{avg}	0.177	0.181	0.182	0.180	0.003	0.000
	T_z	1.76	1.76	1.77	1.76	0.003	0.000
	N	3.3	3.3	3.0	3.2	0.192	0.037
.406	H_{rms}	0.203	0.205	0.203	0.204	0.001	0.000
	H_{avg}	0.203	0.205	0.202	0.203	0.001	0.000
	T_z	1.78	1.76	1.76	1.76	0.011	0.000
	N	4.0	3.7	3.7	3.8	0.192	0.037

Table B14: Cont.

Wave Number		8					
Burst/Variable		a	b	c	Average	St. Dev.	Variance
Water Depth	Value						
0.203	H_{rms}		0.101	0.105	0.103	0.003	0.000
	H_{avg}		0.091	0.096	0.093	0.003	0.000
	T_z		1.80	1.75	1.78	0.035	0.001
	N		4.0	4.0	4.0	0.000	0.000
0.254	H_{rms}			0.182	0.182		
	H_{avg}			0.181	0.181		
	T_z			2.35	2.35		
	N			3.7	3.7		
0.305	H_{rms}		0.214	0.206	0.210	0.006	0.000
	H_{avg}		0.213	0.205	0.209	0.006	0.000
	T_z		2.35	2.34	2.35	0.006	0.000
	N		4.00	4.00	4.0	0.000	0.000
.356	H_{rms}	0.224	0.220	0.231	0.225	0.005	0.000
	H_{avg}	0.223	0.220	0.230	0.224	0.005	0.000
	T_z	2.23	2.23	2.23	2.23	0.000	0.000
	N	4.0	4.0	4.0	4.0	0.000	0.000
.406	H_{rms}	0.218	0.218		0.218	0.000	0.000
	H_{avg}	0.216	0.215		0.216	0.000	0.000
	T_z	2.23	2.23		2.23	0.000	0.000
	N	4.0	4.0		4.0	0.000	0.000

Table B15: ReefBLK^{SM} raw experimental data of transmitted wave properties. The burst values are the average of the gage data. Areas of omitted data are indicative of incomplete or inconsistent data. All physical dimensions are in meters.

Wave Number		1					
Burst/Variable		a	b	c	Average	St. Dev.	Variance
Water Depth	Value						
0.203	H_{rms}	0.019	0.019	0.019	0.019	0.000	0.000
	H_{avg}	0.019	0.019	0.019	0.019	0.000	0.000
	T_z	1.37	1.36	1.37	1.36	0.006	0.000
	N	3.0	3.0	3.0	3.0	0.000	0.000
0.254	H_{rms}	0.023	0.024	0.025	0.024	0.001	0.000
	H_{avg}	0.023	0.024	0.025	0.024	0.001	0.000
	T_z	1.34	1.34	1.35	1.35	0.003	0.000
	N	3.0	3.0	3.0	3.0	0.000	0.000
0.305	H_{rms}	0.028	0.027	0.028	0.028	0.000	0.000
	H_{avg}	0.028	0.027	0.027	0.027	0.000	0.000
	T_z	1.33	1.34	1.34	1.34	0.006	0.000
	N	3.00	3.00	3.00	3.0	0.000	0.000
.356	H_{rms}	0.038	0.037	0.037	0.038	0.000	0.000
	H_{avg}	0.037	0.037	0.037	0.037	0.000	0.000
	T_z	1.35	1.36	1.34	1.35	0.006	0.000
	N	3.0	3.0	3.0	3.0	0.000	0.000
.406	H_{rms}	0.044	0.044	0.044	0.044	0.000	0.000
	H_{avg}	0.044	0.044	0.043	0.044	0.000	0.000
	T_z	1.34	1.34	1.36	1.35	0.006	0.000
	N	3.0	3.0	3.0	3.0	0.000	0.000

Table B15: Cont.

Wave Number		2					
Burst/Variable		a	b	c	Average	St. Dev.	Variance
Water Depth	Value						
0.203	H_{rms}	0.033	0.033	0.033	0.033	0.000	0.000
	H_{avg}	0.033	0.033	0.033	0.033	0.000	0.000
	T_z	2.14	2.14	2.14	2.14	0.000	0.000
	N	3.0	3.0	3.0	3.0	0.000	0.000
0.254	H_{rms}	0.041	0.041	0.042	0.041	0.000	0.000
	H_{avg}	0.041	0.041	0.041	0.041	0.000	0.000
	T_z	2.14	2.14	2.14	2.14	0.000	0.000
	N	3.0	3.0	3.0	3.0	0.000	0.000
0.305	H_{rms}	0.049	0.048	0.049	0.049	0.001	0.000
	H_{avg}	0.049	0.048	0.049	0.049	0.001	0.000
	T_z	2.09	2.08	2.07	2.08	0.011	0.000
	N	3.00	3.00	3.00	3.0	0.000	0.000
.356	H_{rms}	0.062	0.060	0.061	0.061	0.001	0.000
	H_{avg}	0.062	0.060	0.061	0.061	0.001	0.000
	T_z	2.06	2.06	2.05	2.06	0.005	0.000
	N	3.3	3.3	3.7	3.4	0.192	0.037
.406	H_{rms}	0.076	0.077	0.077	0.077	0.001	0.000
	H_{avg}	0.076	0.077	0.077	0.076	0.001	0.000
	T_z	2.08	2.07	2.06	2.07	0.013	0.000
	N	4.0	4.0	4.0	4.0	0.000	0.000

Table B15: Cont.

Wave Number		3					
Burst/Variable		a	b	c	Average	St. Dev.	Variance
Water Depth	Value	0.020	0.021	0.021	0.021	0.000	0.000
0.203	H_{rms}	0.020	0.020	0.020	0.020	0.000	0.000
	H_{avg}	1.07	1.07	1.07	1.07	0.000	0.000
	T_z	2.0	2.0	2.0	2.0	0.000	0.000
	N	0.024	0.024	0.023	0.024	0.001	0.000
0.254	H_{rms}	0.024	0.024	0.022	0.023	0.001	0.000
	H_{avg}	1.12	1.12	1.16	1.13	0.022	0.001
	T_z	2.0	2.0	2.3	2.1	0.192	0.037
	N	0.030	0.029	0.030	0.030	0.000	0.000
0.305	H_{rms}	0.029	0.029	0.029	0.029	0.000	0.000
	H_{avg}	1.13	1.13	1.13	1.13	0.000	0.000
	T_z	2.00	2.00	2.00	2.0	0.000	0.000
	N	0.041	0.040	0.040	0.041	0.000	0.000
.356	H_{rms}	0.039	0.039	0.039	0.039	0.000	0.000
	H_{avg}	1.13	1.15	1.15	1.14	0.010	0.000
	T_z	2.0	2.0	2.0	2.0	0.000	0.000
	N	0.049	0.048	0.046	0.048	0.001	0.000
.406	H_{rms}	0.046	0.045	0.042	0.045	0.002	0.000
	H_{avg}	1.15	1.20	1.15	1.17	0.029	0.001
	T_z	2.0	2.0	2.3	2.1	0.192	0.037
	N	0.020	0.021	0.021	0.021	0.000	0.000

Table B15: Cont.

Wave Number		4					
Burst/Variable		a	b	c	Average	St. Dev.	Variance
Water Depth	Value						
0.203	H_{rms}	0.032	0.032	0.032	0.032	0.000	0.000
	H_{avg}	0.032	0.031	0.031	0.032	0.000	0.000
	T_z	1.67	1.67	1.69	1.67	0.013	0.000
	N	3.0	3.0	3.0	3.0	0.000	0.000
0.254	H_{rms}	0.038	0.039	0.039	0.039	0.000	0.000
	H_{avg}	0.038	0.039	0.039	0.038	0.000	0.000
	T_z	1.71	1.71	1.68	1.70	0.019	0.000
	N	3.0	3.0	3.0	3.0	0.000	0.000
0.305	H_{rms}	0.051	0.052	0.052	0.052	0.001	0.000
	H_{avg}	0.051	0.052	0.052	0.051	0.001	0.000
	T_z	1.72	1.72	1.72	1.72	0.000	0.000
	N	3.00	3.00	3.00	3.0	0.000	0.000
.356	H_{rms}	0.072	0.074	0.075	0.074	0.001	0.000
	H_{avg}	0.072	0.074	0.074	0.073	0.001	0.000
	T_z	1.74	1.74	1.72	1.74	0.013	0.000
	N	3.0	3.0	3.0	3.0	0.000	0.000
.406	H_{rms}	0.096	0.097	0.098	0.097	0.001	0.000
	H_{avg}	0.095	0.097	0.097	0.096	0.001	0.000
	T_z	1.71	1.73	1.72	1.72	0.011	0.000
	N	3.0	3.0	3.0	3.0	0.000	0.000

Table B15: Cont.

Wave Number		5					
Burst/Variable		**a**	**b**	**c**	**Average**	**St. Dev.**	**Variance**
Water Depth	**Value**						
0.203	H_{rms}	0.030	0.031	0.032	0.031	0.001	0.000
	H_{avg}	0.029	0.030	0.031	0.030	0.001	0.000
	T_z	1.08	1.10	1.10	1.09	0.010	0.000
	N	2.0	2.0	2.0	2.0	0.000	0.000
0.254	H_{rms}	0.037	0.037	0.037	0.037	0.000	0.000
	H_{avg}	0.036	0.036	0.036	0.036	0.000	0.000
	T_z	1.08	1.10	1.08	1.09	0.010	0.000
	N	2.0	2.0	2.0	2.0	0.000	0.000
0.305	H_{rms}	0.062	0.059	0.057	0.060	0.003	0.000
	H_{avg}	0.059	0.055	0.054	0.056	0.003	0.000
	T_z	1.04	1.05	1.08	1.06	0.021	0.000
	N	2.33	2.00	2.00	2.1	0.192	0.037
.356	H_{rms}	0.074	0.075	0.072	0.074	0.001	0.000
	H_{avg}	0.071	0.073	0.069	0.071	0.002	0.000
	T_z	1.08	1.07	1.07	1.07	0.006	0.000
	N	2.7	3.0	2.0	2.6	0.509	0.259
.406	H_{rms}	0.092	0.091	0.094	0.092	0.002	0.000
	H_{avg}	0.088	0.087	0.090	0.089	0.001	0.000
	T_z	1.07	1.10	1.08	1.08	0.017	0.000
	N	3.0	3.0	3.0	3.0	0.000	0.000

Table B15: Cont.

Wave Number		6					
Burst/Variable		a	b	c	Average	St. Dev.	Variance
Water Depth	Value						
0.203	H_{rms}						
	H_{avg}						
	T_z						
	N						
0.254	H_{rms}						
	H_{avg}						
	T_z						
	N						
0.305	H_{rms}						
	H_{avg}						
	T_z						
	N						
.356	H_{rms}						
	H_{avg}						
	T_z						
	N						
.406	H_{rms}						
	H_{avg}						
	T_z						
	N						

Table B15: Cont.

Wave Number		7					
Burst/Variable		a	b	c	Average	St. Dev.	Variance
Water Depth	Value						
0.203	H_{rms}						
	H_{avg}						
	T_z						
	N						
0.254	H_{rms}						
	H_{avg}						
	T_z						
	N						
0.305	H_{rms}		0.115	0.110	0.112	0.004	0.000
	H_{avg}		0.114	0.109	0.111	0.003	0.000
	T_z		1.76	1.75	1.75	0.004	0.000
	N		3.00	3.00	3.0	0.000	0.000
.356	H_{rms}	0.130	0.132	0.131	0.131	0.001	0.000
	H_{avg}	0.130	0.132	0.131	0.131	0.001	0.000
	T_z	1.78	1.78	1.78	1.78	0.000	0.000
	N	3.3	3.3	3.3	3.3	0.000	0.000
.406	H_{rms}	0.167	0.162	0.161	0.163	0.003	0.000
	H_{avg}	0.167	0.162	0.160	0.163	0.003	0.000
	T_z	1.80	1.78	1.79	1.79	0.008	0.000
	N	3.0	3.3	3.3	3.2	0.192	0.037

Table B15: Cont.

Wave Number		8					
Burst/Variable		a	b	c	Average	St. Dev.	Variance
Water Depth	Value						
0.203	H_{rms}						
	H_{avg}						
	T_z						
	N						
0.254	H_{rms}	0.114	0.103	0.123	0.113	0.010	0.000
	H_{avg}	0.114	0.103	0.122	0.113	0.010	0.000
	T_z	2.23	2.21	2.24	2.23	0.015	0.000
	N	4.0	4.0	4.0	4.0	0.000	0.000
0.305	H_{rms}	0.148	0.146	0.147	0.147	0.001	0.000
	H_{avg}	0.148	0.146	0.147	0.147	0.001	0.000
	T_z	2.28	2.29	2.30	2.29	0.009	0.000
	N	4.00	4.00	4.00	4.0	0.000	0.000
.356	H_{rms}	0.147	0.142	0.141	0.143	0.003	0.000
	H_{avg}	0.147	0.142	0.141	0.143	0.003	0.000
	T_z	2.24	2.21	2.23	2.23	0.015	0.000
	N	4.0	4.0	4.0	4.0	0.000	0.000
.406	H_{rms}	0.177	0.168	0.169	0.171	0.005	0.000
	H_{avg}	0.176	0.168	0.168	0.171	0.005	0.000
	T_z	2.25	2.23	2.24	2.24	0.009	0.000
	N	4.0	4.0	4.0	4.0	0.000	0.000

BIOGRAPHICAL SKETCH

BIOGRAPHICAL SKETCH

Name of Author: Richard J. Allen

Place of Birth: Alabama, USA

Date of Birth: March 25, 1985

Graduate and Undergraduate Schools Attended:

University of South Alabama, Mobile, Alabama
Auburn University Montgomery, Montgomery, Alabama

Degrees Awarded:

Bachelor of Science in Civil Engineering, 2011, *cum laude*, Mobile, Alabama

Awards and Honors:

Research Assistant, 2010
Graduate Teaching Assistant, 2011
Graduate Research Assistant, 2012
Civil Engineering Student of the Year, 2011
Tau Beta Pi Engineering Honor Society, 2011
Dean's Honor List, 2009 - 2011
President's List, 2009
ASBPA Student Education Award, 2011
ASBPA Nicholas Kraus Coastal Scholar Award, 2012